CHARACTERIZATION OF RECEPTOR PROTEIN TYROSINE

PHOSPHATASE PTP69D IN THE GIANT FIBER CIRCUIT

by

LaTasha Hoskins Lee

A Dissertation Submitted to the Faculty of

Charles E. Schmidt College of Science

In Partial Fulfillment of the Requirements for the Degree of

Doctor of Philosophy

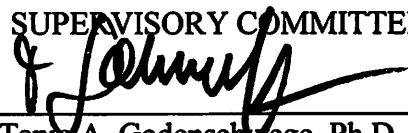Florida Atlantic University

Boca Raton, Florida

December 2014

CHARACTERIZATION OF RECEPTOR PROTEIN TYROSINE

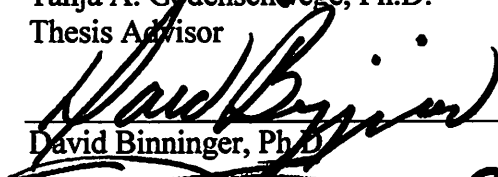# PHOSPHATASE PTP69D IN THE GIANT FIBER CIRCUIT

by

LaTasha Hoskins Lee

This dissertation was prepared under the direction of the candidate's dissertation advisor, Dr. Tanja A. Godenschwege, Department of Biological Sciences, and has been approved by the members of her supervisory committee. It was submitted to the faculty of the College of Science and was accepted in partial fulfillment of the requirements for the degree of Doctor of Philosophy.
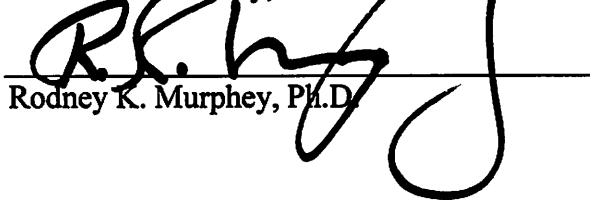
SUPERVISORY COMMITTEE:
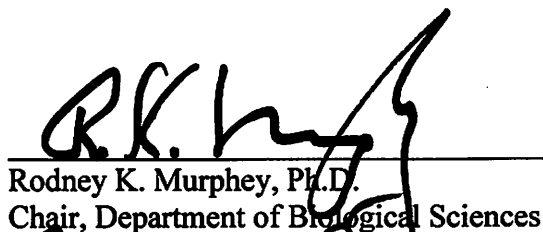
Tanja A. Godenschwege, Ph.D.
Thesis Advisor

David Binninger, Ph.D

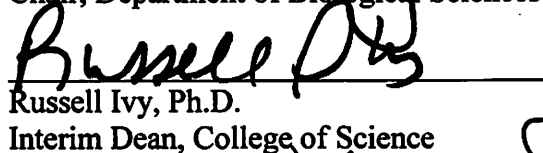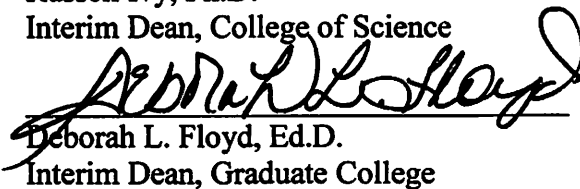Ken Dawson-Scully, Ph.D.

Rodney K. Murphey, Ph.D

Rodney K. Murphey, Ph.D.
Chair, Department of Biological Sciences

Russell Ivy, Ph.D.
Interim Dean, College of Science

Deborah L. Floyd, Ed.D.
Interim Dean, Graduate College

11/10/2014

Date

iii

ACKNOWLEDGEMENTS

God in his infinite wisdom often sends people our way to help mold us into a more meaningful existence. However, more often than not, like my beloved fruit fly that metamorphosis is not even recognized until we have eclosed and are well into adulthood. With that being said, I have a host of individuals I wish to acknowledge for nurturing, motivating and supporting me through my doctoral studies. I am deeply appreciative of the many individuals who have been my support system, both through my graduate program and through the writing of this dissertation. The list is extensive so I apologize in advance if I forget to name you here, but nevertheless without your time, attention, encouragement, thoughtful feedback, and patience, I would not have been able to see it through.

Sir Francis Crick stated that, "science has shown you that your joys and your sorrows, your memories and your ambitions, your sense of identity and free will, are in fact no more than the behaviour of a vast assembly of nerve cells and their associated molecules." With that being said, I thank science and the neuroscientists that have shaped me. I want to acknowledge Tanja and my committee – Drs. Binninger, Dawson-Scully, Murphey and Nambu – for all of their guidance, expertise, and support throughout this long journey. Special thanks to my advisor for her "tough love," support, and criticisms which have made this dissertation into a body of work I hope she is proud of. I am grateful for her financial support as well, because my work was supported by her grants (R01HD050725) and a Research Supplement to Promote Diversity in Health-

iv

your constant love and encouragement over the years. I know it was a gamble having only one child so I hope I've made you proud, and God willing one day after I "birth" this dissertation I can birth some long awaited grandkids. To my grandmothers I thank each of you for instilling in me the attributes which I have utilized throughout my academic career. Grandma Ruth you were my first science teacher and you have always encouraged my curiosity. Grandma "Red" thanks for encouraging me to study hard and take advantage of the opportunities you and grandpa didn't have. Thanks also for feeding me nearly every Sunday, your meals were food for my soul. Also thanks to my numerous aunts, uncles, cousins and friends for encouraging their "professional student" friend, your jokes actually kept me motivated to finish.

Thank you all from the bottom of my heart.

ABSTRACT

Author: LaTasha Hoskins Lee

Title: Characterization of Receptor Protein Tyrosine Phosphatase
                     PTP69D in the Giant Fiber Circuit

Institution: Florida Atlantic University

Thesis Advisor: Dr. Tanja A. Godenschwege

Degree: Doctor of Philosophy

Year: 2014

PTP69D is a receptor protein tyrosine phosphatase (RPTP) with two intracellular

catalytic domains (Cat1 and Cat2), which has been shown to play a role in axon

outgrowth and guidance of embryonic motorneurons, as well as targeting of

photoreceptor neurons in the visual system of *Drosophila melanogaster*. Here, we

characterized the developmental role of PTP69D in the giant fiber (GF) neurons; two

interneurons in the central nervous system (CNS) that control the escape response of the

fly. In addition to guidance and targeting functions, our studies reveal an additional role

for PTP69D in synaptic terminal growth in the CNS. We found that inhibition of

phosphatase activity in catalytic domain (Cat1) proximal to the transmembrane domain

did not affect axon guidance or targeting but resulted in stunted terminal growth of the

GFs. Cell autonomous rescue and knockdown experiments demonstrated a function for

PTP69D in the GFs, but not its postsynaptic target neurons. In addition,

complementation studies and structure-function analyses revealed that for GF terminal growth, Cat1 function of PTP69D requires the immunoglobulin and the Cat2 domain but not the fibronectin type III repeats nor the membrane proximal region. In contrast, the fibronectin type III repeats, but not the immunoglobulin domains, were previously shown to be essential for axon targeting of photoreceptor neurons. Thus, our studies uncover a novel role for PTP69D in synaptic terminal growth in the CNS that is mechanistically distinct from its function during earlier developmental processes.

DEDICATION

I dedicate this work in memory of my late grandfathers, Dewey Henry Hoskins and Larry "Bobby" Lee, Sr, whom I lost during my Ph.D. Thank you both for your unconventional wisdom, your spirits live on in me. Though not educated, Papa "Bobby" you encouraged me to seek higher education but never forget from whence I came. I also dedicate it to my grandmothers, Willie Ruth Hoskins and Mary Lou "Red" Lee, who have inspired me in so many ways.

Sankofa

.

CHARACTERIZATION OF RECEPTOR PROTEIN TYROSINE

PHOSPHATASE PTP69D IN GIANT SYNAPSE FORMATION

LIST OF TABLES

LIST OF FIGURES

1   GUIDANCE, TARGETING AND SYNAPSE FORMATION: THE COMPLEX PROCESS OF WIRING THE BRAIN

"The budding neuron has to detect the local environment it is growing through and decide where it is, and whether to grow straight, move to the left or right, or stop. It does this by mixing and matching just a handful of protein products to create complexes that tell a growing neuron which way to go, in the same way that a car uses the GPS signals it receives to guide it through an unfamiliar city."

- Sam Pfaff, PhD

During embryonic development, the nervous system is challenged with an enormous and complex task of transforming from simple cells to a network of neuronal connectivity, with the ability to process sensory information. In other words, the basic physiological function of these cells is to sense and respond to the plethora of intracellular and extracellular inputs it receives, and then process this information into an appropriate and efficient response. This is not an easy feat; rather, it requires the integration of signal transduction pathways, which are organized into quite complex

signaling networks. The nervous system is the most complex system in any living organism. In humans, it consists of between 10-100 million axons, equating to 10-100 trillion synapses integrating signaling information from all types of inputs that function in the wiring of our brains (Benson, Colman, & Huntley, 2001). Therefore, a major question in neuroscience involves addressing, how are axons guided to their targets and how proper circuits are formed?

Throughout development, neurons seek out their respective targets, respond to molecular cues which guide them along the appropriate path and finally determine which cells in their target area to connect with to form functional synapses. Thus, axon guidance and synapse formation are significant neurodevelopmental processes required for establishing functional neuronal circuits. The nervous system is essentially the body's electrical wiring. Like an electrical wire, neurons of the body must make appropriate connections or synapses to make a functional circuit. Neuronal connections are formed by the outgrowth of an axon towards its synaptic target. The axon of a neuron is responsible for transmitting voltage changes from the dendrite to the presynaptic terminal, where it releases neurotransmitters onto the proper postsynaptic neuron or other target. The processes underlying brain wiring and the key molecules involved in controlling neurodevelopment are fundamental to our understanding of normal brain function.

It was once thought that the cellular processes of guidance and synapse formation were mediated by distinct molecular signals. These axon guidance molecules were thought to be responsible for guiding the axon toward its specific target area, while other adhesion or receptor molecules were responsible for specifying synapse formation within

the target area. However, increasing evidence has shown that axon guidance molecules also play an important role in regulating synapse formation, the localization and formation of pre- and post-synaptic machineries. The processes regulating both the formation and modification of synapses will help us to understand how the nervous system develops and responds.

1.1   Phosphorylation and Neurodevelopment

The processes of axon guidance, targeting, and synapse formation, are complicated and highly regulated events that occur at critical periods during the development of the nervous system. This regulation is dependent on sophisticated communication and signaling between cells and their extracellular environment. Research has focused over the past several decades on the molecules required for these processes, focusing on receptors, effectors, modulators, and other structural components. Protein phosphorylation and dephosphorylation are well recognized regulatory mechanisms that are integral in a variety of cellular processes. These cellular events include, but are not limited to, proliferation, differentiation, cell adhesion, and migration (Ariño & Alexander, 2004). Phosphorylation of proteins leads to various conformational changes in the protein, which as a result alters biological function. Furthermore, the regulation and balance between the phosphorylated and dephosphorylated state of proteins, by kinases and phosphatases respectively, is recognized as an important developmental mechanism, especially during neurodevelopment.

Phosphorylation of proteins can occur on serine, threonine or tyrosine residues (Ariño & Alexander, 2004). In particular, phosphorylation of tyrosine residues has been shown to have developmental importance in the nervous system (Ensslen-Craig & Brady-Kalnay, 2005; Van Vactor, 1998). Protein tyrosine kinases, PTKs, are responsible for adding phosphate moieties from ATP to the tyrosine residues of proteins via hydroxyl groups, whereas the removal of phosphate groups from these same proteins is accomplished by protein tyrosine phosphatases, PTPs (Figure 1.1) (Fischer, Charbonneau, & Tonks, 1991). Tyrosine phosphorylation and dephosphorylation are key regulatory events which impact neuronal morphogenesis in a variety of organisms.
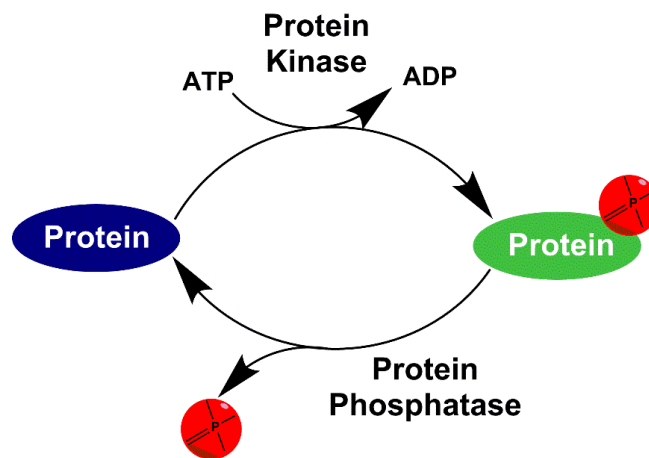
Figure 1.1 The Reversible Process of Protein Phosphorylation and Dephosphorylation.

Adenosine triphosphate (ATP) acts as a donor molecule for kinases which transfer a phosphate group to proteins. This process can be reversed by phosphatases, which remove phosphate groups from proteins.

Phosphorylation has been identified as a critical step in a variety of central nervous system (CNS) processes. Protein tyrosine phosphorylation is a post-translational modification ubiquitously used in biological processes (especially in the nervous system,) and is thought to be involved in the regulation of neuronal function (Bixby, 2001).

4

Furthermore, the tyrosine phosphorylation of proteins has been shown to be important in synapse formation and synaptic plasticity within the peripheral nervous system (PNS); specifically at the neuromuscular junction (Arregui, Balsamo, & Lilien, 2000). The phosphorylation of numerous proteins and molecules is regulated by a balance in activity of both protein kinases and phosphatases. Furthermore, PTKs and PTPs are highly regulated molecules, supporting their role in developmental processes.

1.2   Classification of Protein Tyrosine Phosphatases

Protein tyrosine phosphatases constitute a large enzyme superfamily with hundreds of members (Zinn, 1993). They are conserved from prokaryotes to mammals. All PTP enzymes are single polypeptides with a catalytic domain consisting of approximately 250 amino acids (A. Stoker & Dutta, 1998). Based on their structure and function, PTPs can be grouped into three subfamilies: the "classical" PTPs, the dual-specificity phosphatases (DSPs), and the low molecular weight phosphatases (LMW-PTPs) (Zhang, 1998). Although the PTPs within each subfamily share significant sequence homology, there is very little amino acid sequence similarity exhibited among PTPs of different subfamilies. The common feature that defines the PTP superfamily is the unique active site sequence (I/V)HCxAGxxR(S/T)G in the catalytic domain, also known as the PTP signature motif (Tonks & Neel, 1996). The capital letters in this motif refer to the single-letter amino acid code that is conserved, while the x's refer to any amino acid. The cysteine and arginine of the signature motif are highly conserved. The catalytic domain contains approximately 240 exceedingly conserved residues that share high sequence homology throughout the subfamily (Zhang, 1998). However, the three-

dimensional structure around the active site is highly conserved, despite their lack of homology in their amino acid sequences. The subfamily of the classical PTPs can then be further divided into receptor-like and intracellular (non-receptor) PTPs, primarily based on their cellular localizations (Ariño & Alexander, 2004).

Cytosolic, non-receptor PTPs contain a single highly conserved catalytic domain and as well as a highly variable non-catalytic domain, located at either the amino- or carboxyl-terminus. They contain additional non-catalytic intracellular domains such as Src homology domains, PDZ and PEST motifs (Ariño & Alexander, 2004). These non-catalytic domains of intracellular PTP appear to have regulatory and/or targeting functions, with the net effect of conferring some sort of in vivo substrate specificity among the various PTPs. For example, a carboxyl-terminal hydrophobic region was identified in PTP1B that is both necessary and sufficient to target PTP1B in the endoplasmic reticulum (Frangioni, Beahm, Shifrin, Jost, & Neel, 1992). In fact, a particular family of PTPs, which include PTP-MEG1 and PTPH1, contain non-catalytic domains that show significant homology with the band-4.1 superfamily of cytoskeletal proteins. The band 4.1 domains may actually direct these PTPs to the actin filaments near the plasma membrane (Li & Dixon, 2000). Furthermore, cytosolic phosphatases are grouped into classes based on their PTPase and accessory domain structures (Andersen et al., 2001).

The receptor-like protein tyrosine phosphases (RPTPs) are transmembrane receptors whose structure suggests that they function as an interface between the extracellular environment of a cell and the signaling pathways occurring within a cell. In terms of structure, all known RPTPs are made up of a variable-length extracellular

6

domain, followed by a transmembrane region and a C-terminal catalytic cytoplasmic domain (Fischer et al., 1991). Their extracellular domains are highly variable, but they have the tendency to contain motifs that are implicated in cell adhesion events. Some of the receptor PTPases contain fibronectin type III (FNIII) repeats, immunoglobulin-like (Ig) domains, MAM domains, or carbonic anhydrase-like domains in their extracellular region (Ariño & Alexander, 2004; Beltran & Bixby, 2003). In general, the cytoplasmic region contains two phosphatase domains. Though RPTPs usually possess two intracellular phosphatase domains, there are some members wherein only one domain exists. With few exceptions, the majority of RPTPs are expressed in the nervous system. The tyrosine kinases have been extensively studied, yet still most RPTPs are orphan receptors because their ligands and modes of action remain unknown (Bixby, 2001).

1.2.1   Structural Motifs of Protein Tyrosine Phosphatases

The members of PTP superfamily all contain the PTP signature motif (H/V)CXsR(S/T), in which the cysteine and arginine residues are invariant and catalytically essential (Tonks & Neel, 1996). Although the signature motif is localized to different sites in the three subfamilies of PTPs and there is a general lack of sequence similarity outside the motif, it is interesting that the three-dimensional structures of all PTPs catalytic domains have demonstrated extraordinarily similar structural features (Andersen et al., 2001; Barford, Das, & Egloff, 1998). The phosphate-binding loop – also known as P-loop – as well as the adjacent surface loop contain an essential Aspartic acid residue that are structurally conserved. There is an invariant Cysteine residue sitting at the base of the P-loop that is essential for both the phosphatase activity and formation

of the phosphoenzyme intermediate (Fischer et al., 1991; Tonks & Neel, 1996). Also, an invariant Arginine residue makes hydrogen bonds with the bound oxyanion, which resembles the phosphate group of a phosphotyrosine through its guanidinium group. It is this moiety that is thought to play an important role in substrate binding and stabilization during hydrolysis (Zhang, 1998). Furthermore, structural comparison of the ligand-bound and ligand-free forms of some classical PTPs reveals two different conformations: an "open" and "closed" state (Fauman & Saper, 1996). Ligand binding induces the closure of the surface loop (WPD loop) containing the Aspartic acid residue into the catalytic site. Though these biochemical studies have been carried out for some PTPs, this particular ligand-induced loop closure has not yet been confirmed, though it may be applicable to the entire PTP family (Stewart, Dowd, Keyse, & McDonald, 1999).

The majority of the catalytic activity of PTPs is attributable to the membrane proximal or Cat1 phosphatase domain, while for the majority of PTPs the membrane distal or Cat2 phosphatase domain is hypothesized to bind to downstream regulatory partners (Johnson & Van Vactor, 2003). Not all PTPs contain a second phosphatase; thus it is not at all surprising that the cytoplasmic domains are the most highly conserved domains in all PTP members. In fact, evidence for an accessory function of this second phosphatase domain comes from findings that suggest it does not exhibit any catalytic activity in vivo; however, it was shown that the non-catalytic domain can be converted into a catalytically active phosphatase by mutating two particular amino acids (Ariño & Alexander, 2004). Additionally, there is speculation that the second phosphatase domain requires a cofactor for catalysis.

1.2.2   Receptor Protein Tyrosine Phosphatases (RPTPs)

Receptor protein tyrosine phosphatases (RPTPs) are evolutionary conserved proteins, which are required for nervous system development in both vertebrates and invertebrates (Johnson & Van Vactor, 2003; Van Vactor, 1998). The RPTPs are expressed in high levels in the nervous system, serving key roles in signal transduction, growth, differentiation, cell adhesion, neurite outgrowth, and axon guidance (A. Stoker & Dutta, 1998). Nevertheless, the role of many PTPs in synaptogenesis is limited.

Receptor protein tyrosine phosphatases (RPTPs) are a family of cell surface signal transduction molecules identified approximately two decades ago (Streuli, Krueger, Hall, Schlossman, & Saito, 1988; Streuli, Krueger, Tsai, & Saito, 1989; Tonks, Charbonneau, Diltz, Fischer, & Walsh, 1988). This family of transmembrane proteins is strongly expressed in the nervous system, and is crucial for the formation of functional neuronal circuits (Ensslen-Craig & Brady-Kalnay, 2005; Van Vactor, 1998). Moreover, neural RPTPs are evolutionary conserved from *C. elegans* to humans.

RPTPs have modular ectodomains, which resemble cell adhesion molecules, and intracellular tyrosine phosphatase domains, which antagonize tyrosine kinase signaling. Similar to many cell adhesion molecules – like NCAM, fasciclin II, neuroligin and DSCAM – many of these molecules are defined by their adhesion molecule-like extracellular domains consisting of immunoglobulin (Ig) domains and fibronectin type III (FN III) repeats (Streuli et al., 1988; Streuli et al., 1989). While intracellullarly these RPTPs contain one or two phosphatase (PTP) domains, typically it is the membrane proximal PTP domain that is assumed to contain the majority of the catalytic activity. Like previously described features of PTPs, the membrane distal PTP domain is thought

to have a regulatory role. This non-catalytic phosphatase domain is thought to primarily serve as a binding site for downstream factors or mediate subcellular localization of the RPTP (Serra-Pagès, Streuli, & Medley, 2005; Wallace, Fladd, Batt, & Rotin, 1998; Wills, Bateman, Korey, Comer, & Van Vactor, 1999). Furthermore as a result of their structure, RPTPs are generally considered as axon guidance receptors. In fact, mutants of a variety of RPTPs display a broad range of neurodevelopmental axon guidance defects.

Receptor-like protein tyrosine phosphatases (RPTPs) span the cellular membrane have the potential to transduce extracellular signals via ligand binding which results in activation of their catalytic activity. The receptor-like PTPs (RPTPs) are type 1 transmembrane proteins containing an extracellular domain, a single transmembrane region and a cytoplasmic domain. The heterogeneity of the RPTP extracellular domains (ECDs) and phosphatase domains results in the division of this class into seven distinct subfamilies (Figure 1.2). The intracellular domain (ICD) of RPTP types I, II, IV, V and VI have tandem phosphatase domains, whereas types III and VII phosphatases often have just a single catalytic domain (Fischer et al., 1991; Soulsby & Bennett, 2009). Their division into these distinct subfamilies is primarily based upon the structural motifs in the extracellular domains. The structural motifs include domains resembling immunoglobulin, fibronectin, carbonic anhydrase, MAM (Meprin-Xenopus A2-Mu) domains or cysteine rich regions, suggesting that RPTPs may function in cell-cell or cell-matrix adhesion (den Hertog et al., 1999; Soulsby & Bennett, 2009). The cytoplasmic region of the receptor PTPs contains one or two PTP domains, in which the membrane-proximal PTP domain (Cat1) is responsible for the majority – if not all – of the phosphatase activity. The membrane distal (Cat2) domain of some RPTPs also displays

intrinsic (although weak) phosphatase activity, while the Cat2 domain of others is catalytically inactive. Evidence suggests that the Cat2 domain plays a regulatory role. The Cat2 domain of the CD45 appears to be required for interleukin-2 secretion and substrate recruitment of TCR-£ in vivo (Kashio, Matsumoto, Parker, & Rothstein, 1998). Additionally, it was found that calmodulin might be a specific modulator of PTPα by binding to its Cat2 domain (Liang, Lim, Seow, Ng, & Pallen, 2000). However, the biological significance of the second PTP domain remains largely obscure for many PTPs.

In *Drosophila*, six RPTPs – *Drosophila* LAR (DLAR), PTP69D, PTP99A, PTP10D, PTP52F and PTP4E – have thus far been identified. DLAR and PTP69D are members of the cell adhesion molecule-like type IIa subfamily of RPTPs, whereas the remaining RPTPs in the fly are members of the type III subfamily. The majority of RPTPs in *Drosophila* are expressed in the CNS and are continuing to emerge as important signaling molecules in axons and their growth cones (Johnson & Van Vactor, 2003; A. W. Stoker, 2001).
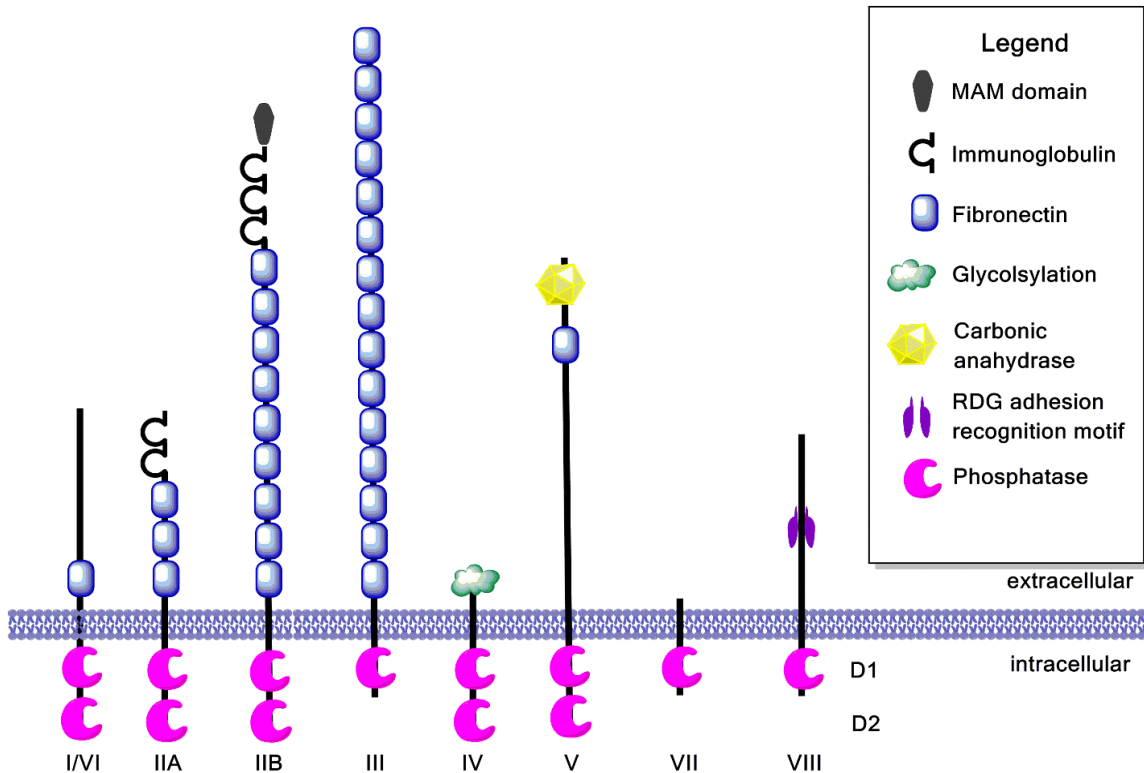
Figure 1.2 The Receptor Protein Tyrosine Phosphatases (RPTP) Family

RPTPs have diverse extracellular structures with fairly conserved intracellular catalytic domains. They are classified into eight specific subfamilies based on their extracellular domain composition. Type I/VI RPTPs contain a single FNIII domain extracellularly and two cytoplasmic phosphatase domains. Type IIa RPTPs have large extracellular domains consisting of immunoglobulin-like (Ig) domains and FNIII domains, while T]type IIb RPTPs have an extracellular meprin-A5-PTP-μ (MAM) domain, Ig domain, and multiple FNIII domains. The type III RPTPs have a series of FNIII domains extracellularly but only have a single cytoplasmic phosphatase domain. Type IV RPTPs have the shortest extracellular domains, which are often heavily glycosylated. The type V RPTPs have an extracellular carbonic anhydrase domain and FNIII domain. Type VII RPTPs have one cytoplasmic phosphatase domain and a short extracellular domain that spans the membrane. Lastly type VIII RPTPs have an extracellular RDG adhesion recognition motif and a single intracellular phosphatase domain which is thought to be catalytically inactive. Several subfamilies are implicated in the regulation of neuronal morphogenesis, these include type IIa, type IIb, type III, and type IV subfamilies. This schematic is generalized for the member of the subfamily and does not reflect the exact structure of each RPTP in the subfamily. (Adapted from (Soulsby & Bennett, 2009)

1.2.3 The RPTP type IIa subfamily

The type IIa subfamily are the most well-characterized family of RPTPs. The founding member of this large RPTP subfamily is LAR (Leukocyte antigen-related protein), thus it is often called the LAR subfamily. Members of this subfamily include *Drosophila* LAR (DLAR) and PTP69D, multiple invertebrate members and three vertebrate homologs. Type IIa RPTPs are initially translated as proproteins of approximately 200 kDa in size, which then undergoes post-translational modifications (Johnson & Van Vactor, 2003).

Members of the type IIa subfamily of RPTPs are characterized by an extracellular domain consisting of Ig-like domains in series with fibronectin type III (FNIII) domains. Thus, type IIa RPTPs are members of the Ig-superfamily and resemble cell adhesion molecules such as NCAM and L1 (Walsh & Doherty, 1997). As a result it is suggested that type IIa RPTPs are involved in the cell adhesion and cell-to-cell signaling in the nervous system. The first support of a role of these RPTPs in CNS development came from studies in *Drosophila*, whereby it was demonstrated that type IIa RPTPs are specifically expressed in the CNS (Tian, Tsoulfas, & Zinn, 1991). Type IIa RPTPs have been shown to have roles in regulating nervous system development (Johnson & Van Vactor, 2003). For instance, *Drosophila* DLAR was shown to exhibit axon pathfinding defects in flies mutant for DLAR (Krueger et al., 1996). Many of these RPTPs have been found to be inactivated by dimerization, whereby reciprocal interaction of domain Cat1 of one dimer pair with Cat2 of the other is believed to systematically cause inhibition (Barr et al., 2009).

Receptor tyrosine phosphatases are not simply scavengers of phosphotyrosine residues; they actually have been implicated in the regulation of a wide range of signaling pathways. In fact, they control diverse processes such as focal adhesion dynamics, cell-cell adhesion and others. While little is known about downstream signaling of type IIa RPTPs, nor many of their substrates, there is evidence suggesting that these RPTPs modify the actin cytoskeleton through interactions with Rho GTPases (Chagnon, Uetani, & Tremblay, 2004). Furthermore, it has been suggested that the catalytic PTP domains of RPTPs may be regulated and temporarily impeded by oxidation (A. W. Stoker, 2005).

1.2.4 Extracellular ligand binding and regulation of RPTPs

The identification of substrates and *in vivo* ligands of RPTPs will be vital to understanding the physiological function of the molecule and development of an accurate model of PTP signal transduction. In fact, most RPTPs remain characterized as orphan receptors because no ligands have yet been identified (A. Stoker, 2005). Thus, identification of their ligands will be critical in understanding their roles in signal transduction cascades and their regulation. At present, two important regulatory mechanisms controlling RPTP activity have been identified.

The first mechanism is regulation of alternative splice variants. The majority of well characterized RPTP mRNAs have been shown to be alternatively processed. In particular, RPTP mRNAs alter exons translated into the juxtamembrane region of the molecule, an intracellular membrane proximal region just prior to the catalytic domain that is critical for the regulation of signal transduction. (Besco, Popesco, Davuluri,

Frostholm, & Rotter, 2004). It is this juxtamembrane region that is thought to be the site of protein interaction between RPTPs and their substrates; therefore it is hypothesized that the function of RPTPs in various signaling cascades is dependent on particular splice variants.

The other regulatory mechanism of RPTPs involves dimerization. While it is known that ligand binding to receptor tyrosine kinases causes dimerization and autophosphorylation of these receptors, the effect of ligand binding on RPTP activity remains unclear. However it is logical to assume that RPTPs could also be regulated by dimerization, whereby inhibition might occur via dephosphorylation of dimer pair. In fact, the "wedge" domain of RPTPs, a cytoplasmic consensus sequence between the transmembrane and phosphatase domains, is predicted to interact with the phosphatase domain of other receptor monomers. It subsequently inhibits the enzymatic activity of the RPTP via this interaction.   There is evidence from some RPTPs that homodimerization may result in negative regulation of phosphatase activity by occluding the active site by juxtaposition of the wedge domain of one monomer onto another (Jiang et al., 1999). This phenomenon was confirmed by biochemical analysis of the type I/VI RPTP CD45 (Majeti, Bilwes, Noel, Hunter, & Weiss, 1998).

1.3   The *Drosophila* Receptor Protein Tyrosine Phosphatase PTP69D

The *Drosophila melanogaster* receptor protein tyrosine phosphatase 69D, abbreviated as PTP69D (or DPTP69D) is one of three *Drosophila* RPTPs recognized as a key player involved in motor axon guidance (C. J. Desai, Gindhart, Goldstein, & Zinn,

1996; C. J. Desai, Krueger, Saito, & Zinn, 1997). It was first identified, along with DLAR, through an examination of the *Drosophila* cDNA library for sequences coding for VHCSAGV, a PTPase domain consensus sequence (Streuli et al., 1989). However, unlike DLAR, PTP69D does not have a vertebrate homologue.

The protein has a 23-aa signal peptide, 782-aa extracellular region, 18-aa transmembrane segment, and 639-aa cytoplasmic domain (Streuli et al., 1989). It was also identified during pull-down experiments to identify target proteins using an anti-Horseradish Peroxidase (α-HRP) antibody, which recognizes carbohydrate epitope on glycoproteins selectively expressed in the insect nervous system (C. J. Desai et al., 1996; C. J. Desai, Popova, & Zinn, 1994). PTP69D, like the previously characterized RPTPs, in the embryo is localized to CNS axons. In third instar larvae, its expression is restricted to subsets of neuronal processes within the brain, eye disc, and the ventral nerve cord. Additionally, in each of the three thoracic ganglia PTP69D is expressed at high levels in the neuropil. Furthermore, in the optic lobes, PTP69D is localized to the lamina and medulla; while, in the eye-antennal disc it is localized to photoreceptor axons of the optic stalk (C. J. Desai et al., 1994). Immunohistochemistry revealed that PTP69D is expressed in the ventral nerve cord (VNC), brain, and eye disc of the fly (C. J. Desai et al., 1994). PTP69D is also an essential gene involved in motor, central and retinal axon guidance, suggesting a pivotal role in nervous system development.

Characteristic of members of type IIa RPTPs, PTP69D is comprised of a large extracellular domain, containing two N-terminal immunoglobulin (Ig) domains and three fibronectin type III (FNIII) repeats, followed by a membrane proximal region (MPR) (Figure 1.3). A proteolytic cleavage site within the MPR was shown to be required for

16

functional cleavage of the PTP69D protein (Garrity et al., 1999). The cytoplasmic tail of PTP69D consists of two phosphatase domains, whereby the membrane-proximal domain has been shown to be crucial for catalytic activity (C. Desai & Purdy, 2003). There are however studies that have shown that the second phosphatase domain may also exhibit catalytic activity (Garrity et al., 1999).
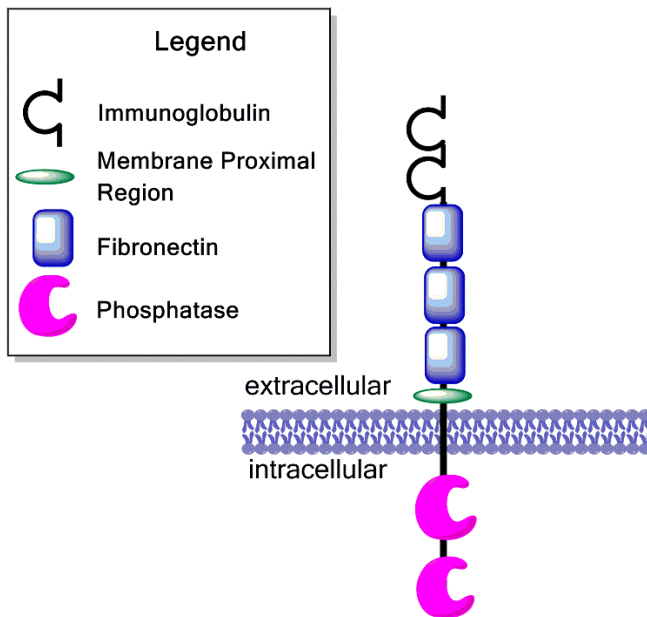
Figure 1.3 Structure of PTP69D

The extracellular domain of PTP69D consists of two immunoglobulin domains (Ig), three fibronectin type III (FNIII) domains, and a membrane proximal (MPR) region. Intracellularly the protein has two cytoplasmic tyrosine phosphatase domains (*Cat*1 and *Cat*2).

1.3.1 PTP69D is required for motor axon guidance

Receptor protein tyrosine phosphatases have emerged as critical regulators of axon growth and guidance. Mutations in PTP69D cause penetrant targeting defects in embryonic motor neurons (C. J. Desai et al., 1996). The receptor tyrosine phosphatases PTP69D and PTP99A are expressed on motor axons in *Drosophila* embryos and are required for motor axon guidance, with partially redundant functions during development of the neuromuscular system. Flies genetically homozygous null for PTP69D typically do not eclose and die as late pupae. Furthermore they exhibit numerous motor neuron guidance defects in SNb and SNa axons (C. J. Desai et al., 1996).

The most well-characterized of these nerves is the SNb, which exits from the CNS with another nerve the ISN (intersegmental nerve) and subsequently splits off from the ISN as both nerves enter the muscle field. The axons of the SNb then defasiculate from the primary nerve at various points to innervate the ventrolateral muscles. In embryos mutant for PTP69D abnormal SNb, morphologies are exhibited ranging from bypass, detour and stall phenotypes. In the bypass phenotype, the majority of the SNb axons are incapable of defasciculating from the intersegmental nerve and innervating the ventrolateral muscle field. Rather in these mutant animals, the SNb axons pass their target and project dorsally within the ISN. Phenotypically these mutants appear denser; this density is the result of their inability to defasciculate plus the contribution of misrouted axons, while in complete bypass phenotypes, the ventrolateral muscles are apparently uninnervated (C. J. Desai et al., 1996).

Another group of axons which have been studied are the SNa axons, which exit the CNS from the SN root and proceed along a distinct course to the distal portion of the ventrolateral muscle field. It then bifurcates and extends one branch to lateral muscles 21-24, and another to muscles 5 and 8. Double mutants of *Ptp69D* and *Ptp99A* exhibit a variety of SNa guidance defects (C. J. Desai et al., 1996). Several phenotypes are exhibited; the most prominent of these defects results when the SNa axons leave the ISN abnormally and stall prior to reaching their targets. A second example of these branching defects results when the SNa axon actually defasciculate into three fascicles rather than just two. In contrast to *Ptp69D* mutants, DLAR knockouts show a more severe phenotype, and die in the late instar stage with target recognition defects in SNb and SNd. When all three phosphatases, DLAR, PTP69D, and DPTP99A, are functionally

knocked out, a much more severe phenotype is seen, suggesting that DLAR and DPTP99A may have similar roles in forming the larval neuromuscular junction (Desai et al., 1997). In this mutant construct, the majority of SNb nerves either defasciculate appropriately and then stall, failing to form their proper muscle synapses, or miss their separation point and continue to grow with the ISN as a fusion bypass.

Mutations of DPTP10D, another *Drosophila* PTP, was studied in combination with the *Drosophila* RPTPs DLAR, PTP69D, and DPTP99A (Sun, Schindelholz, Knirr, Schmid, & Zinn, 2001). DPTP10D was found to work in conjunction with DLAR, PTP69D, and DPTP99A to facilitate the outgrowth and bifurcation of the SNa nerve. In fact, DPTP10D opposes the action of the other 3 RPTPs in regulating extension of the ISN past intermediary targets. These three phosphatases appear to be involved in partially redundant signaling pathways involved in both muscle targeting and fasciculation decisions. Surprisingly, triple mutants did not exhibit a phenotype and the nerves appeared to be unaffected, suggesting a potential pathfinding role for DPTP10D and DPTP4E. It also suggests that a specific combination of phosphatases is required for correct signal transduction. Additionally, this study examined the role of these RPTPs on axons within the CNS and found that all four 4 RPTPs participate in guidance of interneuronal axons within longitudinal tracts of CNS. However, it found that any single mutant lacking either DPTP10D or PTP69D expression exhibits only a mild CNS phenotype, while quadruple mutants lacking all four RPTPs had a severe CNS phenotype. In the CNS of this mutant, most longitudinal pathways become commissural and cross the midline, similar to the phenotype seen in the robo mutants (Sun et al., 2001).

DPTP52F is the most recently discovered RPTP in *Drosophila*. It has an extracellular domain consisting of five fibronectin type III repeats, and one intracellular phosphatase domain. Researchers utilized RNA interference (RNAi) techniques to ablate DPTP52F expression in the CNS (Schindelholz, Knirr, Warrior, & Zinn, 2001). In DPTP52F mutants, the pioneer axons in the longitudinal tracts and the SNa motor axons were selectively affected by ablation. While DLAR/DPTP52F double mutants rescued the phenotype, indicating functionally opposing roles in axon guidance, it appears that that DPTP52F shows partially redundant function with DPTP10D and PTP69D in regulation of growth cone guidance choices of axons within the ISN and SNb motor nerves.

PTP69D was also found to facilitate neurite outgrowth (C. Desai & Purdy, 2003) and along with other RPTPs, such as DLAR and PTP99A, was found to be required for proper motor axon guidance (C. J. Desai, Krueger, et al., 1997). Again using the SNb neuron as a model, it was shown that in double mutants of *Ptp69D* and the related RPTPs, *Dlar* or *Ptp99A*, SNb motor axons fail to defasciculate upon entering their target region. Axon bundling defects are not only restricted to motor neurons. In *Ptp69D* mutants the fasciculated axons of the Bolwig's nerve fail to defasciculate upon approaching their target area. In addition, it was shown to play a role in axon fasciculation and branching in the mushroom bodies (Kurusu & Zinn, 2008).

1.3.2 PTP69D in the Visual System

In the fly visual system, retinal axons from the eye disc send projections through the optic stalk to the optic lobe. In the optic lobe the R1-R6 photoreceptor axons target and terminate in the lamina, while R7 photoreceptor axons target to the medulla (Garrity, 1999). In the development of the *Drosophila* compound eye, PTP69D is required for the axons of the photoreceptors R1-R6 to defasciculate from the R8 axon, which precedes R1-R6 axons into the brain. Axon overshoot or bypass is phenotypic of R1-R6 photoreceptors in *Ptp69D* loss of function mutants. R7 photoreceptor axons, which normally create a distinct layer or demarcation by terminating in the medulla, exhibit a retraction or premature stall phenotype in these same mutants (Newsome, 2000).   The data suggest that PTP69D functions as a defasciculation receptor playing a role in the target layer selection of R7 and R8 axons. Furthermore, transgenic rescue experiments in the retina of *Drosophila* revealed that particular domains of PTP69D were required to rescue the mutant phenotype. Deletion of the extracellular FN III repeats of PTP69D, but not the Ig domains, prevented the rescue of retinal axon targeting defects (Garrity et al., 1999). This finding suggests a role of the FNII repeats in retinal axon targeting in the visual system. Additionally, mutations inactivating the membrane proximal phosphatase domain or deletion of the membrane distal phosphatase domain did not affect the ability to rescue guidance defects. While in contrast, the targeting defects persisted with constructs containing mutations inactivating both phosphatase domains. These results provided evidence that the activity of at least one phosphatase domain is required for proper guidance and targeting in the visual system. In a more recent study, it was shown

that the phosphatase activity of PTP69D was also shown to be involved in R7 targeting to the medulla (Hofmeyer & Treisman, 2009).

From these findings a working model of PTP69D evolves, suggesting that PTP69D is located on the surface of R1-R6 growth cones where it detects a stop signal in the developing lamina plexus and subsequently converts the signal into the shutdown of growth cone motility. The presence of PTP69D on the R1-R6 growth cones suggests that it is capable of responding to the stop signal, because PTP69D overexpression in R7 cells could not induce premature termination of R7 axons in the lamina (Garrity et al., 1999). The study also implies that PTP69D interacts with other R1-R6 specific proteins in order to respond properly to the stop signal, however the identity of the stop signal in the lamina plexus and ligand for PTP69D remains unknown. The generation of *Ptp69D* mosaic mutants in the eye resulted in targeting defects whereby mutant R7 axons failed to reach their targets in the medulla, stopping instead at the same level as the R8 axon (Newsome, Asling, & Dickson, 2000). As a result of the observed phenotype, another working model surfaced in which PTP69D is involved in reducing the adhesion of R1-R7 axons to the pioneer R8 axon. Moreover, R1-R7 axons are able to defasciculate from the R8 axon and respond independently to targeting cues. Thus, two models of the action of PTP69D in the visual system exist, though the chief accuracy of either model remains unclear.

1.3.3 PTP69D signaling

The receptor functions of other RPTPs have been found to be critical for both axon growth and guidance. The phosphatase activity of the *Drosophila* RPTP PTP69D is required for axons to extend out of the mushroom body into the antennal lobes and for proper motor axon guidance (Kurusu & Zinn, 2008). This finding was similar to phenotypes seen in catalytically inactive (D-to-A) *Ptp69*D mutants and in knockout flies (C. Desai & Purdy, 2003; C. J. Desai et al., 1996; C. J. Desai, Krueger, et al., 1997; C. J. Desai, Sun, & Zinn, 1997). The D-to-A mutant exhibited an abnormal phenotype that was similar to those seen in both null- and incomplete-knockdown of PTP69D, as well as a weak missense mutations. This finding was consistent with the view that the defects arising from the catalytically-inactive PTP69D were attributable to the lack of phosphatase activity, and suggests that proper axon guidance is dependent on the receptor function of PTP69D (Kurusu & Zinn, 2008).

These results contribute to the accumulating evidence that RPTP phosphatase activity of PTP69D is important for maintaining proper axonal development. This underscores the necessity of RPTPs as receptors and not just ligands for regulating axon outgrowth. Additionally, it was shown that the kinase activity of Abelson tyrosine kinase (Abl), a substrate downstream of PTP69D along with PTP69D, is necessary for proper formation of the motor nerve (Wills, Bateman, et al., 1999). These along with other findings lend support for a biologically-relevant role for the receptor functions of RPTPs, which may be separate from the RPTP ligand roles, and may have physiological influences in nervous system development. Furthermore, substrates of RPTPs are likely involved in signaling cascades that lead to changes in cytoskeletal dynamics and axon

growth. The Abl and Ena substrates have been reported to play important roles in axon development, and genetic mutation of Abl or Ena was shown to cause motor axon defects in *Drosophila* (Wills, Bateman, et al., 1999; Wills, Marr, Zinn, Goodman, & Van Vactor, 1999). The RPTPs DLAR and PTP69D were found to antagonize the function of Abl and Enabled (Ena), which are known to regulate actin dynamics (Song, Giniger, & Desai, 2008; Wills, Bateman, et al., 1999). Ena Abl were shown to bind to the intracellular domains of PTP69D in vitro, and *Ptp69D* mutants show phenotypic similarity to Ena mutants (Wills, Bateman, et al., 1999). This interrelationship is strengthened by genetic interaction studies which support a functional relationship among PTP69D, Abl, and Ena (Song et al., 2008).

Adding complexity to the signaling potential of PTP69D is evidence that this phosphatase also interacts with Src64B, a src-family kinase (Song et al., 2008). Defects in axon guidance caused by loss of PTP69D function were reversed in flies by a mutation in *Abl,* and exacerbated by a mutation in Src64B (C. J. Desai, Sun, et al., 1997; Song et al., 2008). This is consistent with the idea that Src64B functions in a synergistic manner with PTP69D, while Abl antagonizes it suggesting that Abl and Src64B can thereby mutually antagonize axon guidance instructions delivered by each other. PTP69D can therefore function as a gatekeeper for opposing signals in axon growth and guidance.

"What you need to do is find which is the best system to experimentally solve the problem, and as long as it is general enough you will find the solution there. The choice of an experimental object remains one of the most important things to do in biology and is, I think, one the great ways to do innovative work. The diversity in the living world is so large, and since everything is connected in some way, let's find the best one."

- Dr. Sydney Brenner

1.4   *Drosophila melanogaster* – An ideal Model Organism

The cellular environment of the nervous system is extremely complex and intricate, thus making it particularly challenging to understand the molecular mechanisms mediating neuronal development and connectivity. Therefore, in studying the nervous system it is often advantageous to utilize a model system with a simple circuitry that affords the use of many molecular and genetic tools. Invertebrate systems have thereby historically been studied in place of more complicated systems. *Drosophila melanogaster* is one such model organism. The fly life cycle, from fertilization to adult progeny, is approximately 10 days when reared at a temperature of 25˚C, with conveniently large numbers of progeny being easily produced (Greenspan, 2004). Additionally in the last century a number of powerful forward and reverse genetic tools in the fly have been developed. The genetic and technical tools available when working with *Drosophila* are a great advantage to addressing many biological inquiries. Tools

25

such as tissue-specific drivers, balance chromosomes, and a number of genetic tools greatly ease molecular manipulation of neural circuits.

The segmented body topography of *Drosophila* results in a repeating pattern of highly stereotyped motor neuron trajectories and synapses. Additionally, other axons of the fly, like those in the CNS and visual system, have characteristic morphologies which can be visualized and evaluated. In neurobiology, they serve as suitable model organisms because their neurons can be distinguished morphologically and anatomically, based on their position. This permits the analysis of single cells within the nervous system and the systematic dissection of the complex molecular mechanisms of neurodevelopment. This in turn makes *Drosophila melanogaster* an ideal model organism for the study of axon guidance, targeting and synapse formation.

"The analysis of the neural mechanisms of learning and similar behavioral modifications requires an animal whose behavior is modifiable and whose nervous system is accessible for cellular analysis."

- Dr. Eric R. Kandel

1.5   The Giant Fiber Circuit of *Drosophila melanogaster*

The escape response of *Drosophila* to light-off stimulus is mediated through a simple neuronal circuit called the Giant Fiber Circuit (GFC). The GFC is a simple neuronal circuit that mediates the escape response of the fly, and is characterized by a

jump that is followed by the initiation of the flight (Allen, Drummond, & Moffat, 1998; Allen & Godenschwege, 2010; Allen, Godenschwege, Tanouye, & Phelan, 2006; Trimarchi & Murphey, 1997). This neuronal circuit has been extensively characterized and provides a simple model for studying synapse formation and function. The GF synapse is the largest central synapse in the fly. In fact, it is 10-100 times larger than any other synapse in the fly (Tanouye & Wyman, 1980). The giant fibers are a pair of large bilateral interneurons, approximately 5μm in width, that descend from the brain and terminate in the thoracic ganglion. Due to its size and stereotypic morphology, it serves as an excellent model to examine the cellular and molecular basis of axon guidance, target recognition, and the growth, maturation and formation of synapses in vivo at the single cell resolution anatomically, as well as physiologically. The GFC, in this manner, provides a simple yet elegant circuit through which a number of neurodevelopmental queries can be ascertained.

Anatomically, the giant fibers (GFs) are large bilaterally symmetrical interneurons with cell bodies located in the brain. The main process of the neuron is connected to the cell body via a long neurite. The GF axon projects dorsally and posteriomedially towards the ventral midline into the cervical connective and terminates in the mesothoracic neuromere (King & Wyman, 1980; Tanouye & Wyman, 1980). In the mesothroacic neuromere, or ventral nerve cord, each giant fiber axon makes a prototypic lateral bend. Just prior to this lateral bend each giant fiber electrically synapses with the peripherally synapsing interneuron (PSI). The PSI projects across the ganglion and chemically synapses onto the dorsal longitudinal motorneurons (DLMns,), which innervate the contralateral dorsal longitudinal flight muscles (DLMs) or flight muscles. At the giant

fiber terminal it synapses with the tergotrochanteral motorneuron (TTMn), which innervates the tergotrochanteral or jump (Allen & Murphey, 2007; Blagburn, Alexopoulos, Davies, & Bacon, 1999; Phelan et al., 1996).

The Giant Fiber Circuit is a polysynaptic pathway containing a mixed electrochemical synapse that mediates the *Drosophila* escape response, whereby a fly jumps, then flies away from a visual light-off stimulus (Allen et al., 1998; Trimarchi & Murphey, 1997). Stimuli in the form of sensory input from the visual and antennal centers of the brain is received by the soma of paired giant fibers (GFs) in the brain and relayed to the muscles of the thorax to elicit the escape response. The cell bodies of the two bilateral giant fibers (GF) originating in the brain project a single axon into the thorax of the fly (Figure 1.4). The soma of the GF axons send ipsilateral axonal projections caudally into the second thoracic neuromere of the fly, where they extend lateral projections and form a giant presynaptic terminal onto the Tergotrochanteral Motorneuron (TTMn) (Tanouye & Wyman, 1980). The GF forms a monosynaptic connection with the TTMn; this motor neuron innervates the jump muscle, Tergotrochanteral muscle (TTM), which is involved in escape response. This monosynaptic connection between the GF and TTMn consists of a mixed electrical and chemical synapse, which contain both gap junctions and chemical synaptic machinery (Allen & Murphey, 2007; Blagburn et al., 1999; Phelan et al., 1996). The chemical component of the circuity are cholinergic and glutamatergic (Figure 1.4). Furthermore, in the thorax of the fly the GFs connect outputs through the flight muscle (dorsal longitudinal muscle, DLM) via the PSI (peripheral synapsing interneuron) to the DLMn (dorsal longitudinal motorneuron).
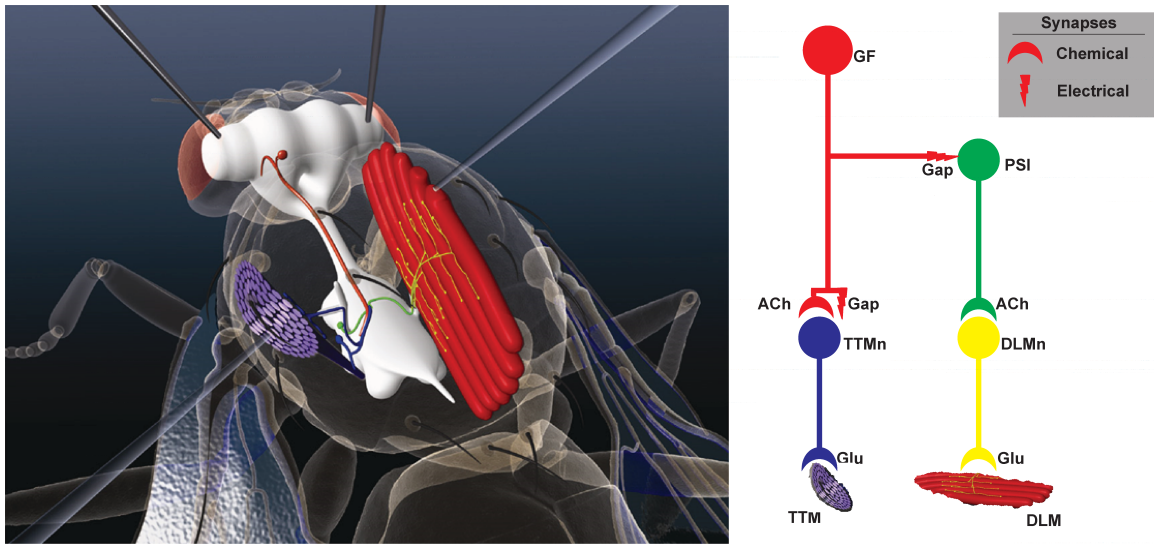
Figure 1.4 Schematic of the Giant Fiber Circuit of *Drosophila*

The Giant Fiber Circuit (GFC) is a simple neuronal circuit mediating the escape response of the fly; it is characterized by a jump followed by the initiation of the flight. The cell bodies of the two bilateral giant fibers (GF) in the brain project a single axon each into the thorax. Here the GFs have outputs to the flight muscle (dorso longitudinal muscle, DLM) and the jump muscle (tergo-trochanteral muscle, TTM). The GF makes an electrical and chemical synapse onto the peripherally synapsing interneuron (PSI, depicted in green). The PSI makes a cholinergic synapse onto the dorsal longitudinal motorneurons (DLMn in yellow) that innervate the flight muscle (DLM). Additionally, the GF through a mixed electrical (Gap) and chemical (acetylcholine, Ach) synapse provides input to the TTMn (tergo-trochanteral motor neuron, depicted in blue, which innervates the TTM. Both the TTMn and the DLMn neuromuscular junctions are of glutamatergic (Glu) nature. (Adapted from (Allen & Godenschwege, 2010)

The development of the Giant Fiber Circuit in the central nervous system (CNS) of *Drosophila* has been well-characterized. During embryogenesis, the cell bodies of the Giant Fibers (GFs) arise and begin their descent into the thoracic neuromere during stage three of larval development. Assembly of constituent parts of the GFs into a functional synapse occurs during pupal development (PD), and includes axon pathfinding, leading to the formation of mature synapses in the thorax (Allen et al., 1998; Jacobs, Todman, Allen, Davies, & Bacon, 2000; Murphey et al., 2003; Phelan et al., 1996) (Figure 1.5). Growth of the TTMn dendrites toward the target area in the second thoracic neuromere

occurs prior to the arrival of the GF axons from the brain into this region. The GFs finally reach the target area and make their initial contact with the TTMn dendrites at 20% PD. This is followed by a phase of synaptogenesis (25-50% of PD), during which each GF makes initial contact with its respective TTMn at around 40% of PD and create a lateral "bend" establishing a presynaptic terminal (Allen et al., 1998; Jacobs et al., 2000; Murphey et al., 2003; Phelan et al., 1996). After 50% of PD, the synapse continues to grow and stabilize to become a fully mature synapse by the time of eclosion.

A number of tools can be exploited to examine the mechanisms at a central synapse. Electrophysiological recordings, transgenic expression of reporter genes, and injections of photosensitive dyes into the neurons allow the assessment of the function of the GF circuit, as well as the anatomy of the individual neurons. In assessing synapse function, the time delay between stimulation and response (response latency) can be used as a measure of the strength and speed of the circuit. Additionally, the ability of the circuit to follow multiple stimuli at higher frequencies is used as a measure of refraction period and reliability of the synapses in the GF circuit. Lastly, the actual structure of the synapse can be assessed using various imaging tools.
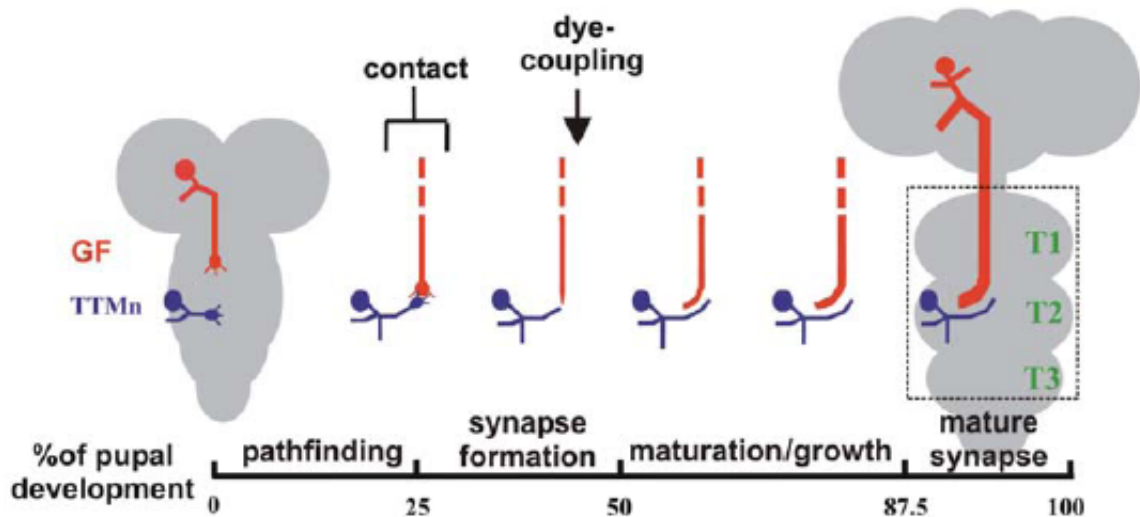
Figure 1.5 The timing of events involved in the development of the giant fiber

During late larval stages (not shown) the Giant Fibers (GFs) begin their decent from the brain into the ventral nerve cord (VNC). The TTMn dendrites grow toward the target area in the second thoracic neuromere prior to the arrival of GF axons. The GF growth cone reaches the target area to make initial contact with the TTMn dendrite by 20% of pupal development (PD). Following pathfinding is the phase of synapse formation (25-50% of PD) during which the GF dye couples with the TTMn at around 40% of PD and forms a lateral "bend" and establishes a presynaptic terminal (Allen et al., 1998; Jacobs et al., 2000; Phelan et al., 1996). After 50% of PD, the synapse continues to grow and stabilize, becoming a fully mature synapse by the time the fly of ecloses from its pupal case. (Adapted from (Murphey et al., 2003)

1.6   The Gal4-UAS System

In *Drosophila* there are a number of unique gene expression systems that have been used for both genetic screen and candidate gene studies. These powerful genetic tools can be used with *Drosophila* to study genes and their interactions in loss and gain of function backgrounds with spatial and temporal control. One of the most utilized systems in this process is the bipartite UAS-Gal4 system used for studying the expression of genes (Brand & Perrimon, 1993). This system consists of two parts: one that contains a gene of interest linked to an Upstream Activation Sequence (UAS), while the second

31

contains GAL4, a yeast *S. cerevisiae* transcription factor. The technique is based on the

Gal4 yeast protein which functions in a transactivator capacity. The system separates a

target gene from its transcriptional activator in two distinct transgenic lines (Perrimon,

1998). The UAS is the DNA binding site for GAL4. The binding of the GAL4 to the

UAS results in the transcription of the gene of interest in an expression pattern defined by

the GAL4 (Figure 1.6). More specifically, it employs the use of transgenic lines,

whereby a fly line has a target gene that remains silent in the absence of an activator. In a

separate fly line the activator protein is present but has no target gene to activate it. It is

only when the two flies are crossed together that the target gene turned on in the resulting

progeny that functional consequences of a mutation can be delineated, spatially in a tissue

specific manner as well as temporally.
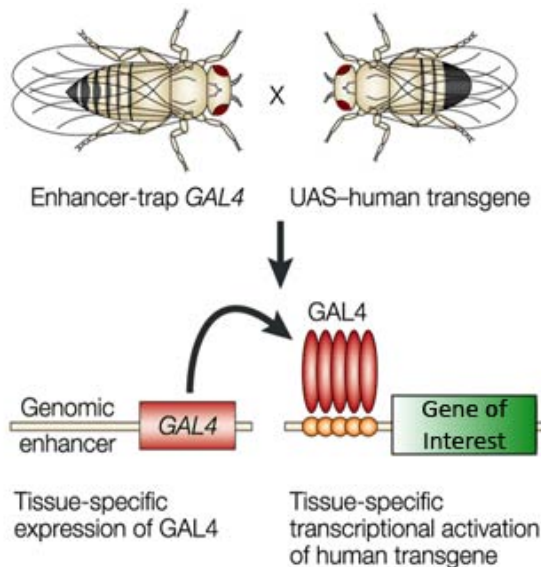
Figure 1.6 The Gal4-UAS System

Two transgenic lines (pattern and target) are crossed. The Pattern line has a tissue specific enhancer or promoter that is used to activate the yeast transcriptional activator Gal4 in a particular pattern. Likewise, the Target line has a Gal4-responsive element called the upstream activating sequence (UAS) that precedes PTP69D, our gene of interest. When the "pattern line" is crossed to the UAS "target line" then the gene of interest is turned on. Modified from (Muqit & Feany, 2002)

There is a large armory of GAL4 lines available in the *Drosophila* research

community, each restricting the UAS transgene to a specific tissue at a particular time

during development. Relevant to this dissertation are six Gal4 driver lines – A307, c17,

ShakB, R78G07, R91H05 and Elav, the first five of whom drive expression in the GFS and the last which drives pan-neuronal expression. The A307 driver has strong presynaptic expression in the GF with weaker expression in postsynaptic targets (Allen et al. 1998). The c17 Gal4-driver, which drives expression in the GF, but not in its target neurons, and the ShakB-Gal4 line, which only drives expression in the postsynaptic target neurons of the GF were described previously (Godenschwege et al., 2002b; Jacobs et al., 2000). The R78G07 and R91H05 lines were identified in a screen of the Janelia Farm Gal4-lines, available from Bloomington, as drivers that express selectively in the GF, but not its postsynaptic target neurons (Jenett et al., 2012; Pfeiffer et al., 2008). Expression of these Gal4 lines in the GF is already present in L3 larval stage during axon outgrowth and is strongly maintained in the adult. The last driver, Elav drives the expression of genes pan-neuronally (both in the central and peripheral nervous systems) during late embryogenesis (Campos, Rosen, Robinow, & White, 1987).

Table 1.1 Expression of GF and Neuronal Gal4 Drivers.	
A307	Pre- and Post-synaptic; in the GF and TTMn throughout development and in adult
c17	Presynaptic; in the GF after it has exited the brain and entered the thoracic ganglion during early pupal stages
Elav	Pan-neuronal expression (PNS and CNS)
R78G07	Presynaptic; in the GF during neurite outgrowth in larvae (L3)
R91H05	Presynaptic; in the GF during neurite outgrowth in larvae (L3)
ShakB	Postsynaptic; in the TTMn but not the GF throughout development and in adult

1.7   Giant Fiber Electrophysiology

The function, or transmission, of the involved synapses can be tested by intracellular, sharp-electrode electrophysiological recordings from the corresponding output muscles: the jump (tergotrochanteral, TTM) muscle and flight (dorsal longitudinal muscle, or DLM) muscle. The GF-TTMn synapse, in particular, is evaluated using two criteria: its response latency and its ability to follow high frequency stimulation (Tanouye & Wyman, 1980). The GFs are stimulated with two tungsten stimulations in the brain, and responses are recorded from the jump muscle (TTM) and the flight muscle (DLM) (Allen & Godenschwege, 2010) (Figure 1.4 & 1.7). Wild type TTM and DLM response latencies are 0.8-1ms and 1.2-1.6ms, respectively. The GF to TTM pathway can follow high frequency stimulation one to one up to 300Hz, the GF to DLM pathway only follows at 100Hz. In mutants, responses are usually either absent or the response late ncy is increased; additionally the ability to follow stimuli at high frequencies is decreased. Thoracic stimulation bypasses the GF and directly activates the TTMn and DLMn motorneurons allowing testing for the presence of potential neuromuscular junction (NMJ) defects.

1.8   Giant Fiber Neuroanatomical Analyses

In addition to circuit function, the GF morphology can be addressed in the very same specimen with reporter gene expression (e.g. Green fluorescent protein, GFP), or with injections of dye into the GF axons (Boerner & Godenschwege, 2010, 2011; Phelan et al., 1996). Large fluorescent dyes like Rhodamine-Dextran and Alexa Fluor® Dyes

remain in the GF, allowing for the assessment of that the neuron morphology. In

contrast, small dyes and molecules, like Lucifer Yellow and Neurobiotin, are able to pass

through gap junctions and label the PSI and TTMn (Figure 1.7). Dye-coupling between

the GF and its postsynaptic target neurons can be used to demonstrate the presence of an

electrical synapse in mutants GF terminals.
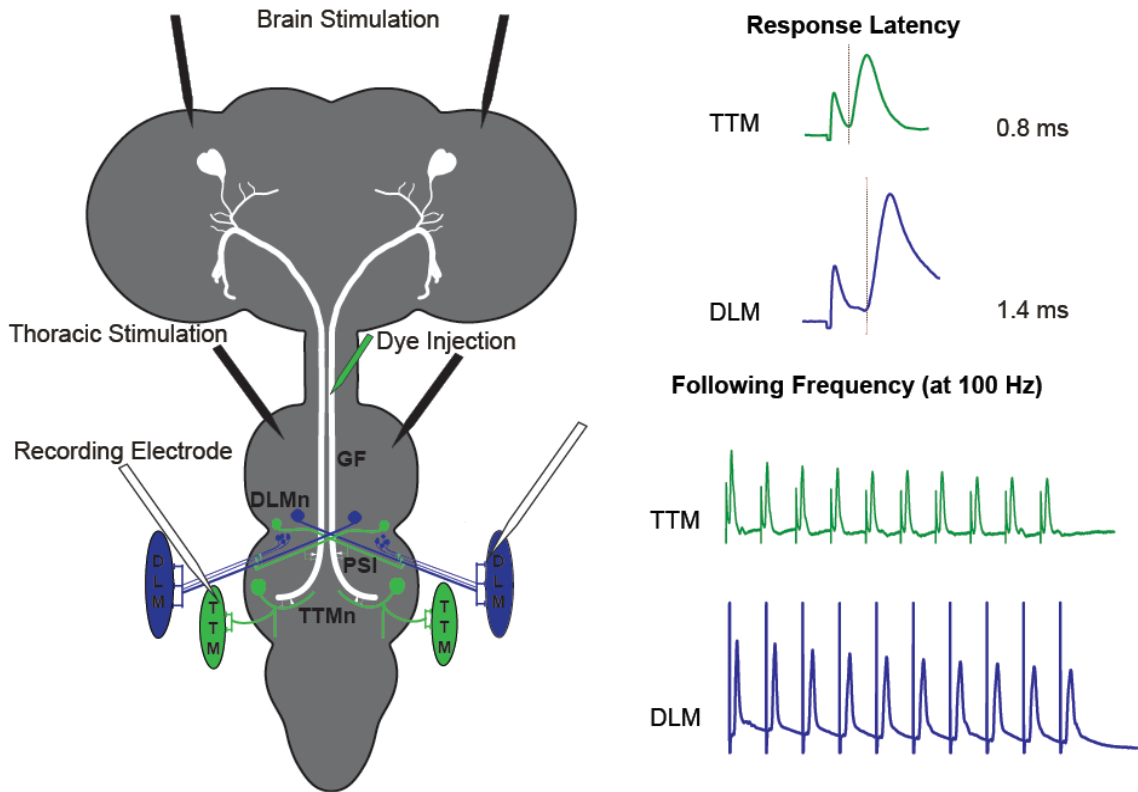
Figure 1.7 Schematic of Electrophysiology and Anatomy of the Giant Fiber Circuit

The image shows giant fiber (GF) circuitry in color as it will be seen in subsequent
confocal images. The GF (white) has its soma and dendrites in the brain and its axons
enter the second thoracic neuromere to make synaptic connections with the Peripheral
Synapsing Interneuron (PSI, green) and the Tergotrochanteral Motorneuron (TTMn,
green). The PSI synapses onto the Dorsal Longitudinal Motorneuron (DLMn, blue). The
TTMn and the DLMn innervate the jump (TTM) and flight (DLM) muscles respectively.
Electrodes (stimulating, depicted in black) seen in the brain are placed in the eyes to
stimulate the GFs, while recording electrodes (depicted in white) placed in the outputs,
the TTM and DLM respectively. Also shown in the schematic are the stimulus (black
electrodes in the thoracic region) and recording arrangement to obtain responses from the
muscle. The recording from the GF circuitry is depicted, and we obtain recordings from
the muscle on both sides. Primary recordings are taken from the TTM, with recordings

from the DLM taken to verify that the GF has indeed reached the target area. Representative recordings from a wild type specimen are shown, whereby via brain stimulation the TTM response latency is 0.8 ms and the pathway is able to follow 1:1 at 100 Hz and 200 Hz (not shown). The DLM pathway has a latency of 1.4 ms and also follows 1:1 at 100Hz, however it fails at 200Hz (traces not shown). Also depicted is placement of electrodes for thoracic stimulation, whereby the GF can be bypassed and the motor neurons are directly stimulated. The NMJ recordings for the TTMn-TTM connection and the DLMn-DLM connection are 0.6 ms and 0.7 ms respectively and can both follow 1:1 at high frequency stimulation (traces not shown).

2   PTP69D: A NEURAL RECEPTOR PROTEIN TYROSINE PHOSPHATASE REQUIRED FOR AXON GUIDANCE AND SYNAPSE FORMATION IN THE ADULT CNS

2.1   Abstract

PTP69D is a receptor protein tyrosine phosphatase (RPTP) which has been shown to play a role in axon outgrowth and guidance of embryonic motorneurons. In addition, PTP69D has a role in targeting photoreceptor neurons in the visual system of *Drosophila melanogaster*. Mutations in the PTP69D result in a broad spectrum of phenotypes ranging from stall, bypass, and detour of the motor axons or photoreceptors. Here, we examine a potential developmental role of PTP69D in the giant fiber (GF) neurons; the GFs are two interneurons in the central nervous system (CNS) that control the escape response of the fly. In addition to guidance and targeting functions, our studies reveal an additional role for PTP69D in synaptic terminal growth in the CNS. Cell autonomous knockdown experiments with RNA interference demonstrated a function for PTP69D in the GFs, but not in the postsynaptic target neurons. Tissue-specific RNAi-mediated knockdown in the Giant Fiber circuit revealed that it can cause the premature termination or stalling of axons in the *Drosophila* giant fiber system. RNAi knockdown of PTP69D reveals a requirement for this protein in the formation of synapses within the Giant Fiber circuit.

"What's really terrific about RNAi is that once it's inside the cell, it enters very

efficiently into the cellular machinery."

- Craig C. Mello, PhD

2.2   Background

The receptor tyrosine phosphatase PTP69D is expressed on motor axons in *Drosophila* embryos. In PTP69D null or mutant embryos the growth cones of the motor neurons either stop growing before reaching their muscle targets or bypass their target muscles, following incorrect pathways (C. J. Desai et al., 1996). *Ptp69D* mutant embryos display a variety of abnormal SNb morphologies, including bypass, detour, and stall SNb phenotypes. In the bypass phenotype, some or all of the SNb axons fail to defasciculate from the intersegmental nerve (ISN), entering the ventrolateral muscle field, where they continue to extend dorsally within the ISN. As a result, the ISN often appears thicker than normal because of the addition of the misrouted SNb axons. On the other hand, in the complete bypass mutant phenotype the ventrolateral muscles are apparently uninnervated (C. J. Desai et al., 1996). PTP69D antagonizes Abl tyrosine kinase to guide axons in *Drosophila* (Song et al., 2008). Furthermore, a mutation of the gene encoding the cytoplasmic Src64B tyrosine kinase exacerbates *Ptp69D* mutant phenotypes, suggesting that two different cytoplasmic tyrosine kinases, Abl and Src64B, modify PTP69D-mediated axon patterning in quite different ways.

In the optic lobes, PTP69D is localized to the neuropils of the lamina and medulla, as well as an array of parallel thick bundles in the developing lobula complex (C. J. Desai et al., 1994). PTP69D was found to promote R1-R6 targeting in response to

extracellular signals by dephosphorylating an unknown substrate or substrates in R1-R6 growth cones (Garrity et al., 1999). The absence of PTP69D in photoreceptors occasionally leads to their projection into the medulla. It is required for the correct targeting of R7 axons into the M6 layer of the medulla, however in its absence R7 axons terminate like R8 axons into the M3 layer. Thus, it has been suggested that PTP69D plays a permissive role in R1-R6 and R7 axonal targeting by helping to defasciculate from the leading R8 axon.

Classical genetic screens have generated various mutations that affect the embryonic central nervous system (CNS), peripheral nervous system (PNS) and visual system, revealing that PTP69D is involved in neuron development and axon pathfinding. Several of these mutations however often result in lethality at later developmental timepoints. In fact, it is an essential gene required in the nervous system during periods of axon guidance and targeting and animals null for PTP69D exhibit lethality, typically not surviving past the larval stage (C. J. Desai et al., 1996). Thus, determining whether PTP69D is required for the establishment of adult neural circuits is more problematic. In order to examine the *Ptp69D* loss of function mutations in adults, other methods must be employed. RNA interference (RNAi) is a powerful technique whereby small double-stranded RNA (dsRNA) fragments can be used to investigate the role of a gene by preventing gene function and observe what effect, if any, this has on the organism's phenotype.

Gene silencing methods can provide valuable approaches to functional analysis of genes. Using double-stranded RNA as a target for inducing gene-specific silencing is a powerful tool for obtaining targeted disruption of a given genes function. Utilizing RNAi

39

methods overcomes the need to generate a series of mutants, while providing evidence for a genes function in various physiological and morphological events. In order to have efficient induction of RNAi in *Drosophila,* the initiating RNA must be double-stranded and be several hundred nucleotides in length (Sharp, 1999). The introduction of dsRNA can be accomplished by injection of dsRNA corresponding to a single gene into an organism, but this injection only interferes with gene expression transiently and is not stably inherited. Therefore, use of RNAi to study gene function in the late stages of development was previously limited. This problem was circumvented in *Drosophila* through the development of a method to express dsRNA as a hairpin-loop (hpRNA) using the Gal-UAS system (Brand & Perrimon, 1993) (Figure 2.1). This hpRNA is a transgenically expressed inverted repeat or palindromic sequence that can be controlled spatially and temporally, thereby enabling the study of gene function late in *Drosophila* development (Kennerdell & Carthew, 2000).
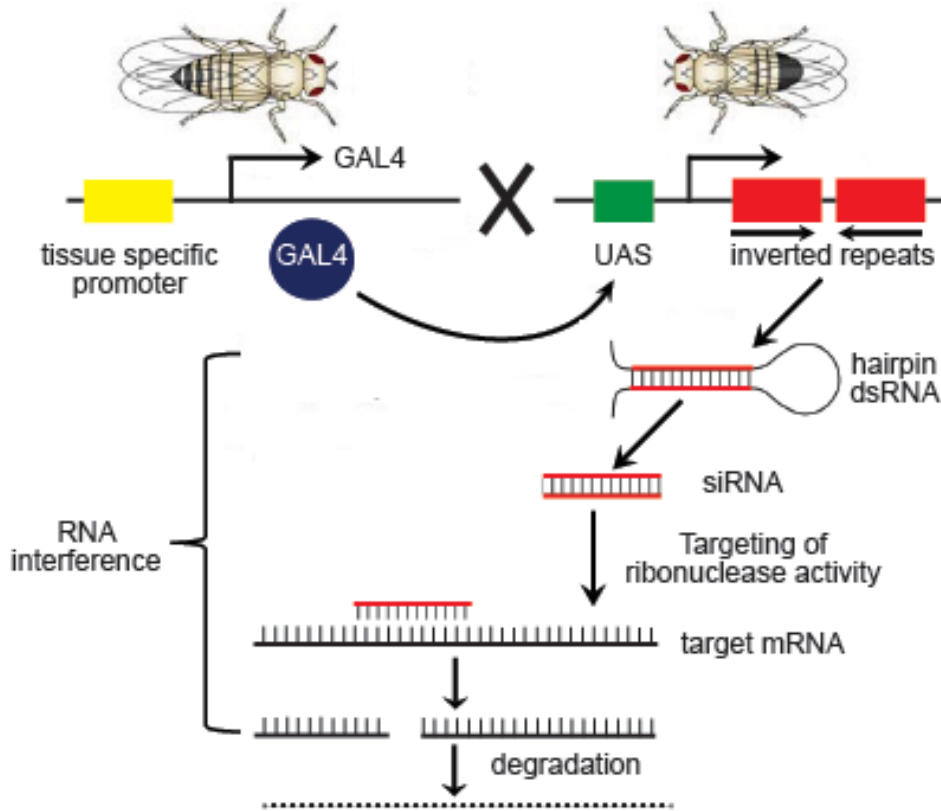
Figure 2.1 Heritable and inducible transgenic RNAi knockdown in *Drosophila*

Two transgenic fly lines—GAL4 driver and UAS-IR—are used in this heritable and inducible RNAi system. The GAL4 driver fly has a transgene containing the yeast transcriptional factor GAL4; GAL4 expression is controlled by a tissue-specific promoter. The UAS-IR fly has a transgene containing an inverted repeat (IR) of the target gene that is ligated to the UAS, a target of GAL4. The GAL4/UAS system induces gene silencing by driving expression of hairpin RNA (hpRNA), then these dsRNAs are processed by Dicer into small interfering RNAs (siRNAs) which degrade endogenous target mRNA in a tissue-specific manner. Figure adapted from http://stockcenter.vdrc.at/control/rnailibrary

2.3   Materials and Methods

2.3.1   Flystocks and expression patterns

The following Flystocks were obtained from Bloomington stock center unless otherwise indicated. The wild type control (w^{1118}) stock served as a control. The *UAS-Ptp69D RNAi* (RNA interference) lines (ID104761, ID27061, ID40631) were acquired

41

from the Vienna *Drosophila* RNAi Center (Dietzl et al., 2007). The A307 Gal4 driver line expresses in the GF and its postsynaptic target neurons, the TTMn and the peripherally synapsing interneuron (PSI) (Allen et al., 1998; Phelan et al., 1996). The c17 and c422 Gal4-drivers drive expression in the GF, but not in its target neurons. The c422 Gal4 driver turns on expression in the second half of pupal development (PD) during giant synapse maturation, but not during GF guidance or initial synapse formation. The c17 Gal4 driver only turns on expression in the GF once it exited the brain and entered the thoracic ganglion during early pupal stages. The *ShakB* Gal4-driver drives expression in the postsynaptic target neurons of the GF but not the GF (Allen et al., 1999; Godenschwege et al., 2002b; Jacobs et al., 2000). The R78G07 and R91H05 lines of the Janelia Farm Flylight Gal4 line collection (Jenett et al., 2012; Pfeiffer et al., 2008) were characterized by our lab in the GFS; they were found to express selectively in the GF but not its postsynaptic target neurons. Expression of these Gal4 lines in the GF is already present in L3 larval stage during axon outgrowth and maintain strong expression in the adult. The driver Elav Gal4 drives expression throughout the nervous system in both the CNS and PNS. All genetic crosses were performed on standard fly media at 25°C and 2-5 day old flies were used in all of the experiments.

2.3.2 Electrical stimulation of GF neurons and analysis of muscle potentials

The method of obtaining electrophysiological recordings from the GFC has previously been described in detail (Allen & Godenschwege, 2010). In brief, the GFs were stimulated (Grass instruments S48 stimulator) with pulses (0.03 ms, 50 V) in the brain using a pair of tungsten electrodes. Glass electrodes (resistances of 40-60 MΩ)

filled with saline were used for recordings from the tergotrochanteral muscles (TTM) and dorsal longitudinal muscles (DLM). The responses were amplified (Microelectrode amplifier Model 5a, Getting Instruments) and the traces were recorded, stored and analyzed using pClamp 10 software (Molecular Devices). To determine the response latencies (RL), ten individual stimuli were given with a five second interval between the stimuli and the shortest RL of each fly was averaged for each genotype. The following frequency (FF) was determined and represents the number of responses in percent of ten trains of ten stimuli at 100 Hz, recorded with a two second interval between the trains. In mutant animals that had a reduced ability to follow stimuli at 100 HZ, we directly stimulated the motorneurons in the thorax to confirm that functional defects were not at the neuromuscular junction but instead at the GF to TTMn (GF-TTMn) connections. Data analysis and Student's t tests were used to determine statistical significance (SigmaPlot 12).

2.3.3 Dye injections and immunohistochemistry of the GFC

Dye injection and immunohistochemistry methods have previously been described in detail (Boerner & Godenschwege, 2010, 2011). In brief, the dissected animal's CNS was mounted dorsal side up on Polylysine coated slides or VECTABOND™ (Vector Labs) coated 0.9-1.1 mm etched slides. A glass electrode (80-100 MΩ) filled or a dye solution of 10% w/v neurobiotin (Vector Labs) and tetramethyl rhodamine-labeled dextran (Invitrogen) backfilled with 2 M potassium acetate was used to inject the dyes into the GF axons by passing depolarizing current. Samples fixed in 4% paraformaldehyde were prepared for confocal microcopy as previously described.

Anti-DPTP69D MAb 3F11 supernatant made in mouse (Developmental Studies Hybridoma Bank) was diluted [1:100] in PBS containing 0.3% TritonX-100 and 2% bovine serum albumin (BSA, Sigma). Following antibody incubation for 2 nights at 4°C, samples were rinsed in PBS with shaking. For detection of PTP69D (MAb), a goat anti-mouse secondary antibody coupled to the Cy2 fluorophore and dyelight 649 against Neurobiotin was used. The secondary antibodies were incubated overnight in PBS at 4°C. The following antibodies were used to visualize the GFs: streptavidine-Cy2 conjugate (Jackson ImmunoResearch; 1:750), anti-GFP A11122 (Invitrogen, 1:500), goat anti-rabbit-Cy2 (Jackson ImmunoResearch, 1:500 dilution) to visualize neurobiotin or GFP. Samples were scanned at a resolution of 1024x1024 pixels, 2.5x zoom, and 0.5 μm step size with a Nikon C1si Fast Spectral Confocal system, using a 60× oil immersion objective lens. Images were processed using Nikon Elements Advance Research 4.0 and Adobe Photosuite CS4 software.

2.4   Results

2.4.1   *PTP69D* is expressed in the adult CNS

The first evidence supporting for a role of RPTPs in CNS development came from studies in *Drosophila*, whereby it was demonstrated that type IIa RPTPs are specifically expressed in the CNS (Tian et al., 1991). More specifically, Type IIa RPTPs, PTP69D and DLAR, have been found to be expressed exclusively in the nervous system and a subset of axons in the CNS. They have been shown to have roles in regulating nervous system development (Johnson & Van Vactor, 2003). These earlier expression studies were conducted in embryos and larvae, however immunohistochemistry to determine the

expression of PTP69D in the adult has yet to be conducted (C. Desai & Purdy, 2003; Garrity et al., 1999). PTPT69D is first present in the germ band extended embryos (stages 9-10). Staining of the axons is first observed at the onset of germ band retraction in embryos. Following this developmental time point the staining becomes primarily localized to CNS axons. In third instar larvae, its expression is restricted to only a subset of neuronal processes in the brain, ventral nerve cord, and eye disc, as well as in the neuropil. .In each of the three thoracic ganglia, PTP69D is expressed at high levels in the neuropil. Additionally, PTP69D has been found to be localized in the posterior ventral nerve cord at the A8 abdominal ganglion.

To determine the expression pattern in adult we examined PTP69D expression in the adult nervous system using whole mount preparations of the brain and ventral nerve cords of wild type animals. The CNS of adult animals was stained with anti-DPTP69D mAb 3F11 (C. J. Desai et al., 1996; C. J. Desai et al., 1994). Diffuse staining was observed throughout the entire CNS, confirming that PTP69D is a neural RPTP expressed in the adult CNS (Figure 2.2). The GFs were dye filled with Dextran and Neurobiotin, co-staining with a monoclonal antibody directed against PTP69D indicates that PTP69D is also present in the GF axons.
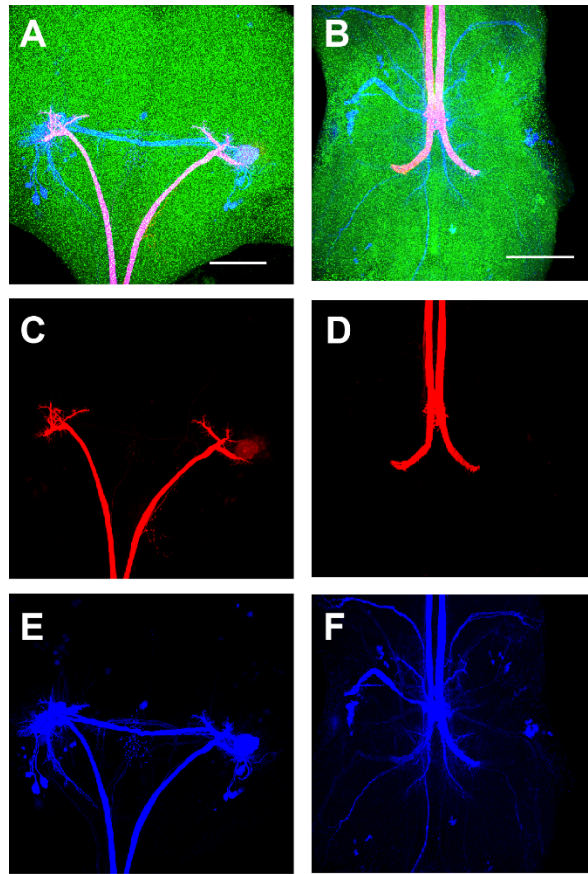
Figure 2.2 Expression of PTP69D in the Adult CNS

Monoclonal antibody staining of PTP69D with 3F11 directed against PTP69D indicates that the phosphatase is expressed in the adult CNS, both in the brain (A) and the ventral nerve cord (B). Dyefills with Rhodamine Dextran (C and D) and Neurobiotin (E and F) show overlap with PTP69D staining. Thus, indicating that PTP69D is present in the GF axons in addition to diffuse staining throughout the nervous system.

2.4.2 Knockdown of PTP69D in the giant fiber system causes aberrant GF morphology

Ptp69D null mutants exhibit lethality and typically do not survive past the larval stage (C. J. Desai et al., 1996). In order to examine the role of PTP69D in later developmental time points, three different *UAS-PTP69D RNAi* lines in the Giant Fiber

Circuit were expressed using the A307 Gal4 line to knock down PTP69D pre- and post-synaptically. To assess the morphology of the GFs and its ability to dye-couple with its postsynaptic target neurons, a mixture of Rhodamine-dextran and neurobiotin was injected into each of the bilateral GFs (Boerner & Godenschwege, 2011; Phelan et al., 1996).

In wild-type animals the GFs projecting from the brain through the cervical connective to the second thoracic ganglia, where it makes a lateral bend and terminates making a synaptic connection with the TTMn (Figure 2.3A) (Blagburn et al., 1999; Thomas & Wyman, 1982). In PTP69D knockdown animals however, the majority of the GFs lacked their characteristic bend in the second thoracic neuromere, and their axons had stunted terminals (Figure 2.3 B-D, upper dextran panel).

In wild type animals, dye coupling between the GF and its postsynaptic target neurons could be observed reliably (Figure 2.3, bottom left image). In P*tp69D RNAi* knockdown animals the GFs strongly dye-coupled with PSI in all cases. However, despite the severely stunted GF terminals, most (90%) GFs of PTP RNA mutants remained dye-coupled to the TTMn albeit severely weakened (Figure 2.3 B-D, middle neurobiotin panel). This suggests that PTP69D is required for GF terminal growth.
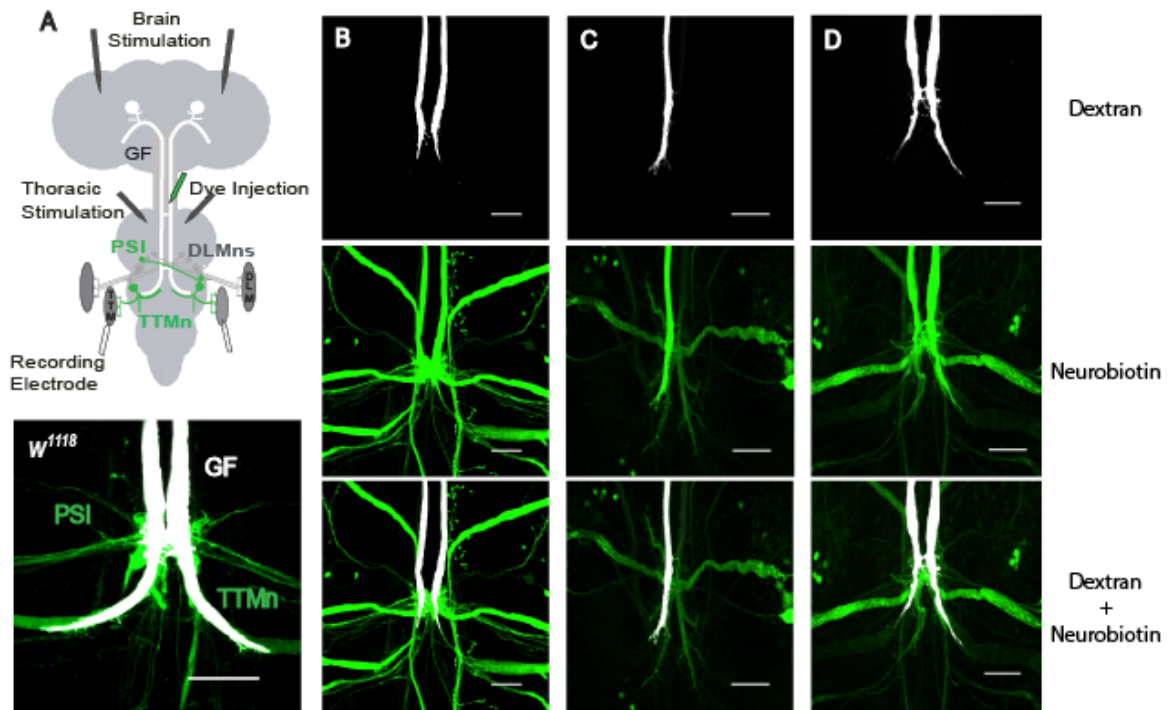
Figure 2.3 Expression of *Ptp69D RNAi* disrupts GF morphology

Whole-mount preparations of the CNS from UAS-Ptp69D RNAi A307 adult flies. Dye fills with Dextran into the GFs make it to the target area but lack their characteristic bend. The preparations are capable of dye coupling as evidence by Neurobiotin staining. Scale bar, 20 μm

2.4.3 PTP69D knockdown disrupts giant fiber function

To assess synaptic function, electrophysiological recordings from the GFC were examined to characterize the response latency and following frequency of mutant and control animals. In control flies, containing the P[GAL4] element or the *UAS Ptp69D RNAi* construct alone, the stereotypical wild type responses were observed (Tanouye & Wyman, 1980). The TTM response latencies were less than 1 msec and the following frequencies at 100Hz were around 96% at 100 Hz (Table 2.1, Figure 2.4). The DLM responses showed the characteristically longer response latencies (~1.3 msec) and the

ability of the GF to DLM pathway to follow stimuli at 100Hz was 94% (Table 2.1). In *Ptp69D RNAi* animals the GF–TTMn connection was abnormal. The TTM response latency was nearly doubled, and repetitive stimulation resulted in either TTM response failures at 100 Hz or no responses being recorded, suggesting a GF disconnect with its post-synaptic target (Table 2.1, Figure 2.4). However, direct stimulation of the motorneurons in the thoracic ganglia in the same preparations resulted in normal muscle responses, which were able to follow stimuli at 100Hz. This suggests that the TTMn neuromuscular junctions (NMJ) were intact and the defect was at the GF to TTMn connection. In contrast, GF to DLM pathway was not significantly different from control animals (Table 2.1, Figure 2.4). Finally, while the majority of *Ptp69D RNAi* mutants were responsive, in some animals no recordings could be obtained from either the TTM or DLM upon brain stimulation although thoracic stimulation revealed normal NMJs (Table 2.1, Figure 2.4). This suggests that PTP69D knockdown may also disrupt axon guidance in addition to GF terminal growth.

Table 2.1 Synaptic function in wild-type and PTP69D RNAi animals

| Genotype | n | TTM | | | DLM | | |
		Latency in msec (±SE)	Following Frequency 100Hz (±SE)	Dis-connected	Latency in msec (±SE)	Following Frequency 100Hz (±SE)	Dis-connected
Control	10	0.917 (±0.11)	95% (±1%)	0%	1.225 (±0.029)	94% (±2%)	0%
A307; 104761 PTP69D RNAi	46	1.964 (±0.114)	16% (±4%)	22%	1.359 (±0.076)	74% (±6%)	11%
A307; 27091 PTP69D RNAi	26	1.648 (±0.112)	20% (±4%)	0%	1.370 (±0.114)	82% (±6%)	0%
A307/40631 PTP69D RNAi	30	1.595 (±0.076)	22% (±4%)	0%	1.211 (±0.043)	86% (±5%)	0%
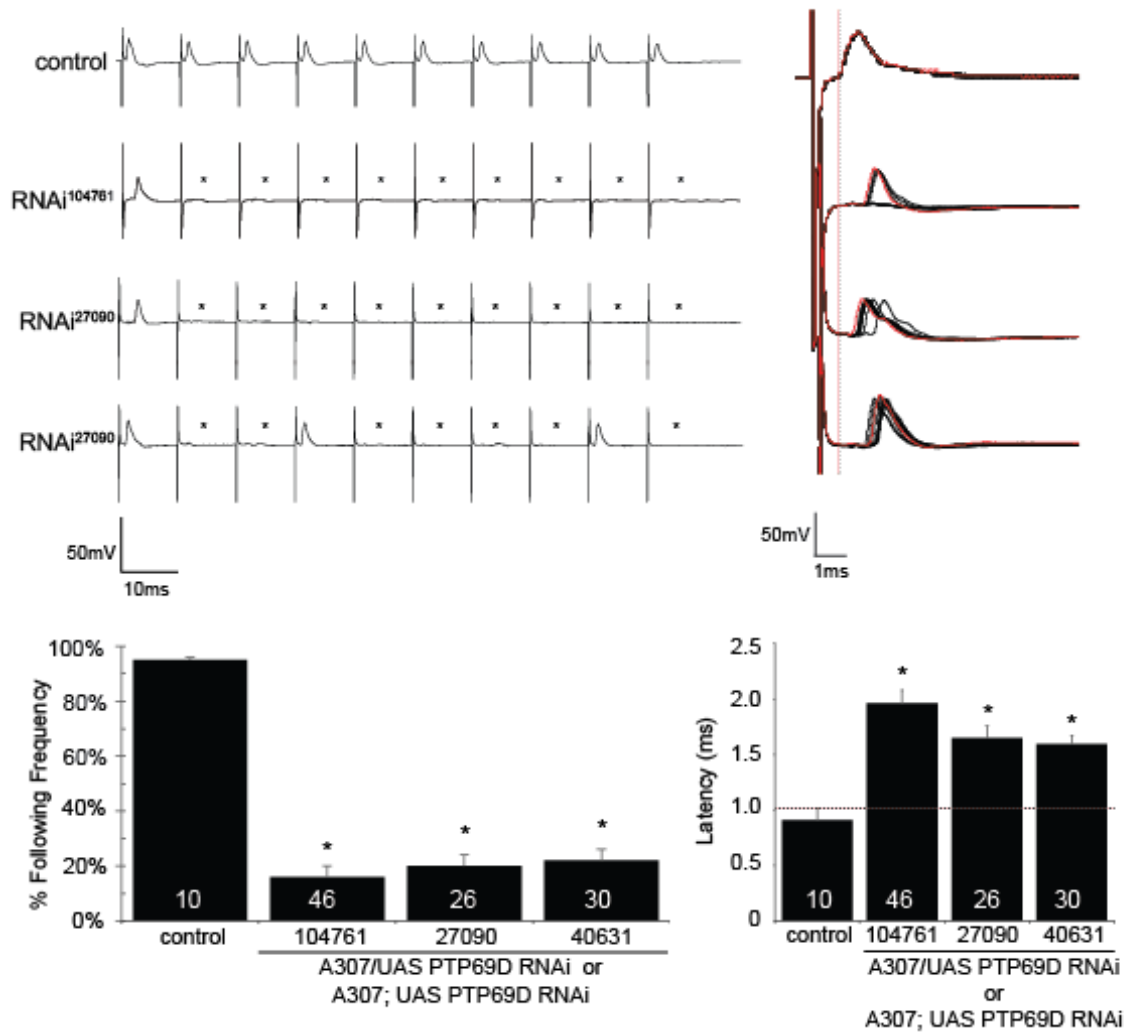
Figure 2.4 The PTP69D RNAi disrupts the physiology of the giant fiber system

Recordings from individual control (w1118) and UAS Ptp69D RNAi lines (104761, 27090, and 40631) driven with A307 Gal4. The TTM of control animals but not PTP69D RNAi mutants were able to respond at a 1:1 ratio when the GFs were stimulated at 100 Hz. The failures to respond to a stimulus are indicated by asterisks. The response latency (RL) for control animals is indicated by the dashed line (0.8 msec); the response latencies for the RNAi animals were greater than 1.5 msec. The quantification of responses to 10 stimuli given at 100HZ is depicted by the average Following Frequencies (FF) in percent. The average FF is significantly reduced (* = p value ≤0.05, ** = p value <0.001, Student's t-test) in PTP69D RNAi mutants, when compared to control animals. The average RL of the GF-TTM pathway in control and PTP69D RNAi mutants shows a significant increase in response time indicated by asterisks (* = p value ≤0.05, ** = p value<0.001, Student's t-test).

2.4.4 Cell-autonomous knock-down of PTP69D in the GF disrupts guidance and terminal growth.

Because A307 Gal4 driver expresses in both the GF and TTMn, it does not permit accurate determination of the site where PTP69D is required (pre- or post-synaptically, or both sides). Therefore, by utilizing various P[GAL4] lines to express shRNA directed against *Ptp69D* in a cell autonomous manner in the GF or its target neurons assessment of the cell-autonomous requirement of PTP69D could be characterized. R78G07, R91H05 and c17 are Gal-4 drivers that drive expression in the GF during development and the adult, but not in the postsynaptic target neurons. However, R78G07 and R91H05 turn on expression in the GF during neurite outgrowth in larvae (L3), while c17 only turns on expression in the GF once it exits the brain and enters the thoracic ganglion during early pupal stages (Godenschwege et al., 2002a; Jenett et al., 2012; Pfeiffer et al., 2008). On the other hand, the c422 Gal4 driver expresses presynaptically in the GF but not in its postsynaptic target. Furthermore, the driver turns on expression in the second half of pupal development (PD), during giant synapse maturation, but not during GF guidance or initial synapse formation (Jacobs et al., 2000). In contrast, the *ShakB*-Gal4 line drives expression in the TTMn but not the GF throughout development and in the adult (Jacobs et al., 2000).

In some animals expressing *UAS-Ptp69D RNAi* with the R78G07 (4 out of 10 recordings) and the R91H05 (8 out of 25 recordings) Gal4-drivers, we were not able to obtain any electrophysiological recordings from the GF to TTM pathway nor the GF to DLM pathway (9 out of 32 recordings), suggesting that these GFs did not reach the target area (Figure 2.5). Because these GFs could not be visualized in the cervical connective

with dye-injection nor Differential interference contrast (DIC) microscopy, we co-expressed the membrane bound UAS-mCD8-GFP with *UAS-Ptp69D RNAi* to label the GF in the brain. Correlating with the electrophysiological phenotype, we found that some GFs failed to exit the brain but often projected towards the retina instead (Figure 2.6B, arrow). This suggests that PTP69D has a role during early stages of GF guidance in the brain. This was further supported by the knockdown of PTP69D with the c17 Gal4-driver, which only drives expression in the GF after it exits the brain, and does not result in any guidance defects (Figure 2.7).
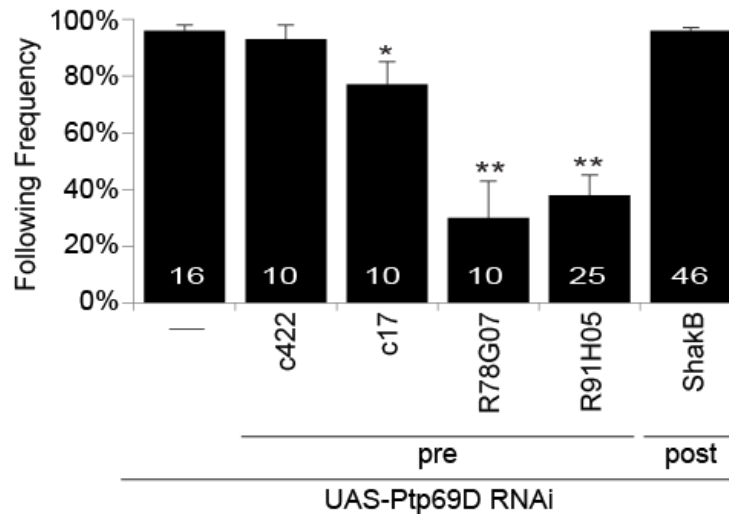
Figure 2.5 Targeted spatial and temporal expression of PTP69D RNAi in the Giant Fiber circuit

Knockdown of PTP69D by RNAi in the GFC was achieved by pre- and postsynaptic expression of shRNA against PTP69D. Quantification of FF from GF-TTM pathway for animals with defects in the synaptic target area. Animals without responses from the DLM and the TTM (indicating a guidance defect) were not included in the calculations. FFs were significantly decreased when UAS-Ptp69D RNAi was expressed with presynaptic drivers, but not with the postsynaptic-expressing ShakB-Gal4 line (* = p value ≤0.05, ** = p value<0.001, Student's t-test).

However, all GFs that exited the brain reached the synaptic target area and dye-coupled with the PSI. We found expression of *UAS-Ptp69D RNAi* with c17, R91H05 and R78G07 affected the growth and function of the GF terminal in the target area (Figure 2.5 and 2.6, Table 2). While the majority of the GFs dye-coupled with the TTM, in some animals it was found that the GF to TTMn terminal was completely lacking (Figure 2.6C). This suggests that PTP69D may also have a function in target recognition of the TTMn, in addition to its function in terminal growth.
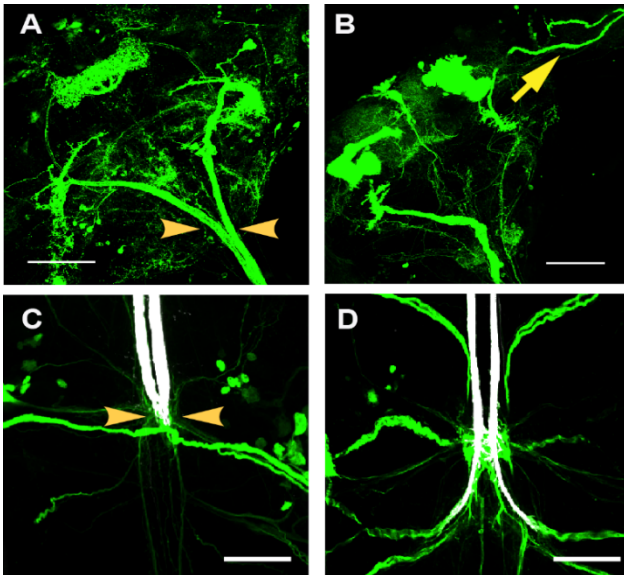
Figure 2.6 Phenotypes of PTP69D knockdown in the GFC

GF morphology in the brain (A, B) and cervical connective (C, D) was revealed with co-expression of mCD8-GFP or by dye-injection, respectively and projections views of confocal stacks are shown. (A) In control animals all GFs exited the brain in the suboesophangeal ganglion (arrowheads), when mCD8-GFP was expressed with the R91H05 line. Scale bar = 50µm. (B) With co-expression mCD8-GFP and shRNA against Ptp69D resulted in some GFs that did not exit the brain but grew towards the retina (arrow). Scale bar = 50µm. (C) Presynaptic expression of shRNA with R91H05 result in some GFs that dye-couple with the PSI but not the TTMn, suggesting a role for PTP69D in TTMn targeting. Scale bar = 20µm (D) Postsynaptic expression of shRNA with ShakB-Gal4 did not affect the GF morphology or its dye-coupling with the PSI and the TTMn. Scale bar = 20µm.

Consistent with the anatomical phenotypes, the function of the GF-TTMn pathway was severely impaired in animals expressing *UAS-Ptp69D RNAi* with c17, R91H05 and R78G07 (Figure 2.5, Table 2).   In contrast, post synaptic expression of PTP69D RNAi with the *ShakB* Gal4 driver resulted in no anatomical (Figure 2.6 and 2.7) nor physiological GF phenotypes (Table, 2, Figure 2.5, <1 msec response latency and 93-96% following frequency).

These data suggest that PTP69D may be required cell-autonomously in the GF, but in not the TTMn during guidance, target recognition, and terminal growth. Finally, expression late in pupal development during GF synapse maturation with the c422 Gal 4driver did not disrupt GF function (Figure 2.5, Table 2), suggesting and that PTP69D is required during early synaptic stages of GF synapse formation for terminal growth. This was further confirmed with use of additional Gal4-drivers (R91D07 and R14A01) from the Janelia Flylight collection (Table 2).
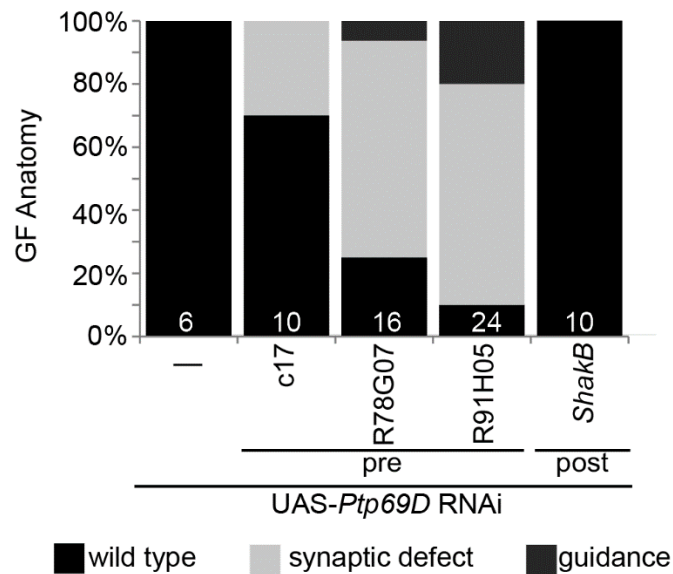
Figure 2.7 Quantification of the GF anatomical phenotypes with knockdown of PTP69D by expressing RNAi pre- or post-synaptically.

It was observed that with knockdown of PTP69D from p5 through eclosion resulted in normal response latencies of 0.89 msec on average, with following frequencies of 62%, and no disconnects. However onset of expression during earlier time periods (P4i-P4ii) severely disrupted the GF function (Table 2). The necessity of PTP69D presence in early developmental periods was demonstrated not only physiologically but also confirmed by examining the morphology of the giant fiber terminals with coexpression of GFP in the GFS (Figure 2.8). Both R91D07 and R14A01 exited the brain, but only PTP69D RNAi expression with R91D07 resulted in mutant GF terminals (Figure 2.8). PTP69D RNAi expression with R91D07 resulted in mutant GF terminals. Collectively, the anatomical and physiological findings indicate a critical period for PTP69D in GF synapse formation prior to P5i.

Table 2. Spatial and Temporal requirement of PTP69D in GF synapse formation

Genotype	GF expression onset	n	TTM		DLM
			Latency in msec (±SE)	Following Frequency 100Hz (±SE)	Dis-connected	Dis connected
c17	~20% PD	10	1.11 (±0.02)	77% (±8%)	0%	0%
C422	~50%PD	10	0.91 (±0.06)	93% (±2%)	0%	0%
R78G07	P1	14	1.18 (±0.11)	30% (±13%)	40%	29%
R91H05	L3	28	1.24 (±0.10)	38% (±7%)	32%	11%
R91D07	P4i-P4ii	18	1.27 (±0.17)	49% (±11%)	44%	27%
R14A01	P5i	14	0.89 (±0.03)	62% (±8%)	0%	0%
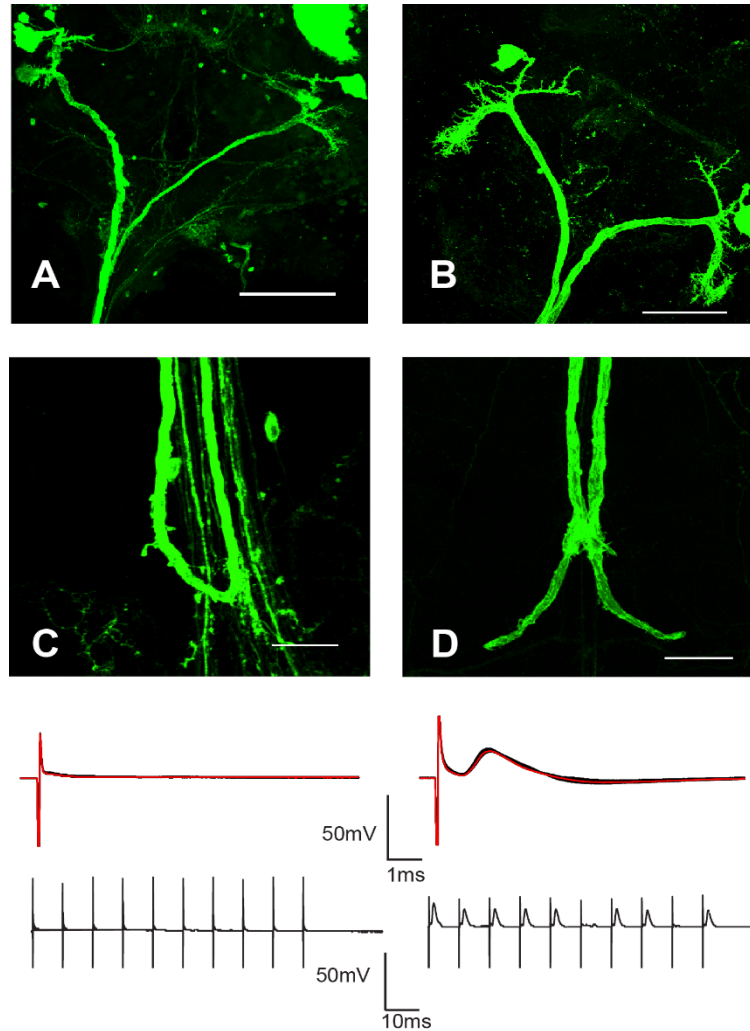
Figure 2.8 Temporal experiments indicating PTP69D requirement in GF synapse formation and function.

GF morphology in the brain (A, B) and ventral nerve cord (C, D) was revealed with co-expression of mCD8-GFP and projections views of confocal stacks are shown. (A) Using the driver R91D07 GFP (A and C), which turns on in P4i, and R14A01 GFP (B and C), which turns from P5i to adult, expression of PTP69D RNAi was driven in the GF circuit presynaptically. In all animals the GFs exited the brain (A, R91D07 GFP; B, R14A01 GFP). Scale bar = 50μm. In the ventral nerve cord co-expression of R91D07 mCD8-GFP and shRNA against Ptp69D resulted in GFs that made it to the target area but did not form appropriate synapses (C). Scale bar = 20μm. While presynaptic expression of shRNA with R14A01 resulted in normal GF morphologies (D). Scale bar = 20μm. Below each GF terminal are representative physiological traces indicating disconnects in the R91D07 animal and normal physiology for R14A01 animal.

2.5 Discussion

Screens to identify genes involved in particular neuronal developmental processes can often be problematic, in that they are often pleiotropic, having multiple vital functions throughout development. This, coupled with the fact that nearly two thirds of the vital genes within the *Drosophila melanogaster* genome (~2,500) are involved in its development (Thaker & Kankel, 1992). Thus, if the appropriate system is not utilized these functions cannot be uncovered or difficult to assess, whether or not a defect was the result of an earlier, rather than later developmental event. The strength of the Giant Fiber circuit in characterizing the development of the GF axon is well established; there are various tools available to assess and characterize GF synapse formation and function adding to its attractiveness. In this study, multiple roles for PTP69D were uncovered in the development of the GF neurons. In addition to previously described functions for PTP69D in guidance and target recognition, it is revealed that PTP69D is also required for terminal growth in the CNS.

In the visual system, PTP69D is required for synaptic targeting (Garrity et al., 1999; Hofmeyer & Treisman, 2009). Here, PTP69D serves as a "stop" signal preventing the R1-6 and the R7 photoreceptor neurons from passing by the target area in the lamina and medulla, respectively. In contrast, in the embryonic nervous system motor neurons of *Ptp69D* mutants did not innervate their respective muscles due to axon outgrowth and guidance defects (C. Desai & Purdy, 2003; Song et al., 2008). In addition, a role for PTP69D in axonal branching of mushroom body neurons has been described (Kurusu & Zinn, 2008).

59

It has been shown that the RPTP PTP69D is expressed in the adult CNS of fruit flies. Furthermore evidence has emerged that RPTP PTP69D is involved in synapse formation within the adult giant fiber (GF) system, in addition to its role in guidance and targeting. Cell-autonomous expression of PTP69D RNAi resulted in two main phenotypes in the Giant Fiber Circuit. In some animals, the GF axons had guidance defects and did not exit the brain. The observed guidance defects in the brain, but not in the ventral nerve cord, when PTP69D was down regulated in the GF using RNA interference during early development was not observed during later developmental stages. In the remaining animals, the GFs exited the brain and reached the target area in the thorax but stalled at the site of synapse formation, exhibiting severe anatomical and physiological defects. This finding indicated that PTP69D is involved in synapse formation.

Knockdown of PTP69D with various GF Gal4 drivers demonstrated a novel role for PTP69D in synapse formation and function in the CNS. The majority of GFs reached the target area in the second thoracic neuromere but exhibited synaptic defects that physiologically and anatomically affected the GF-TTM synapse but not the GF-PSI-DLM pathway. Anatomically, the GFs did not grow along the medial TTMn dendrite thereby appearing to have stunted growth and lacking the characteristic lateral bend. Nevertheless, the GFs were in proximity to their postsynaptic target, but the synaptic connectivity between these two neurons was disrupted, as evidenced by dye coupling experiments which further supported a role for PTP69D in synapse formation. Depending on the dosage of knockdown, these GFs make very weak or undetectable synaptic connections with the TTMn. Physiologically, some animals completely lack a

60

synaptic connection, which was supported by weakened dye coupling to the TTMn. The physiological effects are long latencies but very poor response to repetitive firing. The recordings from the GF-DLM pathway were mostly wildtype and not significantly different from control flies (data not shown). Further spatial experiments with PTP69D RNAi indicate that it is required presynaptically. In fact, pre- but not post-synaptic knockdown of PTP69D with RNAi disrupts the GF-motor neuron synapse. Thus, PTP69D mutations preferentially disrupt the GF-TTM synapse anatomically and physiologically, providing preliminary evidence for a novel role of PTP69D in central synapse formation, in addition to roles in guidance and targeting.

Thus, by targeting the expression of PTP69D RNAi to the giant fiber system, we have provided evidence that this RPTP is required to build a normal synaptic connection between GF and TTM neurons in the *Drosophila* CNS, in addition to the role played in guidance and targeting. Targeted presynaptic RNAi expression against PTP69D in Giant Fiber neurons revealed that it is necessary for GF synapse formation, axon growth, guidance and targeting. This finding expands what was previously known of PTP69D function in the developing nervous system. Despite this, a more in depth analysis is required in order to show that these are synaptic defects and not due to an error in guidance or targeting.

3 CHARACTERIZATION OF *Ptp69D MISSENCE MUTATIONS IN THE GIANT FIBER CIRCUIT*

3.1 Abstract

RNAi expression revealed a role for PTP69D in guidance, targeting and terminal growth of the GF. Herein, three missense mutant alleles of PTP69D in the GFC are functionally characterized. Some alleles were strongly temperature sensitive, and the alleles were characterized at three temperatures for GF function.   In addition, complementation studies indicate that the immunoglobulin and the cat1 domain are necessary for GF terminal growth, but that fibronectin type III and the membrane proximal region domains may be excluded from these requirements,. This is in contrast to previous PTP69D studies that found the Fibronectin type III repeats essential for axon targeting of photoreceptor neurons. Thus, this study provides evidence for a novel role for PTP69D in synaptic terminal growth in the CNS that is mechanistically distinct from its function during earlier developmental processes.

"A final proof of our ideas can only be obtained by detailed studies on the alterations produced in the amino acid sequence of a protein by mutations of the type discussed here."

- Francis Crick, PhD

3.2 Background

The successful wiring of neurons to form proper neuronal connections requires that cells perform a series of critical tasks in coordination with their surrounding environment. In neurons, the cell typically extends processes in search of their synaptic targets. Many proteins have been identified as guidance molecules, however it is not clear whether these same molecules are involved in synapse formation. The regulation and balance between the phosphorylated and dephosphorylated state of proteins, by kinases and phosphatases respectively, is recognized as an important developmental mechanism, especially during neurodevelopment. In particular, phosphorylation of tyrosine residues has been shown to have developmental importance in the nervous system (Ensslen-Craig & Brady-Kalnay, 2005; Van Vactor, 1998).

The mechanisms by which tyrosine kinases affect axon guidance and targeting are relatively well studied, however far less is known about their enzymatic counterparts, tyrosine phosphatases. The receptor protein tyrosine phosphatase (RPTP) family has been gaining attention for its role in neuronal development because they are highly express in the developing nervous systems (C. J. Desai et al., 1994; Vactor, Sink, Fambrough, Tsoo, & Goodman, 1993). Extracellularly, RPTPs resemble cell adhesion molecules (CAMs) in that they contain multiple immunoglobulin domains and fibronectin repeats, while intracellulary they contain phosphatase domains. The

63

intracellular membrane proximal (Cat1) phosphatase domain is thought to possess the majority of the catalytic activity of the RPTP. On the other hand, the Cat2 domain is thought to regulate the activity of the RPTP as well as its localization and substrate specificity. The structure of RPTPs hint to their function in signaling cascades.

PTP69D is one of five *Drosophila* RPTPs in the fly nervous system. Genetic studies have demonstrated wide-ranging functions for PTP69D, a type IIa receptor protein tyrosine phosphatase. These range from guiding axon trajectories in both the central and peripheral nervous system, as well as in the retina. It has been shown to facilitate motor and CNS axon guidance during embryogenesis (C. J. Desai, Krueger, et al., 1997; C. J. Desai, Sun, et al., 1997; Krueger et al., 1996; Sun, Bahri, Schmid, Chia, & Zinn, 2000). In addition, it is required for retinal axon guidance during late larval and pupal stages (Garrity et al., 1999). This essential gene has been shown to exhibit embryonic and larval lethality when mutated or null.

Genetic structure-function studies of RPTPs have shown that extracellular and intracellular mutations in RPTPs can independently disrupt their functions. These studies suggest that signals that are initiated by their extracellular domain can be converted into intracellular signals by their intracellular domains (C. Desai & Purdy, 2003; Garrity et al., 1999; Krueger et al., 2003; Maurel-Zaffran, Suzuki, Gahmon, Treisman, & Dickson, 2001; Newsome et al., 2000; Sun et al., 2001). Additional studies have provided evidence that the catalytic activity of these RPTPs are partially responsible for some of their in vivo functions. Using classical inhibitors, oxidation or involuntary dimerization to inhibit RPTPs has been shown to abrogate particular PTP-mediated functions (Ariño & Alexander, 2004). It would seem obvious that catalytic activity should play a critical role

in PTP signaling and observations support this theory. Mutations in the highly conserved active-site residues of RPTPs result in strong loss of function phenotypes, this is especially the case in the nervous system (Davies & Morris, 2004). Furthermore, catalytically inactive forms of phosphatases fail to rescue mutant phenotypes in transgene rescue experiments (Garrity et al., 1999; Krueger et al., 2003; Newsome et al., 2000; Sun et al., 2001).

Neural receptor tyrosine phosphatases, like PTP69D, have been intensively studied for their role in axon outgrowth, guidance, and targeting, but less is known about their potential role in synapse formation. Though PTP69D has not been explored for its role in synapse formation, the function of other PTP family members has been characterized not only for their role in synapse formation but also synaptic plasticity (Gurd, 1997). In *Drosophila* the most extensively studied phosphatase is DLAR, which is a structurally related family member of PTP69D. The role of DLAR in synapse formation has been assessed in the peripheral nervous system, at the neuromuscular junction. Studies of DLAR found that the phosphatase is required for normal synapse morphology and that synapse complexity is relatively proportional to the amount of gene product (Kaufmann, DeProto, Ranjan, Wan, & Van Vactor, 2002). The results also suggest that DLAR determines the size and shape of the active zone of synapses. Additionally, mammalian protein tyrosine phosphatase receptor type T, PTPRT, has been found to regulate synapse formation via interaction with cell adhesion molecules (Lim et al., 2009). Knockdown of this phosphatase resulted in defects in synapse formation as well as diminished dendritic processes. Furthermore, overexpression of PTPRT in cultured neurons increased the number of synapses. More recently, a study has indicated

that interactions between synaptic cell adhesion molecules and RPTPs are responsible for regulating excitatory synapse formation (Kwon, Woo, Kim, Kim, & Kim, 2010). These studies collectively provide further support of phosphatases playing a role in synapse formation and function.

The molecular aspects of assembly of synaptic circuits in the brain are the focus of these types of studies. Taking advantage of the power of fly genetics and molecular biology to investigate the role of various proteins involved in synapse formation this study utilizes the giant synapse of *Drosophila* as a model system. Though in the previous chapter guidance and targing defects were identified with PTP69D knockdown in the system with a focus is on synapse formation. Expression of shRNA directed against PTP69D disrupted growth and synapse formation in the presynaptic component of the circuit. In this chapter, mutational analysis and over expression of wild type PTP69D was used to further characterize the role of PTP69D in this process. In depth electrophysiological and anatomical analysis was used to further elucidate the phenotypes of various alleles and mutations of the *Drosophila* protein tyrosine phosphatase PTP69D, in the synaptic connection between the Giant Fiber and jump motorneuron. In addition, a classical structure function analysis by expression of various PTP69D mutant constructs was used to assess which domains of the molecule are required for its function in central synapse formation.

3.3 Materials and Methods

3.3.1 Flystocks and genetics

The wild type control (w^{1118}), $Df(3L)^{8ex25}$ and $Df(3L)^{8ex34}$ stocks were obtained from the Bloomington Stock Center. The following PTP69D stocks have been previously described: $Ptp69D^{10}$, $Ptp69D^{18}$, $Ptp69D^{20}$ (C. Desai & Purdy, 2003). The c17 and c422 Gal4-driver, which drives expression in the GF, but not in its target neurons, and the ShakB Gal4-driver, which only drives expression in the postsynaptic target neurons of the GF, described previously (Allen et al., 1999; Godenschwege et al., 2002b; Jacobs et al., 2000). For characterization of temperature sensitivity in $Ptp69D$, mutant alleles animals were reared at 18°C, 22°C and 25°C. All genetic crosses were performed on standard fly media at 25°C and 2-5 day old flies were used in all experiments.

3.3.2 Immunohistochemistry

Adult isolated CNS samples were dye filled with Dextran and Neurobiotin immediately fixed in 4% paraformaldehyde (Fisher Scientific) in phosphate-buffered saline (PBS, Calbiochem). The fixative was removed and samples were rinsed in PBS. Prior to antibody incubation, samples were washed 6×30 minutes in PBS containing 0.5% TritonX-100 (Sigma). Anti-DPTP69D MAb 3F11 supernatant made in mouse (Developmental Studies Hybridoma Bank) was diluted [1:100] in PBS containing 0.3% TritonX-100 and 2% bovine serum albumin (BSA, Sigma). Following antibody incubation for 2 nights at 4°C, samples were rinsed in PBS with shaking. In order to detect PTP69D (MAb), a goat anti-mouse secondary antibody coupled to the Cy2 fluorophore and dyelight 649 against Neurobiotin was used. Incubation with the

67

secondary antibodies was preformed overnight in PBS at 4°C. Finally, samples were rinsed with PBS, submitted to an alcohol series to dehydrate, and embedded in methyl salicylate (MP Biomedicals). The fluorescence signal was then scanned with a Nikon C1si Fast Spectral Confocal system with AOTF laser unit (Nikon) using a 40× oil immersion objective (numerical aperture 1.3). The samples were scanned at an image resolution of 1024 times 1024 pixels, a 1.5 -2.0 × zoom, and a z-step size of 0.5 μm.

3.3.3   Electrical stimulation of GF neurons and analysis of muscle potentials

The method of obtaining electrophysiological recordings from the GFC has been described in the previous chapter.

3.3.4   Dye injections and immunohistochemistry of the GFC

Dye injection and immunohistochemistry methods have previously been described in the preceding chapter.

3.4   Results

3.4.1   PTP69D missense mutations disrupt the GF-TTM synapse physiologically

Ptp69D mutations have been shown to cause a number of different guidance defects in different neurons. Studies of the intersegmental nerve (ISN) and segmental nerve (SN) motor pathways revealed that the phosphatase is involved in the control of growth cone guidance of motorneurons (C. J. Desai, Krueger, et al., 1997). Nearly 20

EMS chemically induced alleles of *Ptp69D* have previously been created with various molecular changes (Table 3.1).   These alleles of *Ptp69D* range in strength from viable to null and are balanced over TM6β. However, due to the fact that studies of the GFC is only amenable for adult flies, and furthermore that null animals are not viable, the study was limited to those alleles which yielded homozygous adults that could be subjected to experiments to assess their GF physiology and morphology.   These alleles provided a means of probing the structure, function, and signaling pathway of PTP69D. Additionally, these alleles exhibit a developmentally relevant temperature sensitive phenotype (Table 3.2).

Table 3.1 Description of molecular changes in *Ptp69D* alleles

Allele	Domain mutated	Base change	Coding change
Ptp69D[1] (null)			
Ptp69D[7]	Cat1	$\Delta 9$ bp	$\Delta D_{1065}\ F_{1066}\ M_{1067}$
Ptp69D[9]	MPR	G-A	G_{812} to D
Ptp69D[10]	Ig1, Ig2	T-A	V_{134} to D
Ptp69D[12]	Ig2	T-A	W_{171} to R
	Fn, MPR	G-A	G_{757} to E
	Cat1	G-T	R_{903} to L
Ptp69D[17]	MPR		W_{821} to stop
Ptp69D[18]	Fn, MPR	G-A	G_{757} to E
Ptp69D[20]	Cat1 active site	G-A	G_{1102} to S
Ptp69D[21]	Cat1 active site	G-A	C_{1097} to Y

The molecular changes in the DNA sequences for each allele is listed in the third column (Base change) and the resulting coding change is indicated in the last column. The column adjacent to the allele notes which domain of the protein is predicted to be effected by the mutation. (adapted from (C. Desai & Purdy, 2003)

Table 3.2   Characterization of *Ptp69D* Alleles by protein expression and temperature sensitivity

Allele	protein expression	25°C viability	18°C viability
Ptp69D[1]	None	lethal	lethal
Ptp69D[7]	WT	0%	4%
Ptp69D[15]	None	1%	4%
Ptp69D[21]	WT	2%	4%
Ptp69D[18]	None	0%	43%
Ptp69D[12]	None	1%	44%
Ptp69D[10]	WT	40%	47%
Ptp69D[20]	WT	49%	51%

Note: viability is % of eclosed animals, not adults, out of 200; Desai excluded animals from count due to "tar-pit" phenotype, whereby upon eclosion flies fall into the food, are unable to escape and die; the alleles have been ranked from strongest to weakest mutant phenotype at 25°C. (adapted from (C. Desai & Purdy, 2003)

Initially eight *Ptp69D* alleles reared at room temperature (22 C) were tested to identify highly penetrant alleles with strong GF phenotypes (Table 3.3).   These heterozygous *Ptp69D* stocks over a TM6β balancer were screened for homozygous animals. After the homozygous animals' eclosed, they were subjected to experiments characterizing the functional relevance of the domains of PTP in synapse formation at the one- to-five day old age. Most homozygous *Ptp69D* mutant alleles showed longer response latencies to a single stimulus and a lower percentage following to 10 stimuli at 100 Hz (Table 3.3). To confirm the defect was at the central synapses and not at the neuromuscular junctions (NMJs), the GFs were bypassed and stimulatation of the motorneurons directly in the preparations was conducted. This resulted in typical short latencies associated with functional NMJs being observed (Allen & Godenschwege, 2010). Responses in DLMs showed no significant differences but were recorded to

confirm that the GFs reached their target area during synaptic development and were being activated directly during electrophysiological testing.

Several alleles exhibited a viability phenotype, whereby we were unable to yield large numbers of homozygous adults to test physiologically. These included $Ptp69D^{12}$, $Ptp69D^{18}$ and $Ptp69D^{21}$ which from previous studies were determined to be especially temperature sensitive alleles (C. J. Desai, Krueger, et al., 1997). An observed the "tar-pit" phenotype was evident in these alleles, in which adult flies appear to have eclosed from their pupal cases however fell into the food and drowned. While $Ptp69D^{7}$ showed a strong GF phenotype, it was omitted for future study because of its identification as a neomorphic allele. Additionally, testing of the line with a new stock number for the allele from Bloomington was unable to confirm the result. Thus to avoid discrepancies, the allele was avoided. Three alleles – $Ptp69D^{10}$, $Ptp69D^{18}$, and $Ptp69D^{20}$ – were selected based on their adult viability, ability to yield adequate number of progeny, and strong GF phenotypes (Figure 3.1). These alleles were further characterized and the focus of this study.

Table 3.3   Assessing Giant Fiber phenotypes of
Ptp69D **alleles (room temperature stocks)**

Alleles	n	TTM Latency (ms)	TTM Following Frequency (%)
PTP69D[1]	☠	☠	☠
PTP69D[5]	☠	☠	☠
PTP69D[7]	28	1.31	24%
PTP69D[10]	34	1.23	27%
PTP69D[12]	10	1.08	89%
PTP69D[18]	24	1.19	52%
PTP69D[20]	30	1.14	30%
PTP69D[21]	10	1.09	57%
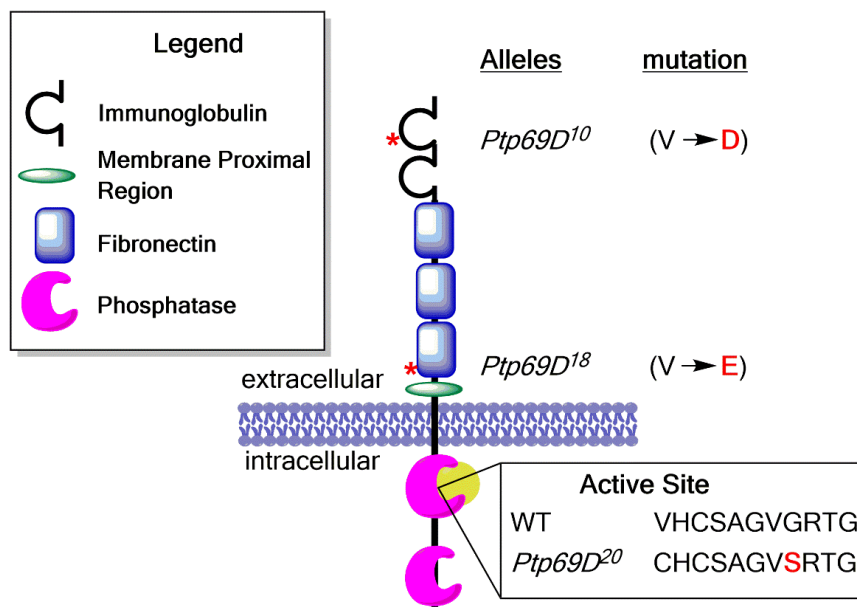
Figure 3.1 Schematic of PTP69D protein structure.

The graphic depicts the domains of PTP69D, with extracellular immunoglobulin domains, fibronectin type III domains, as well as the membrane proximal region and intracellular phosphate domains.   The membrane proximal phosphatase is the catalytically active domain. The mutations and the sites of the mutation are depicted (*) representative of the *Ptp69D[10], Ptp69D[18]* and *Ptp69D[20]* alleles.

3.4.2 Assessing strength and temperature sensitivity of *Ptp69D* alleles

To further determine the strength of the *Ptp69D* alleles, the phenotypes of the viable alleles *Ptp69D*¹⁰, *Ptp69D*¹⁸ and *Ptp69D*²⁰ were characterized. These alleles carry missense mutations in the first Ig-domain, third FNIII-domain, and in the first catalytic domain in the adult GF neurons (Figure 3.1). In control animals, the GF-TTM pathway was able to respond in a 1:1 ratio when the GFs were stimulated with 10 pulses at 100 Hz (Figure 3.2). In contrast, the average following frequency (FF, at 100Hz) of the GF-TTM pathway was severely reduced in *Ptp69D*¹⁰ (FF=27%) and *Ptp69D*²⁰ (FF=32%) animals (Figure 3.2). Correlating with the decrease to follow stimulations at 100 Hz, the average response latency (RL, in milliseconds) of the GF-TTM pathway to an individual stimulus significantly increased in *Ptp69D* mutants (≥ 1 ms) when compared to the control animals (0.8 ms) (Figure 3). In control animals, the RL remained constant in individual flies when 10 stimuli were given at 5 Hz. In contrast, the RL varied in *Ptp69D* mutants with the duration usually increasing further (Figure 3.2), or the GF-TTM pathways failing to respond similarly to repetitive stimulation seen at 100Hz (Figure 3.2), and revealing a severe weakening of the synaptic connection. This failure to respond was particularly evident in PTP *Ptp69D*¹⁰ and *Ptp69D*²⁰ alleles with the demonstration of disconnects (Table 4). These disconnects were primarily in the TTM. The synaptic defects of *Ptp69D*¹⁸ mutants were less severe when compared to *Ptp69D*¹⁰ and *Ptp69D*²⁰ animals. Although slightly increased, the RL was not significantly different from control animals, and the average FF was only reduced to 52% (Figure 3.2). When thoracic stimulation was used to bypass the GFs and activate the TTMns directly, 100% FF of the

neuromuscular junctions and a RL below 0.8 ms were observed (data not shown). This confirmed that the site of the synaptic defect was at the GF-TTMn synapse.

When $Ptp69D^{18}$ homozygous animals were reared at higher temperatures, the animals failed to eclose and exhibited the tar-pit phenotype. Upon closer inspection of the animals, it was noted that they appeared to have locomotor defects, which likely contributed to their inability to escape from the food. Thus, great care was taken to collect homozygous pupae from the $Ptp69D^{18}$ allele and place them in fresh vials on its side to prevent them from falling into the "tar." The $Ptp69D^{18}$ allele exhibited the tar-pit phenotype at all temperatures, but the phenotype was exacerbated at higher temperatures, indicating that this allele was temperature sensitive. At the other end of the spectrum with respect to temperature are the $Ptp69D^{10}$ and $Ptp69D^{20}$ alleles, which are capable of surviving and propagating at all temperatures equally effectively. Thus it was determined that $Ptp69D^{10}$ and $Ptp69D^{20}$ were not temperature sensitive, though the permissive temperature for the $Ptp69D^{18}$ allele was room temperature.
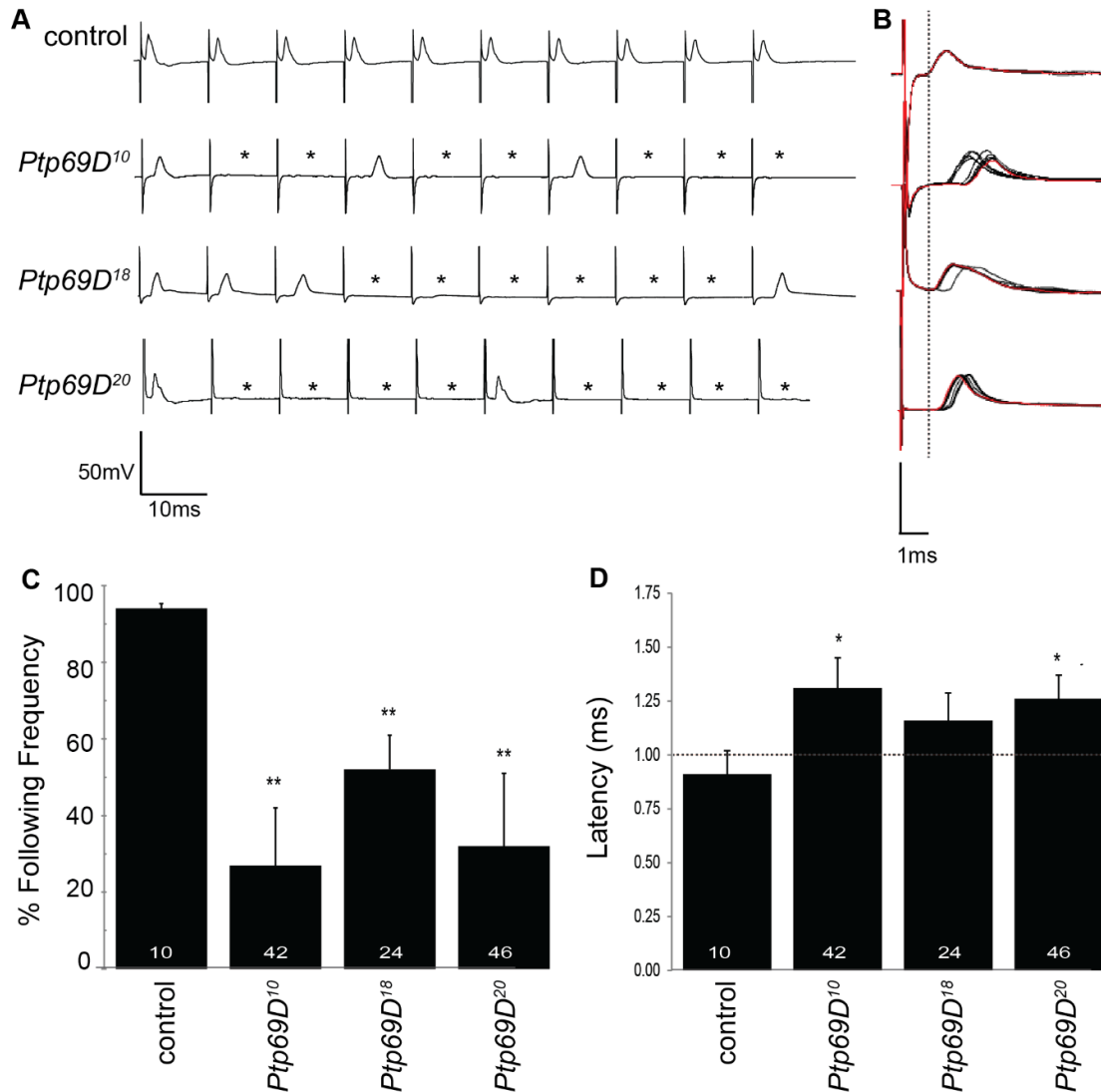
Figure 3.2 Electrophysiological characterization of *Ptp69D* missense mutants in the giant fiber circuit

A) Electrophysiological traces of the GF-TTM pathway from wild type control animals (w[1118]) and *Ptp69D* mutants. Control animals, but not *Ptp69D^10^*, *Ptp69D^18^* and *Ptp69D^20^* mutants, were able to respond at a 1:1 ratio when the GFs were stimulated at 100 Hz. The failures to respond to a stimulus are indicated by asterisks. B) Response Latency (RL) of control animals was 0.87 ms (dashed grey line) but increased in *Ptp69D* mutants. C) The quantification of responses to 10 stimuli given at 100HZ is depicted by the average Following Frequencies (FF) in percent. The average FF is significantly (* = p value ≤0.05, ** = p value <0.001, Student's t-test) reduced in *Ptp69D* mutants, when compare to control animals. D) The average RL of the GF-TTM pathway in control and *Ptp69D* mutants. Significance is indicated by asterisks (* = p value ≤0.05, ** = p value<0.001, Student's t-test)

76

Table 3.4   Characterizing GF-TTM electrophysiological phenotypes of *Ptp69D* Alleles at different temperatures

Alleles	TTM Latency (msec)			TTM Following Frequency			TTM disconnects
	18°C	22°C	25°C	18°C	22°C	25°C	
Ptp69D^{10}	0.96 n = 32	1.23 n = 34	1.31 n = 42	39%	27%	27%	8%
Ptp69D^{18}	1.18 n = 20	1.19 n = 24	☠	58%	52%	☠	0%
Ptp69D^{20}	1.01 n = 30	1.14 n = 30	1.26 n = 46	42%	30%	32%	13%

3.4.3   Disrupted GF terminal in *Ptp69D* mutant alleles

The anatomical phenotypes of the viable alleles *Ptp69D^{10}*, *Ptp69D^{18}* and *Ptp69D^{20}* were characterized in the adult GF neurons. Dye-injections of Rhodamine-dextran and neurobiotin into the GFs were used to reveal the morphology of the terminals and to determine if the GFs are coupled to their synaptic targets via the gap junctions of their electrical-chemical synapses. All GFs in the three mutant alleles reached the synaptic target area in the second thoracic neuromere without any guidance defects, and only anatomically disrupted the GF to TTMn connection but not the GF to PSI connection,. In homozygous *Ptp69D^{10}* (n=22) and *Ptp69D^{20}* (n=20) mutants, the GF terminals were dramatically shorter when compared to control animals (Figure 3.3). However, all GF terminals dye-coupled with the TTMn; however this was often weak, suggesting that terminal growth, and not synaptic targeting, is disrupted in these mutants. These findings were consistent with the physiological phenotypes previously described.

In homozygous *Ptp69D¹⁸* mutants, twelve GF terminals were shorter (Figure 3.3E, arrowhead) similar to the *Ptp69D¹⁰* and *Ptp69D²⁰* alleles. However, three GFs grew a normal-sized terminal to the ispilateral side, while 8 GFs bifurcated (Figure 3.3E, arrow) and grew terminals onto the ispilateral and contra-lateral TTMn. Furthermore, *Ptp69D¹⁸* results in inappropriate midline crossing and dual innervation of both ipsilateral and contralateral TTMns.

In homozygous *Ptp69D^{18}* mutants, twelve GF terminals were shorter (Figure 3.3E, arrowhead) similar to the *Ptp69D^{10}* and *Ptp69D^{20}* alleles. However, three GFs grew a normal-sized terminal to the ispilateral side, while 8 GFs bifurcated (Figure 3.3E, arrow) and grew terminals onto the ispilateral and contra-lateral TTMn. Furthermore, *Ptp69D^{18}* results in inappropriate midline crossing and dual innervation of both ipsilateral and contralateral TTMns.
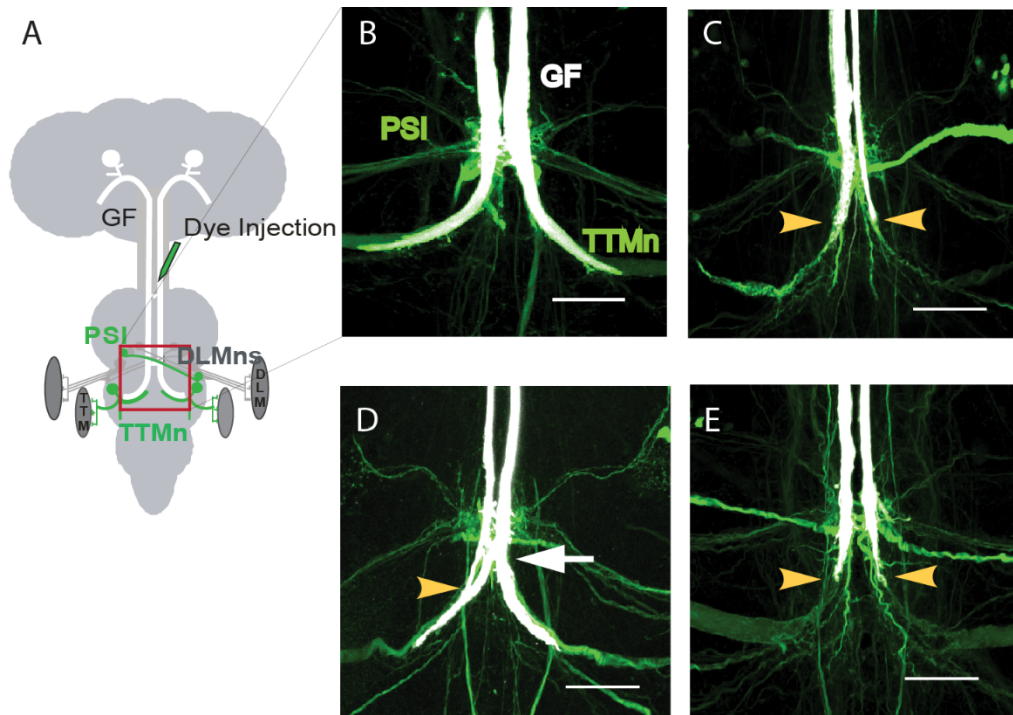
Figure 3.3 Anatomical phenotypes of *Ptp69D* missense mutants in the giant fiber circuit

A) Schematic of the central nervous system (CNS) of *Drosophila* depicting the giant fiber circuit (GFC) within the brain and the ventral nerve cord (modified from (Allen and Godenschwege, 2010)). The two giant fiber (GF, white) somas and dendrites are located in the brain. In the GF to tergo-trochanteral muscle (TTM) pathway, the axons form a large synaptic terminal onto the tergo-trochanteral motorneurons (TTMn, green) in the second thoracic neuromere, which innervate the TTM. In the GF to dorsal longitudinal muscle (DLM) pathway, the GF synapse with Peripheral Synapsing Interneuron (PSI, green). The PSI synapses with the dorsal longitudinal motorneuron (DLMn, grey), which innervate the DLM. Placement of stimulation and recoding electrodes as well as site of dye-injections are indicated. B-E) GF synaptic terminals and dye-coupling to the postsynaptic target neurons were visualized by co-injection of Rhodamine-dextran (white) and neurobiotin (green) into the GF at the cervical connective and projection views of confocal stacks are shown. In w1118 wild type control animals (B), the GFs exhibited large GF terminals and dye-coupled with the TTMn and the PSI. In homozygous Ptp69D10 (C) and Ptp69D20 (E) mutants the GFs were severely stunted (arrowheads) but dye-coupled with the TTMns and the PSIs in all cases. The majority of Ptp69D18 (D) animals exhibited one GF with s short terminal (arrowhead), while the other GF bifurcated (arrow) and innervated the ipsi- and the contra-lateral TTMn, which dye-coupled with the GFs. Scale bars are 20 µm.

79

3.4.4   Complementation of *Ptp69D* mutant alleles

To confirm that the phenotypes observed were the result of disruption in the *Ptp69D* gene, the alleles were crossed to deficiency stocks, which contain a chromosome missing a stretch of the genome that can be mapped to a specific gene locus (Edwards & Mackay, 2009). If the *Ptp69D* alleles overlap with the deficiency, then the phenotype complement and the phenotypes will be worse. However, if the phenotypes of the *Ptp69D* alleles improve, then they are likely due to a secondary mutation outside the locus of *Ptp69D*. The following lines were used of complementation testing of the *Ppt69D^{18}*, *Ptp69D^{10}* and *Ptp69D^{20}* alleles. The *Df(3L)^{8ex25}* stock deletes most or all of the DNA encoding the cytoplasmic domain of *Ptp69D*, and has breakpoints within *Ptp69D* and falls between the fibronectin type III repeats and the PTP enzymatic domain, possibly breaking in the transmembrane domain, removing the carboxy-terminal portion of the molecule. The *Df(3L)^{8ex34}* stock deletes the entire gene plus a kinesin light chain gene (*KLC*), overlapping with *Df(3L)^{8ex25}* (Figure 3.4, (C. J. Desai et al., 1996).

The functional defects in the giant fiber were enhanced when the *Ptp69D^{10}* and *Ptp69D^{20}* alleles were tested over the chromosome deficient (*Df(3L)^{8ex34}*) line (Table 5). The response latencies and following frequencies were significantly disrupted in transheterzygotes. The GF phenotype of homozygous *Ptp69D^{18}* was not as strong as the *Ptp69D^{10}* and *Ptp69D^{20}* alleles. However, both average RL and average FF were strongly disrupted in *Ptp69D^{18}/ Df(3L)^{8ex34}* transheterozygotes.   The results of the complementation test demonstrate that the observed defects were PTP69D-specific.
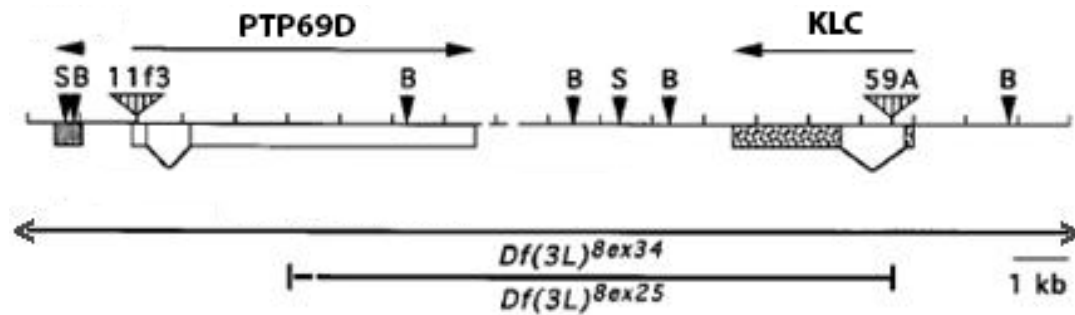
Figure 3.4 Map of *Ptp69D* and Chromosome Deficiencies disrupting genes.

Exons of Ptp69D and klc mRNAs and the snRNP coding region are designated by boxes. The directional arrows designate the direction of transcription of the gene. P elements used to generate deletion mutations are depicted as triangles (not to scale). Below the gene map are the deficiencies which delete all or a portion of the gene(s). All of Ptp69D is deleted by Df(3L)8ex34 (upper bidirectional arrow), while Df(3L)8ex25 deletes portions of Klc and Ptp69D (bottom bidirectional arrow). Borrowed from (C. J. Desai et al., 1996).

Table 3.5 Complementation Analysis of *Ptp69D* Alleles

Genotypes	n	Latency (±SEM)	Following Frequency 100Hz (±SEM)
TM6β/+ (WT)	10	0.91 (±0.11)	94% (±1%)
Ptp69D^10	42	1.31 (±0.14)	27% (±15%)
Ptp69D^10/ Df(3L)^8ex34	20	2.21 (±0.17)	19% (±11%)
Ptp69D^18	24	1.19 (±0.14)	52% (±9%)
Ptp69D^18/ Df(3L)^8ex34	10	1.93 (±0.23)	29% (±16%)
Ptp69D^20	46	1.26 (±0.11)	32% (±19%)
Ptp69D^20/ Df(3L)^8ex34	15	2.05 (±0.20)	24% (±6%)

3.4.5 Transheterozygote *Ptp69D* mutant alleles

Transheterozygote animals were generated in order to test whether *Ptp69D*[18] and *Ptp69D*[10] can complement for the lack of catalytic function in *Ptp69D*[20] animals, or if the Ig and FNIII domains are required for outside-in signaling of the Cat1 domain. In *Ptp69D*[10]/*Ptp69D*[20] transheterozygous animals, the function of the GF to TTMn connection remained severely disrupted (Table 3.6) and the anatomical defects (n=8) were indistinguishable from homozygous *Ptp69D*[10] and *Ptp69D*[20] mutants. In contrast, *Ptp69D*[18] was able to partly complement the synaptic defects of *Ptp69D*[20]. This ability to complement was revealed by a normal RL, an average FF only reduced to 72% (Table 3.6), and an anatomical phenotype (n=4) reminiscent of *Ptp69D*[18] homozygotes.

Table 3.6 Assessing the ability of Transheterozygote *Ptp69D* alleles to complement

Genotypes	n	Latency (±SEM)	Following Frequency 100Hz (±SEM)
TM6β/+ (WT)	10	0.91 (±0.11)	94% (±1%)
Ptp69D[10]	42	1.31 (±0.14)	27% (±15%)
Ptp69D[18]	24	1.19 (±0.14)	52% (±9%)
Ptp69D[20]	46	1.26 (±0.11)	32% (±19%)
Ptp69D[10]/ *Ptp69D*[20]	20	1.75 (±0.22)	43% (±12%)
Ptp69D[18]/ *Ptp69*[20]	14	0.97 (±0.06)	72% (±8%)

3.5 Discussion

PTP69D is a receptor protein tyrosine phosphatase (RPTP) with two intracellular catalytic domains (Cat1 and Cat2), which has been shown to play a role in axon outgrowth and guidance of embryonic motorneurons, as well as targeting of photoreceptor neurons in the visual system of *Drosophila melanogaster*. Here, we characterized the developmental role of PTP69D in the giant fiber (GF) neurons; two interneurons in the central nervous system (CNS) that control the escape response of the fly. A forward genetic approach to identify alleles with strong GF phenotypes was used to determine the structural components which relate to the function of the phosphatase in GF synapse formation.

We found that the missense mutations in the first Ig domain and the Cat1 domain of *Ptp69D^{10}* and *Ptp69D^{20}* mutants did not affect GF guidance, branching or targeting; however synapse formation was affected. Though all GFs dye-coupled with their target TTMn motorneurons, they failed to grow a full-size terminal, resulting in a severely weakened synaptic connection. This suggests a novel role for both the Ig domains and Cat1 domain of PTP69D in synaptic terminal growth in the CNS, which is distinct from its function during earlier developmental processes. Anatomical and functional synaptic defects of *Ptp69D^{10}* animals are indistinguishable from *Ptp69D^{20}* mutants, suggesting a critical role for the Ig domain, in addition to the Cat1 domain, in GF terminal growth. The strength of the *Ptp69D* alleles were assessed, examining their GF phenotypes by complementation analysis, rearing at various temperatures, and quantifying the number of disconnects. Furthermore, *Ptp69D^{10}* and *Ptp69D^{20}* mutants do not complement each other as transheterozygotes because *Ptp69D^{10}/Ptp69D^{20}* animals remained strongly

mutant. While $Ptp69D^{18}/Ptp69D^{20}$ transheterozygotes are still mutant they were slightly improved physiologically when compared to $Ptp69D^{20}$ homozygotes. The strongest alleles were $Ptp69D^{10}$ and $Ptp69D^{20}$. These alleles exhibited a similar phenotype that was observed with RNAi mediated knockdown of PTP69D, further demonstrating that the synaptic defects is due to loss of PTP69D function. Thus, these studies uncover a novel role for PTP69D in synaptic terminal growth in the CNS that is mechanistically distinct from its function during the earlier developmental process. Additionally the study found that inhibition of phosphatase activity in the Cat1 domain, proximal to the transmembrane domain did not affect axon guidance or targeting but resulted in stunted terminal growth of the GFs.

Missense mutation in the fibronectin and membrane proximal region of $Ptp69D^{18}$ mutants, on the other hand, displays a unique phenotype not seen in $Ptp69D^{10}$ and $Ptp69D^{20}$ mutants. This phenotype could be interpreted as a branching, targeting or synaptic defect. The synaptic GF-TTMn connection in $Ptp69D^{18}$ mutants was only mildly impaired, and as a result some GFs did not grow a full-sized terminal. Though only mildly disrupted, nevertheless in most of these cases we found the other GF to bifurcate and grow large GF terminals onto the dendrites of both TTMn motorneurons, while in wild type animals the GF only innervates the ispsilateral TTMn. It is important to note that viability, as well as protein expression levels, of P $Ptp69D^{18}$ mutants are severely temperature-sensitive. This temperature sensitivity was previously demonstrated (Desai and Purdy, 2003), suggesting that the missense mutation renders the protein unstable and subsequently could be degraded when misfolded. Therefore, it is not clear if the observed phenotypes are due to a specific loss of the function of the FNIII

84

domain or result from varying protein levels in $Ptp69D^{18}$ animals during development. Furthermore, the FNIII domains could have a specific function in either preventing axonal branching or targeting the GF only to one synaptic target. Alternatively, varying protein levels in these $Ptp69D^{18}$ mutants may prevent GF terminal growth in some cases, with the other GF compensating for the lack of a contralateral innervation by bifurcation.

In *Ptp69D* null mutants, bouton numbers at the larval neuromuscular junction are reduced (Hofmeyer and Treisman, 2009) suggesting a synaptic function for PTP69D, though the functional requirements remain to be determined. Here, it is demonstrated that PTP69D is required for terminal growth in the CNS. The lack of Cat1 phosphatase activity in $Ptp69D^{20}$ mutants is sufficient to prevent the GF growth in all animals without affecting guidance or targeting.

4   STRUCTURAL FUNCTIONAL ANALYSIS OF PTP69D IN THE GIANT

FIBER CIRCUIT

4.1   Abstract

Evidence has been previously provided supporting the developmental role of PTP69D in the giant fiber (GF) neurons. To further elucidate the function and potential signaling pathways, a detailed structure-function analysis of PTP69D was conducted. It was found that inhibition of phosphatase activity in the Cat1 domain, proximal to the transmembrane domain, did not affect axon guidance or targeting but instead resulted in stunted terminal growth of the GFs. Cell autonomous rescue experiments have demonstrated a function for PTP69D presynaptically in the GFs, but not its postsynaptic target neurons. Hthat both the immunoglobulin and fibronectin domains of the PTP69D ectodomain serve important, non-redundant functions. The structure-function experiments revealed that for GF terminal growth the catalytic function of PTP69D requires the immunoglobulin and the catalytic domains. Additionally, the experiments indicate a novel role of the fibronectin domains and membrane proximal region in inhibiting midline crossing. In contrast, the fibronectin but not the immunoglobulin domains were previously shown to be essential for axon targeting of photoreceptor neurons. Thus, this study uncovers a novel role for PTP69D in synaptic terminal growth in the CNS that is mechanistically distinct from its function in photoreceptor targeting.

86

"If you want to understand function, study structure."

- Francis Crick, PhD

4.2   Introduction

During the formation of the central nervous system, a number of complex interactions occur between cells and tissues that have been well characterized. As the developing CNS shifts from a collection of undifferentiated cells into a functional neuronal circuit, neurons undergo a complex set of morphogenetic changes, including outgrowth, guidance, targeting, and synapse formation. Many of these processes require regulation and involve the coordinated interaction of kinases and phosphatases. Due in part to extensive study of kinases, there is a greater understanding of the role that kinases play in CNS development., Alternatively, phosphatases are beginning to gain attention, and studies are finally beginning to elucidate the function of phosphatases in neurodevelopment. In particular, the receptor protein tyrosine phosphatases have gained attention and studies demonstrating how they function in regulating proper development of the nervous system.

Receptor protein tyrosine phosphatases (RPTPs) are a family of transmembrane proteins strongly expressed in the nervous system and crucial for the formation of functional neuronal circuits (Ensslen-Craig & Brady-Kalnay, 2005; Van Vactor, 1998). They consist of an extracellular variable N-terminal domain; a transmembrane domain and an intracellular region. The intracellular variable region is followed by one or two catalytic phosphatase domains. The membrane proximal phosphatase (Cat1) domain

provides the main catalytic activity, while the second phosphatase (Cat2) domain may be involved in the regulation of enzyme activation, protein- protein interaction, substrate specificity, and presentation of substrates to the active catalytic domain. The RPTPs are classified based on structural differences in the extracellular domain. In general, type II RPTPs have one to three extracellular immunoglobulin (Ig)-like domains, followed by up to 10 fibronectin III (FNIII)-like domains. As a result of their cell adhesion-like structure, the type IIa receptor protein tyrosine phosphatases are believed to function as cell-adhesion receptors, regulating tyrosine dephosphorylation in response to cell contact.

The majority of RPTPs are orphan receptors, meaning that their ligands are largely unknown, and as such often their physiologic function in cellular processes are also unknown. Interestingly, the type IIa RPTPs, also known as the LAR family of RPTPs, have been more studied than many of the other RPTPs. In the nervous system this family has been demonstrated to have roles in axonal morphology, guidance, targeting, presynaptic assembly and the formation of active zones (Davies & Morris, 2004).

The literature has described PTP69D as a pivotal molecule involved in axon outgrowth, guidance and targeting, and earlier a novel role in synapse formation at a central synapse was described (C. Desai & Purdy, 2003; C. J. Desai et al., 1996; Garrity et al., 1999; Hofmeyer & Treisman, 2009). Though mutant phenotypes allowed the identification of the overall biological processes in which PTP69D is involved in, the challenge now is to understand how the structure of the ectodomains and phosphatase domains related to their functions in nervous system development. Form often hints to the function of molecules thus structural functional analysis is an excellent opportunity to

delve into the role of this RPTP in central synapse formation. *Ptp69D* is an essential gene, as animals lacking the phosphatase die early in development (C. J. Desai et al., 1996). Initial rescue experiments found that neuron-specific expression of a wild type *Ptp69D* transgene rescues this lethality, suggesting it is required in the nervous system for viability (Garrity et al., 1999). Furthermore, genetic structure-function studies of RPTPs have revealed that extracellular and intracellular mutations in these molecules are separable and thus can independently disrupt in vivo functions. These studies have suggested that extracellular signals received by the extracellular domain can be converted into intracellular signals (Krueger et al., 2003; Maurel-Zaffran et al., 2001).

Studies have suggested that the catalytic activity of RPTPs is at least partially required for their in vivo functions. The phosphatase (Cat) domain of PTP69D contains two amino acids that are essential for catalytic activity. The first is the conserved cysteine, which acts as a nucleophile initiating the dephosphorylation reaction (Zhang, 1998). The second amino acid is an aspartic acid that aids in the reversibility of the phosphorylation reaction by catalyzing hydrolysis; it thereby enables the dephosphorylated substrate to release the phosphate from the active site. However, if this aspartic acid is mutated, then catalysis prematurely terminates and the substrate remains attached to the RPTP forming a "substrate trap" version of the RPTP (Flint, Tiganis, Barford, & Tonks, 1997). This D-to-A mutation has been previously explored for its function in the Cat1 and Cat2 domains. Additionally, mutations disrupting the function of both Cat1 and Cat2 domains prevent proper targeting of R1-R6 to the lamina, but catalytic activity of one of the two domains is sufficient for normal development. Rescue experiments suggest that the catalytic activity of PTP69D may not be essential for all of

its *in vivo* functions in *Drosophila*. A point mutation in the active site of the Cat1 domain of PTP69D causes defects in the guidance of R1-R6 photoreceptor axons, suggesting that the Cat1 domain may not be able to compensate in this loss of function background (Newsome et al., 2000). In fact, the catalytically inactive Cat2 domain alone can rescue most neuromuscular and retinal axon guidance defects of *Ptp69D* mutants (Garrity et al., 1999; Sun et al., 2001). Thus, the role of catalytic activity in PTP69D signaling *in vivo* remains unresolved.

The extracellular domains of PTP69D have been investigated for their role in various neurodevelopmental processes. In the visual system of *Drosophila*, the functional importance of a number of PTP69D protein domains in R1-R6 axon targeting was illustrated by expressing *Ptp69D* transgenes with various deletions under the control of neural specific promoters (Garrity et al., 1999). These structure-function studies of PTP69D revealed that the FNIII domains, but not the Ig domains, are required for proper axon targeting of the photoreceptor neurons. The axon targeting defects of R1-R6 photoreceptors in *Ptp69D* mutant animals are rescued by expression of transgenes containing all three fibronectin type III (FNIII) domains, and at least one catalytically active cytoplasmic tyrosine phosphatase domain. Additional studies of extracellular mutants indicates that extracellular functions are separable from catalytic functions. Extracellular mutations between the Ig and FNII domains in the *Ptp69D*[10] allele results in longitudinal midline crossing defects in the embryo and stronger ISNb defects than seen in null mutants (C. Desai & Purdy, 2003). Though structural rescue experiments were not conducted, reduced viability is observed in *Ptp69D*[10] animals indicating that they retain some of the essential function associated with PTP69D in the nervous system.

While ligands have not been identified for *Drosophila* RPTPs, it has been suggested that the extracellular domains are required for proper RPTP function. This hypothesis is supported by functional studies of Dlar in photoreceptor axon guidance. Expression of full-length *Dlar* in R7 or R8 photoreceptor, or expression of only the extracellular domains in R8 photoreceptors in a null background, is able to rescue the mutant phenotypes demonstrating a cell-autonomous and nonautonomous function of Dlar (Maurel-Zaffran et al., 2001). Thus, RPTPs may serve as both receptors and ligands.

Redundancy of PTP function has been observed; it has been proposed that the similarity of the extracellular domains that are the underlying cause of this phenomenon. The intracellular domains of RPTPs are interchangeable, suggesting that they share common signaling mechanisms. While PTP69D is not required for ISN axon guidance per se, in null mutant *Dlar* embryos the ISN defects increase from 32% to 85% when PTP69D is reduced (C. J. Desai, Krueger, et al., 1997). Rescue of the *Dlar* mutant phenotype by overexpressing *UAS-Ptp69D^{WT}* further supports the hypothesis of partial compensation or redundancy among the RPTPs. Additionally, it was found that *Dlar* rescues *Ptp69D* mutant defects but not vice versa in the adult visual system (Maurel-Zaffran et al., 2001).

To further elucidate the synaptic requirement of the neural receptor tyrosine phosphatase PTP69D in the Giant Fiber circuit, a detailed structure-function analysis was undertaken. To better understand the function of PTP69D in central synapse formation, the use of a series of point mutant and deletion mutant *Ptp69D* transgenes were employed for their ability to rescue GF phenotypes. These experiments determined which portions

of the complex ectodomains and cytoplasmic phosphatase-like domains were required for PTP69Ds function in GF synapse formation and function.

4.3 Materials and Methods

4.3.1 Flystocks and genetics

The following PTP69D stocks have been previously described: $Ptp69D^{10}$, $Ptp69D^{18}$, $Ptp69D^{20}$, UAS-$Ptp69D^{WT}$, UAS-$Ptp69D^{ΔIg}$, UAS-$Ptp69D^{ΔIg,FNIII}$, UAS-$Ptp69D^{ΔFNIII}$, UAS-$Ptp69D^{ΔFNIII,MPR}$, UAS-$Ptp69D^{Cat1-DA}$, UAS-$Ptp69D^{Cat1/2-DA}$, UAS-$Ptp69D^{ΔCat2}$ and UAS- $Ptp69D^{Δintra}$ (C. Desai & Purdy, 2003; Garrity et al., 1999). The $Ptp69D$ constructs are shown in Figure 4.1. Five P[GAL]4 drivers were used to determine the spatial requirement in the GFC. The A307 drives strong presynaptic expression in the GF along with weaker expression in postsynaptic targets (Allen et al., 1998). The c17 drives weak expression in the GF, but not in its target neurons while the $ShakB$ Gal4-driver only drives expression in the postsynaptic target neurons of the GF (Godenschwege et al., 2002a; Jacobs et al., 2000). The R78G07 and R91H05 lines of the Janelia Farm Flylight Gal4 line collection (Jenett et al., 2012; Pfeiffer et al., 2008) were previously described (Chapter 2). The A307/CyO; $Ptp69D^{*}$/TM6β, c17/CyO; $Ptp69D^{*}$/TM6β and $ShakB$/CyO; $Ptp69^{*}$/TM6β stocks were generated (whereby the * is representative of each of the three alleles: $Ptp69D^{10}$, $Ptp69D^{18}$, $Ptp69D^{20}$) for the rescue experiments and crossed to the various UAS-$Ptp69D$ lines (Table 4.1) that had been previously recombined onto the $Df(3L)^{8ex34}$ deficiency chromosome (Garrity et al., 1999). All genetic crosses were performed on standard fly media at 25°C and 2-5 day old flies were used in all of the experiments.
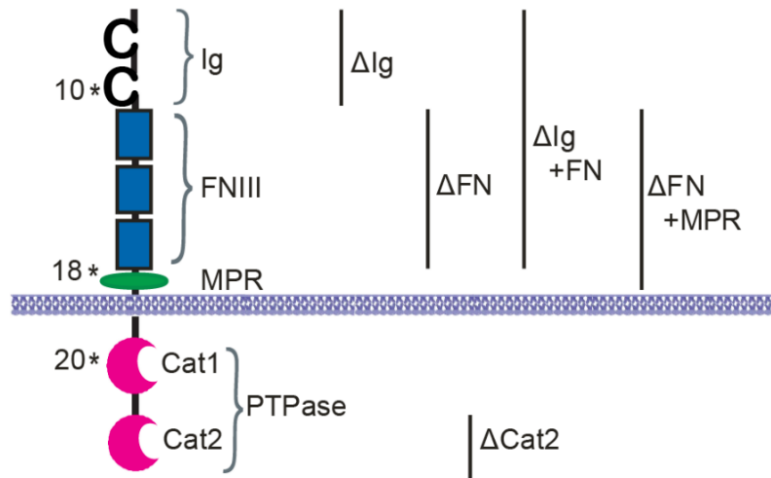
Figure 4.1 The UAS-*Ptp69* Constructs.

Schematic of PTP69D protein structure, indicating the mutation sites (*) representative of the Ptp69D[10], Ptp69D[18] and Ptp69D[20] alleles (C. Desai & Purdy, 2003). Deletions (Δ) in transgenic constructs used for structure-function analysis are depicted by lines adjacent to the molecule (Garrity et al., 1999). Additionally a construct with aspartic acid to alanine (D-A) conversions in the both catalytic domains (Cat1 and Cat2) was used that is not depicted.

Table 4.1 Description of *UAS-Ptp69D* Constructs

Construct	Description
UAS-*Ptp69D*$^{\Delta Ig}$	deletes both Ig domains (residues 30–225)
UAS-*Ptp69D*$^{\Delta FNIII}$	deletes all three FNIII domains (residues 236–534)
UAS-*Ptp69D*$^{\Delta Ig,FNIII}$	deletes Ig and FNIII domains (residues 30–534)
UAS-*Ptp69D*$^{\Delta FNIII,MPR}$	deletes FNIII domains and MPR (residues 236–796)
Ptp69D$^{\Delta Cat2}$	deletes second phosphatase domain (residues 1174–1462)
UAS-*Ptp69D*$^{Cat1-DA}$	point mutation in catalytic aspartate residue (aspartate→alanine at residue 1065) of the first phosphatase domain
UAS-*Ptp69D*$^{Cat1/2-DA}$	point mutations in catalytic aspartate residues of both phosphatase domains (aspartate→alanine at residues 1065 and 1354, respectively)

4.3.2   Electrical stimulation of GF neurons and analysis of muscle potentials

The method of obtaining electrophysiological recordings from the GFC has been described previously (Chapter 2).

4.3.3   Dye injections and immunohistochemistry of the GF.

Dye injection and immunohistochemistry methods have previously been described (Chapter 2).

4.4 Results

4.4.1 Over-expression of wild type and mutant PTP69D in the GFC

In order to determine potential gain of function phenotypes, over-expression of PTP69D in the GFC was assessed. Weak presynaptic over-expression of *UAS-Ptp69D^{WT}* with the c17 Gal4-driver had no effect on anatomy or function of the GF (Figure 4.2 A, F). However, strong presynaptic overexpression using the R91H05 (FF= 75%) and R78G07 (FF=65%) driver lines mildly affected the function of the GF-TTM pathway (Figure 4.2F), which was associated with slightly shorter and skinnier GF terminals (Figure 4.2B). In contrast, post-synaptic over-expression using the ShakB-Gal4 line had no effect on anatomy or function of the GF (Figure 4.2 E, F). This suggests that regulation of target protein dephosphorylation by PTP69D is critical and delicately balanced for the development of a functional GF terminal.

Although both catalytic domains in RPTPs are capable of dephosphorylating substrates, the catalytic domain that is more proximal to the membrane is thought to catalyze the majority of dephosphorylation reactions (Streuli et al., 1989). The glycine to serine missense mutation, in the Cat1 domain in *Ptp69D^{20}* mutants, was shown to inhibit catalytic activity (Marlo and Desai, 2006). Similarly, an aspartic acid to alanine (D-A) conversion in the catalytic domain is predicted to prevent dephosphorylation, consequently the RPTPs function as "substrate traps" because they remain tightly bound to the target protein (Flint et al., 1997). To further assess the structural-functional relation of PTP69D, a previously generated *Ptp69D* construct with the D-A mutation in the Cat1 domain in wild type GFs either pre- or post-synaptically was expressed (Garrity et al., 1999; Tiganis and Bennett, 2007). Strong presynaptic expression with the R91H05

and R78G07 drivers caused morphological and functional phenotypes similar to *Ptp69D²⁰* mutants, albeit with less severity. The majority of GF terminals were severely stunted (Figure 4.2 D, E), and the ability of the GF-TTM pathway to follow high frequency stimulation was impaired (Figure 4.2F). Consistent with our previous result, no anatomical or electrophysiological phenotypes were observed with postsynaptic expression (Figure 4.2 C, E, F).
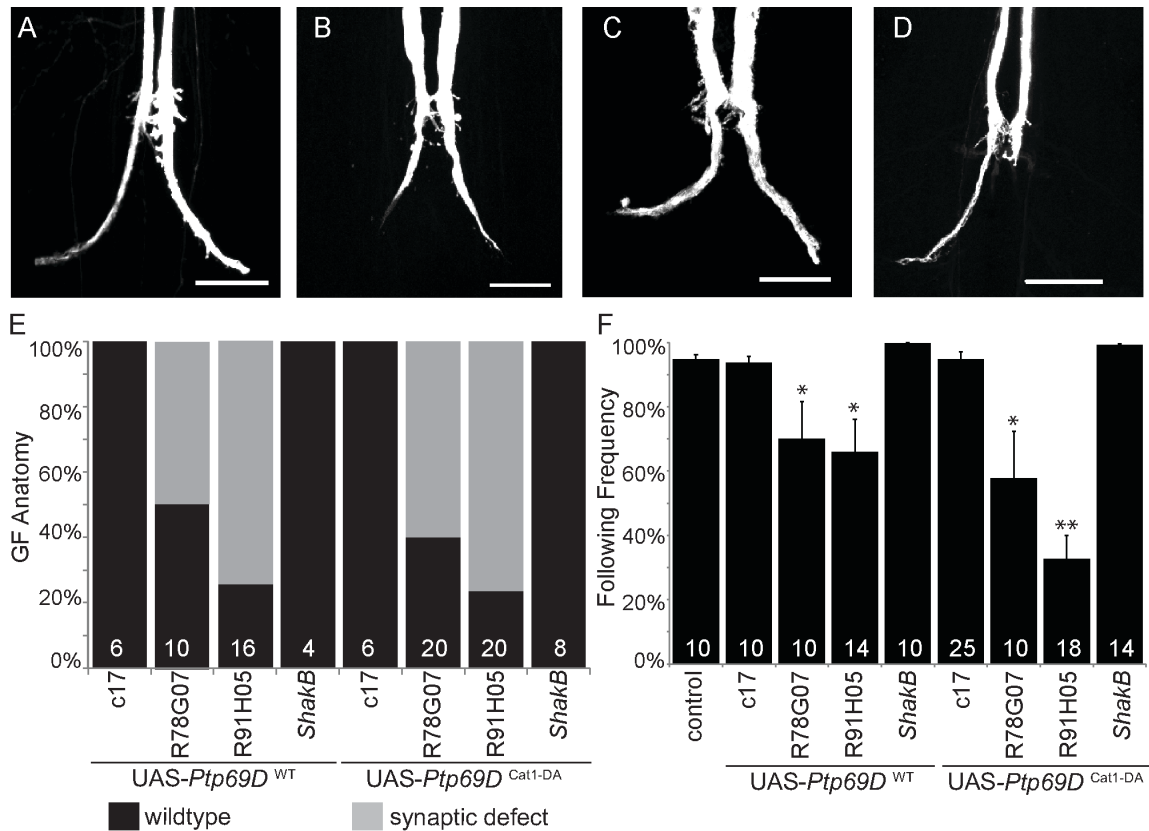
Figure 4.2 Expression of wild type PTP6D and its catalytically inactive mutant in the Giant Fiber Circuit.

A-D) GF morphology was revealed with injections of Rhodamine-dextran into the GFs. Scale bars are 20 μm. A) Weak presynaptic overexpression of wild type PTP69D with the c17 Gal4-driver did not affect the morphology of the GF terminal. B) Strong presynaptic overexpression *of Ptp69D^{WT}* in the R78G07 line resulted in a shorter and skinnier GF terminal. C) Expression of *UAS-Ptp69D^{WT}* in the ShakB-Gal4 line did not affect GF morphology. D) Expression of *Ptp69D$^{Cat1-DA}$* in the GF of the R78G07 line prevented the growth of a GF terminal. E) Quantification of morphological GF defects when the *Ptp69D^{WT}* and *Ptp69D$^{Cat1-DA}$* constructs were overexpressed pre- or postsynaptically. F) Quantification of FF defects of the GF-TTM pathway when *Ptp69D^{WT}* and *Ptp69D$^{Cat1-DA}$* constructs were expressed pre- or postsynaptically in the wild type background. Mild electrophysiological effects were seen in strong presynpatic drivers (R78G07 and R91H05) with overexpression of both constructs (* = p value ≤ 0.05, ** = p value <0.001, Student's t test: two sample assuming unequal variance).

A role for tyrosine phosphorylation in axon growth and guidance has been established; however there is some evidence that some RPTPs may exhibit non-catalytic

functions as well. To explore the possibility of an activity-independent function of PTP69D a construct lacking the intracellular domain of PTP69D, UAS- $Ptp69D^{\Delta intra}$ was expressed in the giant fiber circuit. The resulting progeny had severe synaptic phenotypes. Anatomically the GFs terminated well above the area of the PSI, but did dye couple with the PSI (Figure 4.3B), failing to make contact with the TTMn. In fact, physiologically the DLM and TTM failed to respond (Figure 4.3C), correlating with the anatomical disconnect. This phenotype was exhibited with all GF drivers, however expression of the construct postsynaptically with the ShakB-Gal4 driver did not disrupt the GF anatomy or function (Table 2).

Figure 4.3   Expression of Δintra disrupts synapse formation

A) graphic depicting the deletion of the intracellular domain in the *UAS-Ptp69D^{\Delta intra}*. B) Expression of the *UAS-Ptp69D^{\Delta intra}* construct with c17 presynaptically in the GF results in severely stunted GFs, which terminate prior to the region of the PSI. Scale bar represents 20μm. C) Representative physiological trace of a c17/ *UAS-Ptp69D^{\Delta intra}* animal indicating the inability of neither the DLM nor TTM to follow high frequency stimulation (100Hz).

Table 4.2 Summary of Physiological Phenotypes of *UAS-Ptp69D^{Aintra}* Expressed in the GFC

Genotype	n	TTM Latency in msec (±SE)	TTM Following Frequency 100Hz (±SE)	TTM disconnected	DLM disconnected
A307	36	–	–	94%	100%
c17	10	–	–	100%	100%
c4222	10	–	–	100%	100%
elav	8	–	–	100%	100%
ShakB	12	1.86 (±0.16)	10% (±1%)	0%	0%

4.4.2   PTP69D has a cell autonomous pre-synaptic function

The *Ptp69D* mutant phenotypes clearly demonstrate an endogenous function for PTP69D in GF circuit development. However, it is not yet clear whether PTP69D function is required in the GF, the TTM or both for the proper development of the GF to TTM synapse. In order to address this question the spatial requirements for PTP69D was determined with a cell-autonomous rescue approach of the *Ptp69D^{10}, Ptp69D^{20}* and *Ptp69D^{18}* phenotypes.

Figure 4.4 *Ptp69D²⁰* **rescued presynaptically by wild type PTP.**

Quantification of the GF-TTM response of wild type and mutant Ptp69D20 animals with pre or postsynaptic expression of UAS-Ptp69DWT in a Ptp69D20/Df(3L)8ex34 deficient background. The pathway was restored with expression of wild type protein with the c17 Gal-driver, increasing the ability to follow high frequency stimulation at 100Hz (** = p<0.001).

To analyze the spatial requirement for the signaling of the Cat1 domain, a wild type *Ptp69D* construct in a *Ptp69D²⁰/Df(3L)^8ex34* background was utilized. Pre-and postsynaptic expression of UAS-*Ptp69D^WT, Df(3L)8ex34* in *Ptp69D²⁰* mutants using A307, significantly rescued the physiology of the GF mutant phenotype (Figure 4.4). Presynaptic expression of UAS-*Ptp69D^WT* with the c17 Gal4 driver in this mutant background restored the synaptic function in virtually all animals as well (Figure 4.4) and resulted in normal sized terminals (Figure 4.5A). In contrast, postsynaptic expression of wild type PTP69D protein using the *ShakB*-Gal4 driver did not rescue the function of the GF-TTM pathway, and the GF terminal remained severely stunted in these animals

(Figures 4.4 and 4.5B). This suggests that Cat1 activity of PTP69D is required in the GF for terminal growth.
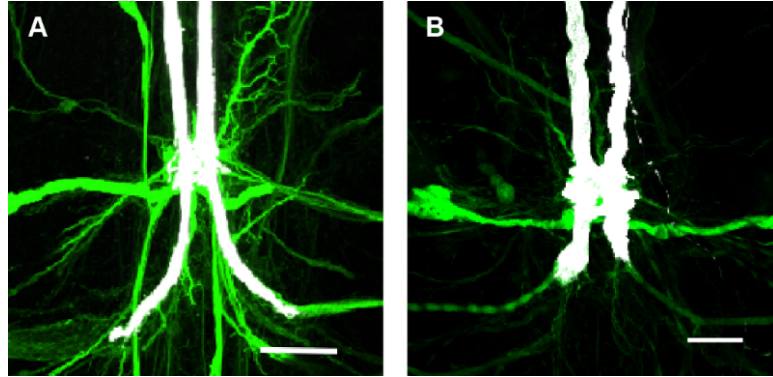
Figure 4.5   Ability of wild type contructs to rescue synaptic defects of *Ptp69D[20]* mutants presynaptically.

A) The GF morphology and dye-coupling to the postsynatic target neurons is normal in c17/+; Ptp69D[20]/UAS-PTP69D[WT], Df(3L)[8ex34] animals. B) The GF terminal was stunted in ShakB-Gal4/+; Ptp69D[20]/UAS-Ptp69D[WT], Df(3L)[8ex34] animals.

The extracellular domains of PTP69D are important for the function of the molecule. Examination of the ability of wild type PTP69D to rescue the *Ptp69D[10]* and *Ptp69D[18]* phenotypes spatially was next addreesed.   Expressing the same UAS-Ptp69D[WT, Df(3L)8ex34] rescue construct in both *Ptp69D[10]* and *Ptp69D[18]* mutant backgrounds produced similar results. In both cases, simultaneously driving expression both pre- and post-synaptically in the GFC rescued the GF-TTM synapse anatomically and physiologically.   In *Ptp69D[10]* the following frequency increased from 19% to 91% (Figure 4.6A), while in *Ptp69D[18]* it improved from 29% to 94% (Figure 4.7A).   To dissect the spatial requirement further the c17 and ShakB Gal4 drivers were tested. The morphological and functional phenotypes were rescued with presynaptic but not

postsynaptic expression in both *Ptp69D[10]* (Figure 4.6B, C) and *Ptp69D[18]* (Figure 4.7B, C). The stunted synaptic terminal persisted when wild type protein was expressed postsynaptically in a *Ptp69D[10]* mutant background, while it restored to a normal sized terminal with presynaptic expression. Similarly with *Ptp69D[18]*, presynaptic expression restored the GF morphology but left the terminal bifurcated with post synaptic expression.
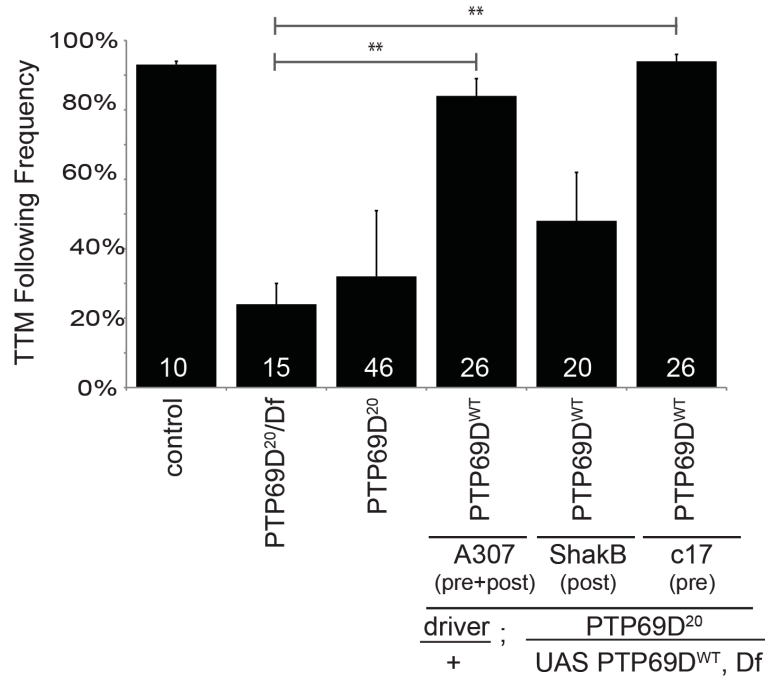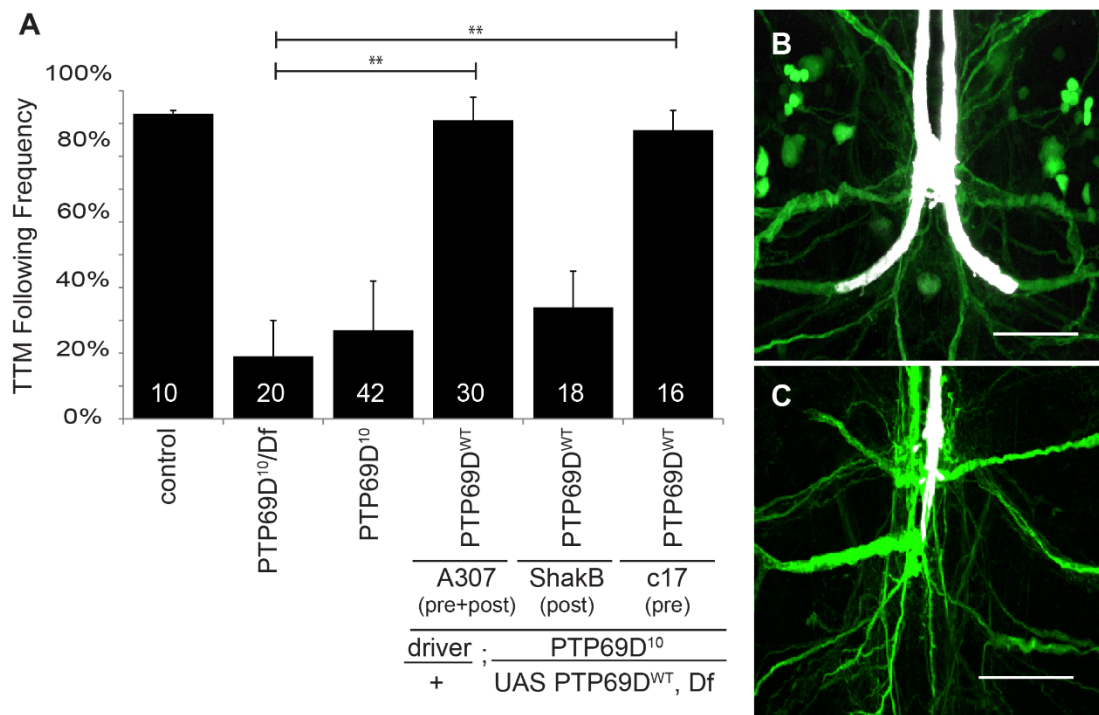

Figure 4.6 *Ptp69D[10]* rescued presynaptically by wild type PTP.

A) Quantification of the GF-TTM pathway in wild type and mutant Ptp69D[10] animals with pre or postsynaptic expression of UAS-Ptp69D[WT] in a Ptp69D[10]/Df(3L)[8ex34] deficient background. The c17 Gal-driver improved the ability of the GF-TTM pathway to follow stimuli at 100Hz to wild type levels (** = $p < 0.001$). B) The GF morphology and dye-coupling to the postsynaptic target neurons is normal on c17/+; Ptp69D[10]/UAS-PTP69D[WT], Df(3L)[8ex34] animals. C) The GF terminal remained stunted in ShakB-Gal4/+; Ptp69D[10]/UAS-Ptp69D[WT], Df(3L)[8ex34] animals note only one GF is shown.
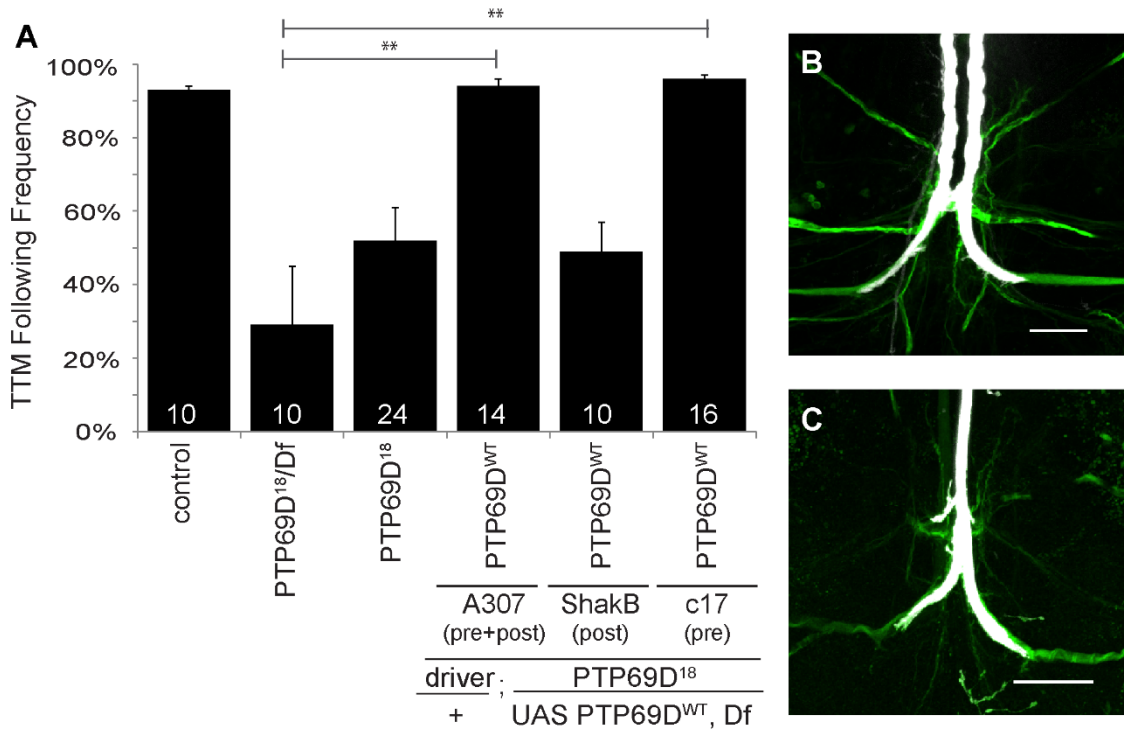
Figure 4.7 *Ptp69D^{18}* **rescued presynaptically by wild type PTP.**

A) Quantification of FF defects of the GF-TTM pathway in wild type and mutant Ptp69D^{18} animals with pre or postsynaptic expression of UAS-Ptp69D^{WT} in a Ptp69D^{18}/Df(3L)^{8ex34} deficient background. The GF-TTM pathway was restored with expression of wild type protein with the c17 Gal-driver, increasing the ability to follow high frequency stimulation at 100Hz (** = p<0.001). B) The GF morphology and dye-coupling to the postsynaptic target neurons is normal on c17/+; Ptp69D^{18}/UAS-PTP69D^{WT}, Df(3L)^{8ex34} animals. C) With postsynaptic expression the GF was still bifurcated in ShakB-Gal4/+; Ptp69D^{18}/UAS-Ptp69D^{WT}, Df(3L)^{8ex34} animals, note only one GF is shown.

In conclusion, our results demonstrate a cell autonomous role of PTP69D in the GF, which has a function in terminal growth. This is consistent with the earlier described knockdown experiments using RNAi, which suggest a presynaptic role for PTP69D in the GF, but not its post synaptic targets.

103

4.4.3 Structure-function analyses of PTP69D signaling via Cat1 domain

The glycine to serine missense mutation in the Cat1 domain in $Ptp69D^{20}$ mutants was shown to inhibit catalytic activity (Marlo & Desai, 2006). In order to determine what domains are required for outside-in signaling of PTP69D, mutant constructs of $UAS\text{-}Ptp69D^*$ (* indicates the various constructs utilized see Table 4.1) presynaptically in a $Ptp69^{20}/Df(3L)^{8ex34}$ background were expressed for ability to rescue. The various $Ptp69D$ constructs (Table 4.1) lacked either the Ig domains (ΔIG), FNIII domains (ΔFN), both domains (ΔIG+FN), or FNIII and MPR domains (ΔFN+MPR, Figure 4.1). In addition, constructs with an intracellular deletion of the Cat2 domain (ΔCat2) or aspartic acid to alanine missense mutations in both catalytic domains (Cat1/2-DA) were tested to examine if they could rescue the defects of $Ptp69^{20}/Df(3L)^{8ex34}$ animals.

The data revealed that expression of constructs with deleted Ig domains (ΔIG and ΔIG+FN) did not rescue the function of the GF synaptic terminal (Figure 4.8A). This suggests that PTP69D requires the Cat1 and the Ig domains for GF terminal growth. Similarly, neither the expression of $UAS\text{-}Ptp69D^{\Delta Cat2}$ nor $UAS\text{-}Ptp69D^{Cat1/2\text{-}DA}$ with the c17 driver was able to rescue the synaptic or morphological defects of $Ptp69D^{20}/Df(3L)^{8ex34}$ animals. Thus, GF terminal function and growth involves both catalytic domains (Figure 4.8B). In contrast, expression of $UAS\text{-}PTP69D^{\Delta FN}$ and $UAS\text{-}PTP69^{\Delta FN+MPR}$ in $Ptp69D^{20}/Df(3L)^{8ex34}$ mutants was able to rescue the synaptic function, as well as the GF terminal anatomy (Figure 4.8C). This demonstrates that Cat1 function does not require the FNIII or the MPR domains in GF terminal growth.

Finally, it should be noted that the failure of constructs lacking the Ig domain or the Cat2 did not attribute to a lack of expression at the cell surface as the same constructs

have previously been shown to recue photoreceptor targeting when expressed in a loss of function background (Garrity et al., 1999). In addition, the expression of the diverse mutant constructs had little or no effect on the function of the GF-TTM pathway when they were expressed with the c17 Gal4 driver in a wild type background (Figure 4.8D). This suggests that inability of mutant *Ptp69D* constructs to rescue the synaptic phenotypes in a *Ptp69D^{20}/Df(3L)^{8ex34}* background is not due to a poisonous or dominant negative effect, but rather due to a lack of a specific function.

Figure 4.8 Rescue of *Ptp69D^{20}* mutants with targeted presynaptic expression of mutant *Ptp69D* constructs.

A) Quantification of FF defects of the GF-TTM pathway when wild type and mutant *Ptp69D* constructs were expressed pre- or postsynaptically in a *Ptp69D^{20}/Df(3L)^{8ex34}* background. Only presynaptic expression of UAS-*Ptp69D^{ΔFN}* and UAS-*Ptp69D$^{ΔFN+MPR}$* with the c17 Gal4-driver improved the the ability of the GF-TTM pathway to follow stimuli at 100 Hz to wild type levels (** = p value<0.001).   Expression of UAS-*Ptp69D^{ΔFN}* **(B)** with the c17 Gal4driver line resulted in normal sized GF terminals, while GF terminals were severely stunted in c17/+; *Ptp69D^{20}*/UAS-*Ptp69D$^{Cat1/2-DA}$, Df(3L)^{8ex34}* animals **(C)**. **D)** Quantification of the FF of the constructs indicating they do not have dominate negative effects.

106

4.4.4 Structure-function analyses of PTP69D signaling via extracellular domains

Utilizing the same constructs, the functionality and anatomy of domain relevant for the rescue of *Ptp69D^{10}* were assessed. Remarkably, *Ptp69D^{10}* and *Ptp69D^{20}* alleles had GFs who were morphologically indistinguishable and physiologically similar. However, structure-function analysis of these two alleles for rescue experiments yielded differing results. Expression of a construct lacking all Ig domains in *Ptp69D^{20}/Df(3L)^{8ex34}* animals did not yield any progeny. Expression of constructs with deleted fibronectin domains (ΔIG+FN) did not rescue the function of the GF synaptic terminal (Figure 4.9A). Though not statistically significant, the ability to follow high frequency stimulation reduced from 19% to 16%. However, the morphology of the GF remained stunted in *c17/+; Ptp69D^{10}/UAS-Ptp69$^{ΔIG+FN}$, Df(3L)^{8ex34}* animals (Figure 4.9B). Conversely, three constructs – *UAS-Ptp69D^{ΔFN}, UAS-Ptp69D$^{ΔFN+MPR}$* and *UAS-Ptp69D$^{Cat1/2-DA}$* – exhibited the ability to rescue the defects of *Ptp69D^{10}/Df(3L)^{8ex34}* animals. These findings support the conclusion that the immunoglobulin domains are necessary for the function of PTP69D and lack of these domains led to lethality.
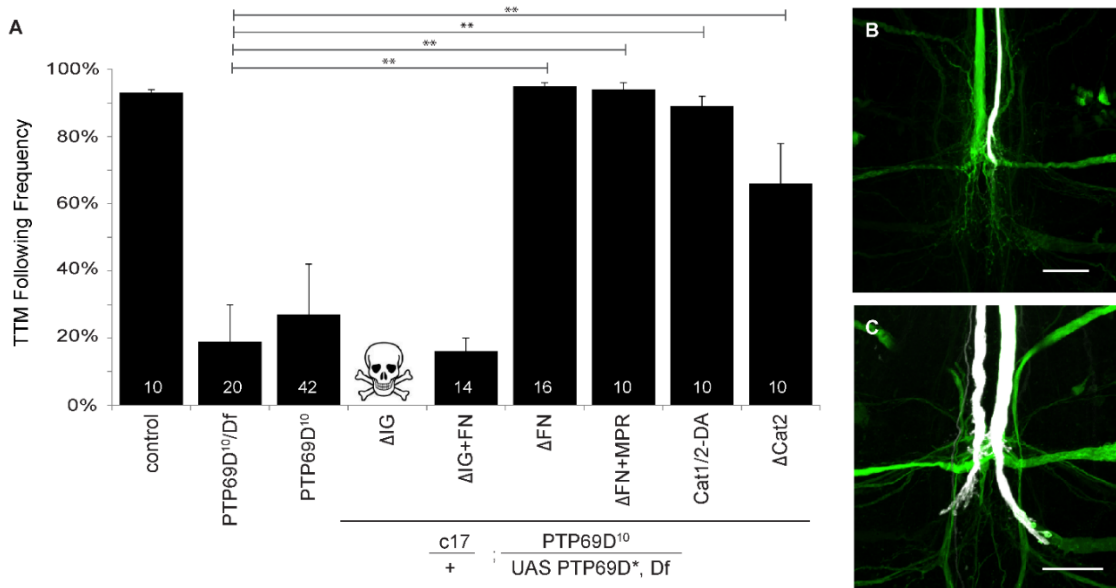
Figure 4.9 Rescue of *Ptp69D*^{10} mutants with targeted presynaptic expression of mutant *Ptp69D* constructs.

A) Quantification of FF defects of the GF-TTM pathway when wild type and mutant Ptp69D constructs were expressed pre- or postsynaptically in a Ptp69D10/Df(3L)8ex34 background. Only presynaptic expression of UAS-Ptp69DΔFN, UAS-Ptp69DΔFN+MPR and UAS-Ptp69DCat1/2-DA with the c17 Gal4-driver improved the the ability of the GF-TTM pathway to follow stimuli at 100 Hz to wild type levels (** = p value<0.001). B) The GF terminals remained severely stunted in c17/+; Ptp69D10/UAS-Ptp69ΔIG+FN, Df(3L)8ex34 animals. C) Expression of UAS- Ptp69DCat1/2-DA with the c17 Gal4driver line partially rescued the GF terminals in c17/+; Ptp69D10/UAS-Ptp69DCat1/2-DA, Df(3L)8ex34 animals.

Structure-function analysis of *Ptp69D*^{18} yielded results which may be the result of the temperature sensitivity of the allele. As described in Chapter 3, *Ptp69D*^{18} is a highly temperature sensitive allele which was characterized by lethality at 25°C and a mutant GF morphology, in which the GF terminals varied between stunted and bifurcated. Interestingly, structure-function experiments was only able to yield a partial rescue in *c17/+; Ptp69D*^{18}*/UAS-Ptp69D*$^{Cat1/2-DA}$*, Df(3L)*^{8ex34} animals (Figure 10B), whereby one GF terminal is wild type while the other GF terminal is bifurcated. These findings

support the model of the fibronectin type III repeats in PTP69D function and indicate that

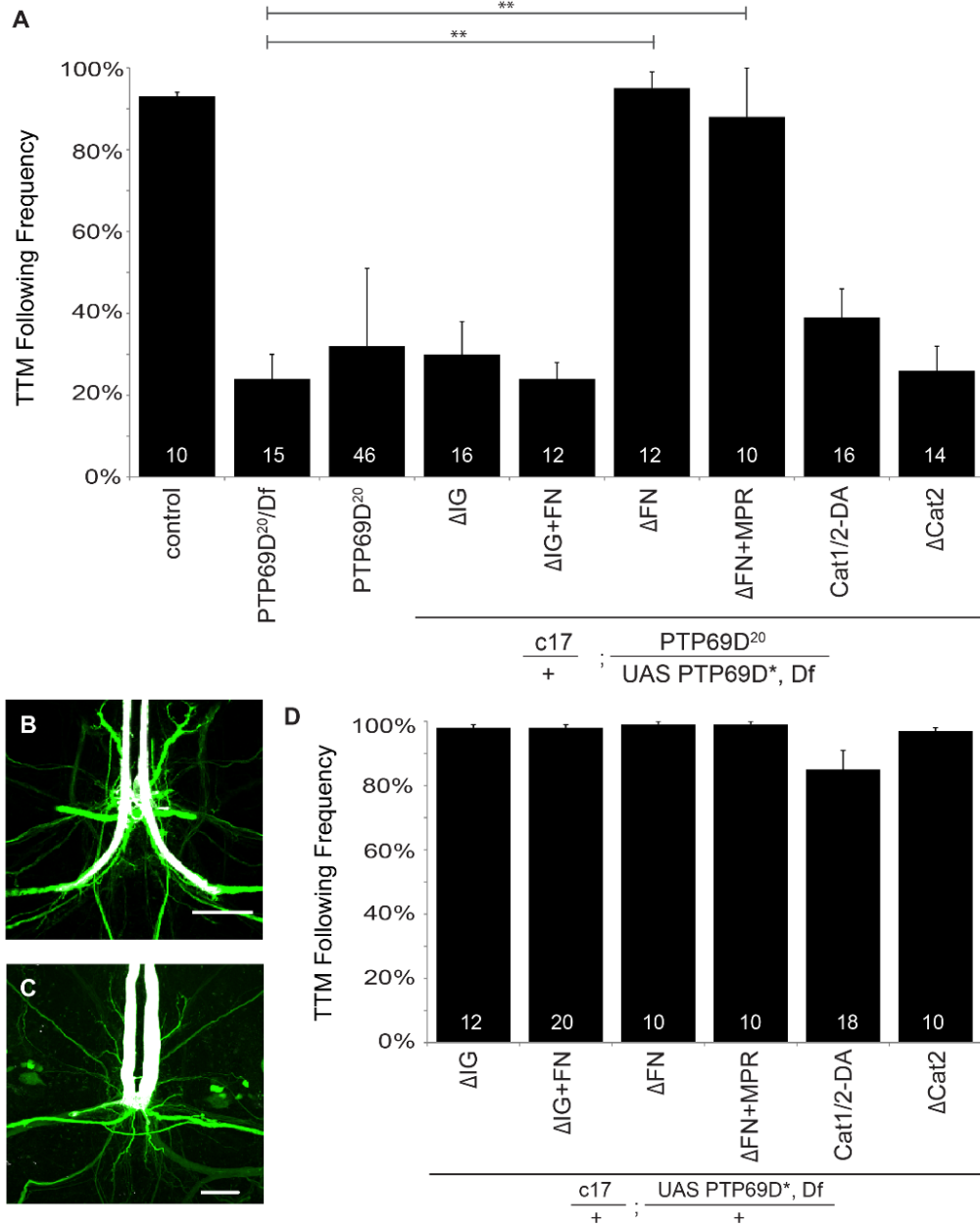they are essential for proper GF terminal growth and maturation.
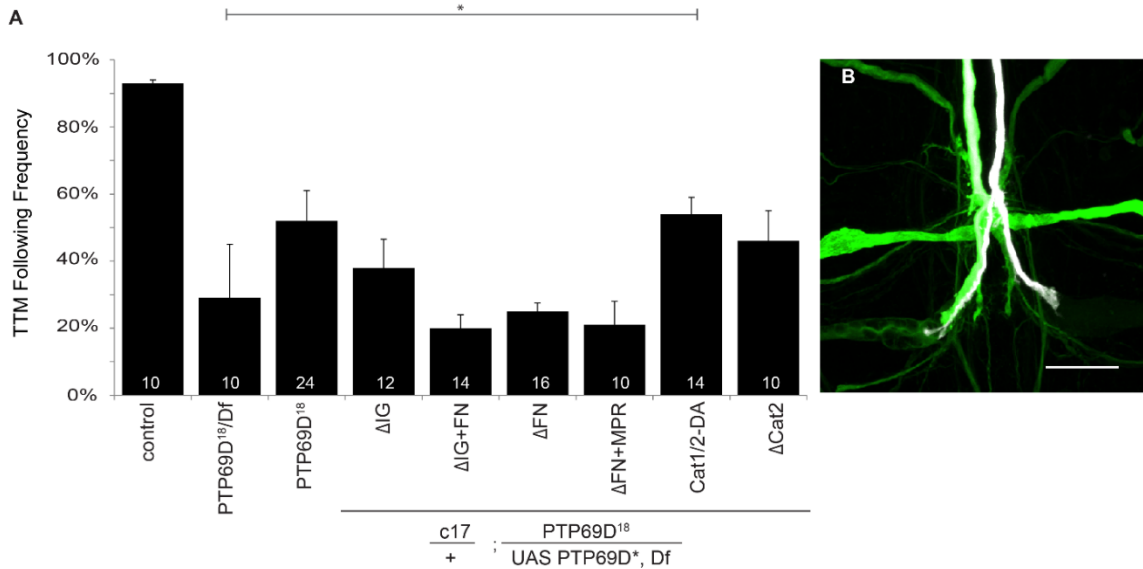
Figure 4.10 Rescue of *Ptp69D*[18] mutants with targeted presynaptic expression of mutant *Ptp69D* constructs.

A) Quantification of FF defects of the GF-TTM pathway when wild type and mutant *Ptp69D* constructs were expressed pre- or postsynaptically in a *Ptp69D*[18]*/Df(3L)*[8ex34] background. Only presynaptic expression of *UAS-Ptp69D*[Cat1/2-DA] with the c17 Gal4-driver improved the the ability of the GF-TTM pathway to follow stimuli at 100 Hz to wild type levels (* = p value<0.05). **B)** Expression of *UAS- Ptp69D*[Cat1/2-DA] with the c17 Gal4driver line partially rescued the GF terminals in *c17/+; Ptp69D*[18]*/UAS-Ptp69D*[Cat1/2-DA]*, Df(3L)*[8ex34] animals.

4.5 Discussion

In this study, we uncovered and characterized a novel role for PTP69D in synaptic

terminal growth in the CNS, which is distinct from its previously described functions in

guidance and target recognition. A potential function for PTP69D in terminal growth in

the peripheral nervous system has been previously implied by the finding that bouton

numbers at the larval neuromuscular junction are reduced in *Ptp69D* null mutants, but

functional requirements have not been determined (Hofmeyer & Treisman, 2009). Here,

we used structure-function analyses to reveal the domains required in synaptic terminal growth of the GF.

4.5.1 Structural and Functional requirements for PTP69D in terminal growth.

In *Ptp69D* null mutants, bouton numbers at the larval neuromuscular junction are reduced (Hofmeyer & Treisman, 2009), suggesting a synaptic function for PTP69D; however the functional requirements remain to be determined. Here, PTP69D is shown to be required for terminal growth in the central nervous system. The lack of phosphatase activity in the Cat1 domain in *Ptp69D*[20] mutants is sufficient to prevent the GF growth in all animals without affecting guidance or targeting. Cell autonomous expression of full-length *Ptp69D* almost completely restores proper GF synapse formation when it is expressed in the GF itself in all three alleles, *Ptp69D*[10], *Ptp69D*[18] and *Ptp69D*[20], but not in its postsynaptic target. This demonstrates that there are various functions of PTP69D in the formation of a proper synapse, relating to the distinct structure of the RPTP.

Anatomical and functional synaptic defects of *Ptp69D*[10] animals are indistinguishable from *Ptp69D*[20] mutants, suggesting a critical role for the Ig-domain and the Cat1 domain, in GF terminal growth. Furthermore, *Ptp69D*[10] and *Ptp69D*[20] mutants do not complement each other. In addition, expression of PTP69D lacking the fibronectin domains, but not PTP69D lacking the Ig-domains, was able to rescue the synaptic function of the GFs. This finding suggests that the Ig-domains, but not the FNIII domains, are involved in outside-in signaling of PTP69D via the Cat1 domain during terminal growth. In contrast, R1-R6 targeting to the lamina did not require the Ig-domains, but was dependent on the FNIII domains. In addition, while catalytic activity

of either Cat1 or Cat2 was sufficient for normal development in the visual system, this was not the case for GF terminal growth, as demonstrated by the synaptic defects of $Ptp69D^{20}$ mutants. However, the function of both catalytic domains in terminal growth is implied by our finding that expression of $Ptp69D^{\Delta Cat2}$ did not rescue the synaptic defects of $Ptp69D^{20}$ mutants. A potential explanation is that Cat1 and Cat2 domains regulate each other forming PTP69D dimers. Additionally, the results of expression of the construct lacking the intracellular domain suggests that it likely functions as a dominant negative, possibly forming a dimer with wildtype PTP69D, either by preventing its activation or by sponging the ligand preventing its interaction with wiltype PTP69D. Interestingly, R7 targeting to the medulla requires the FNIII domains of tyrosine phosphates Dlar, while the catalytic activity is provided by PTP69D and not Dlar (Hofmeyer & Treisman, 2009). This demonstrates that the mechanisms of PTP69D signaling during GF terminal growth and photoreceptor targeting are distinctive. The results suggest a general function for the FNIII domains of tyrosine phosphatases in axon targeting. In contrast, this study demonstrates that regulation of catalytic activity via the Ig-domain is critical during growth of the synaptic terminal, which does not require the FNIII domains or the membrane proximal domain.

Aside from the catalytic function of PTP69D our results suggest that the extracellular domains play critical functions in the function of the molecule in synapse formation. Like other receptor protein tyrosine phosphatases, it likely has the ability to communicate external signals across the cell membrane to direct intracellular activity. Expression of PTP69D lacking the fibronectin domains and membrane proximal region was able to rescue the synaptic function of the GFs in $Ptp69D^{10}$ mutants. This finding

suggests that the Ig-domains, but not the FNIII domains, are required for GF terminal growth. The observance of the split terminal in *Ptp69D[18]* mutants indicate that targeting is a likely function of the fibronectin repeats of PTP69D. Alternatively, the phenotype of these mutants could be described as a midline crossing defects suggesting a role of the fibronectin domain in this phenomenon. In fact, DPTP10D and PTP69D were found to be positive regulators of Slit/Roundabout repulsive signaling (Sun et al., 2000). Thus, this midline crossing phenotype evident in *Ptp69D[18]* mutants may be the result of a disrupted Slit/Robo signaling pathway. Collectively, the extracellular structure function experiments highlight differing roles for the immunoglobulin and fibronectin domains in PTP69D function at a central synapse.

Another likely model for PTP69D signaling is that the extracellular Ig domains mediate crucial interactions with other transmembrane proteins, or that PTP69D may function as homodimers presynaptically in coordinating proper synapse formation. The explanation for the phenotype seen by *PTP69D[20]*, the catalytic mutant allele, is that the active site functions not only as a typical phosphor-tyrosine binding domain but also as an adapter domain (Marlo & Desai, 2006). Thus, the point mutation in this domain disrupts proper recruitment, localization, and signaling in a yet uncharacterized signaling cascade, causing aberrant synaptic phenotypes. This study furthermore implicates an outside-in signaling paradigm, whereby the Ig domain binds in cis with other PTP6D molecules, bringing the regulatory phosphatase domains in proximity to one another. This allows the inactivation of the catalytic function of the molecule during early neurodevelopment, when guidance and targeting are critical. When developmentally necessary, a switch is flipped that disables the inhibition, and allows the extracellular

domains to recruit to synaptic hubs whereby the phosphatase can act on substrates critical for proper synapse formation.

In summary, PTP69D is essential for proper GF development and regulation of the Cat1 activity involves the Ig domains, but not the FNIII and MPR domains, during GF terminal growth. Additionally, the extracellular domains likely serve disparate roles in synapse formation and function. The results suggest a general function for the FNIII domains of PTP69D in either preventing axonal branching or targeting the GF only to one synaptic target, while the Ig domains are possibly involved in forming homodimers in cis.

5   CONCLUSIONS AND FUTURE DIRECTIONS

5.1   Future Directions

The future of PTP69D function in neurodevelopment circle around three major goals. The first and possibly most important is to identify the substrates of PTP69D. Secondly, future directions should seek out to understand the function of the second catalytic domain of PTP69D. Lastly, the next challenge for continuing research will be to identify the signaling pathways with which PTP69D is involved.

5.1.1   Identification of PTP69D Substrates

The identification of PTP69D substrates will be imperative to the development of models of action of PTP69D, as well as determining its function in various signaling cascades throughout development. Since the finding that a mutation in the conserved aspartic acid in the WPD loop is responsible for the stabilization of substrate binding by decreasing the rate of catalysis of the enzyme, many studies have sought to identify PTP substrates (Ariño & Alexander, 2004). The development of tools such as "substrate trap" constructs should provide knowledge of the interacting partners of PTP69D. The catalytic cleft of tyrosine phosphatases contains a unique aspartate residue that acts as a proton acceptor for the catalytic cysteine of the enzyme. The mechanism "substrate trapping" is mediated by a D-to-A mutation, whereby a mutation changes the amino acid aspartate into alanine in the catalytic domain of the phosphatase. This point mutation

in this substrate trap version of a PTP should cause it to bind and fail to release bound substrate (Flint et al., 1997; Tonks & Neel, 1996). This mutation yields the phosphatase nearly functionally and catalytically inactive (Blanchetot, Chagnon, Dube, Halle, & Tremblay, 2005). Alternatively, the substrate trapping mutants still permits binding to substrates but hinders the phosphatase from dephosphorylating them. Hence the substrates become "trapped" or bound so that they can subsequently be identified. By using a tagged substrate trapping construct rather than a tagged wild type PTP69D construct, there will be an increased likelihood of being able to pull down a substrate. This is due to the fact that the interaction with a wildtype PTP69D and a substrate is only temporary – "kiss and leave" – and maybe also easily disrupted by the protein extraction conditions required for co-immunoprecipitation protocols.

The present work attempted to utilize "substrate trap" mutants to trap, pull down and identify trapped substrates with mass spectroscopy, but without success. Structurally PTP69D is a transmembrane protein, and as such removal of the protein from the membrane proved extremely difficult. The disruption of the membrane required finesse to remove the transmembrane protein while keeping it functionally relevant. Often detergents used to solubilize the protein from the membrane render the protein inactive and useless for future functional studies. Though the generation of "substrate trap" mutants has been developed there has been very few studies demonstrating of successful use of this technique (Blanchetot et al., 2005). Future explorations will require strong biochemical backgrounds to utilize "substrate traps" for the identification of PTP69D substrates.

This study suggests that outside-in signaling mechanism whereby the action via the Cat1 domain involves the Ig-domains of PTP69D during GF terminal growth. Thus, an additional strategy for identification of ligands of PTP69D might exploit extracellular mutations. As such, *Ptp69D[10]* may prove a useful tool for identification of PTP69D-specific ligands. Immunoglobulin domains are known to be involved in a variety of binding functions, including their involvement in cell-cell recognition and role as cell-surface receptors. Thus additional, studies can be used to test the ability of substrates to enhance or disrupt the binding of substrates to PTP69D extracellularly.

5.1.2 Determining the function of the Cat2 phosphatase domain of PTP69D

The distal phosphatase or Cat2 domain of the receptor protein tyrosine phosphatases have many conserved motifs which are present in the membrane proximal phosphatase. Additionally, they bear sequences highly conserved among members of their family. These similarities suggest that the Cat2 phosphatase is functionally important. Though the second phosphatase domain is proposed to have regulatory function in most RPTPs, the function in PTP69D remains unknown. Earlier studies, using a deletion mutant found that the Cat2 domain of PTP69D was required for restoring viability of *Ptp69D* mutants (Garrity et al., 1999). On the other hand, this study found that expression of an intracellular deletion of the CAT2 domain (ΔCat2) or aspartic acid to alanine missense mutations in both catalytic domains (Cat1/2-DA) did not rescue the defects of *Ptp69[20]/Df(3L)[8ex(34)]* animals (Chapter 4). These findings suggest that the function of the phosphatase domains may be dependent on one another for function, however currently constructs haven't been developed to test this theory. Thus, additional

mutants in both phosphatase domains of PTP69D must be constructed to identify the regions of the Cat2 domain important for its function.

5.1.3   Signaling Pathways of PTP69D

The function of PTP69D in axon guidance, targeting, and now synapse formation has been established; however the mechanisms by PTP69D function in these axons is still largely not understood. How PTP69D is activated and the proteins with which it interacts are unknown. Future research would benefit from seeking to gain further understanding of the signaling pathways regulated by PTP69D in the nervous system. These studies should also seek to identify the proteins that they bind to and genetically interact. Investigating these interactions should yield further understanding into the pathways that regulate these processes in vivo.

5.2   Concluding Remarks

Mutant alleles of *Ptp69D* have been subjected to physiological, anatomical and genetic analysis.   The *Ptp69D* mutant alleles displayed a range of phenotypic physiologies and morphologies. Additionally, they provided a unique opportunity to investigate the structural determinants of PTP69D function in synapse formation and function. Structural functional experiments further examined the ability to spatially rescue the phenotypes and to identify the structures or domains necessary for the function of the molecule. Exploration of these alleles along with the constructs provided evidence that, in addition to its role in axon guidance and targeting, that the function of this protein

requires the phosphatase and immunoglobulin domains. This dissertation is the first detailed characterization of the *Drosophila* receptor protein tyrosine phosphatase PTP69D in synapse formation in the adult central nervous system.

APPENDICES

A.1   Examination of Neuroglian and PTP69D Genetic Interaction

Our lab has described a novel role for Neuroglian (Nrg), the *Drosophila* ortholog to the human L1 cell adhesion molecule (CAM), in giant synapse formation and the phosphorylation status of the tyrosine in the FIGQY ankyrin binding motif is important for its function in synapse formation (Enneking et al., 2013; Godenschwege, Kristiansen, Uthaman, Hortsch, & Murphey, 2006).   Neuroglian is a transmembrane protein consisting of a variable extracellular domain and a distinct and conserved cytoplasmic domain that interacts with various cytoskeletal proteins.   The extracellular domain is comprised of immunoglobulin (Ig) domains and membrane proximal fibronectin type three repeats (Maness & Schachner, 2007).   The cell adhesion molecule is integrated with the cytoskeleton via cytoskeletal linker proteins interacting with the distinct binding sites within the cytoplasmic domain of L1-type proteins.   There have been several well characterized binding sites, however of interest to this proposal is the highly conserved stretch of amino acids which bind Ankyrin and Doublecortin, called the FIGQY motif (Garver, Ren, Tuvia, & Bennett, 1997; Kizhatil, Wu, Sen, & Bennett, 2002).   This motif is often referred to as the ankyrin binding motif and it the binding site for the Ankyrin adapter protein.   Ankyrin can only bind this motif when the tyrosine of this motif is unphosphorylated and it couples to F-actin by associating with Spectrin (Figure A.1). Conversely, in vertebrates the phosphorylated motif binds to a microtubule stabilizing protein called Doublecortin (DCX), which is important for neuronal migration (Maness & Schachner, 2007). This suggests that phosphorylation of Nrg and CAMs may play a key

120

role in modulating cytoskeletal and membrane dynamics during the assembly of the nervous system (Garver et al., 1997).

Neuroglian contains the highly conserved ankyrin-binding motif (FIGQY) and its function is regulated by phosphorylation of the tyrosine (Y) residue in the motif. The tyrosine phosphorylated Nrg ankyrin binding motif has been shown to co-localize with the protein Lis1, which possibly in combination with Doublecortin, is involved in microtubule stabilization (Pilz et al., 1998; Williams, 2009). However, the unphosphorylated ankyrin binding motif binds Ankyrin, thereby linking to the actin/spectrin cytoskeleton (Garver et al., 1997) (Figure 6.1). The missense mutation in the *nrg*^{849} allele was shown to be associated with reduced phosphorylation of the FIGQY
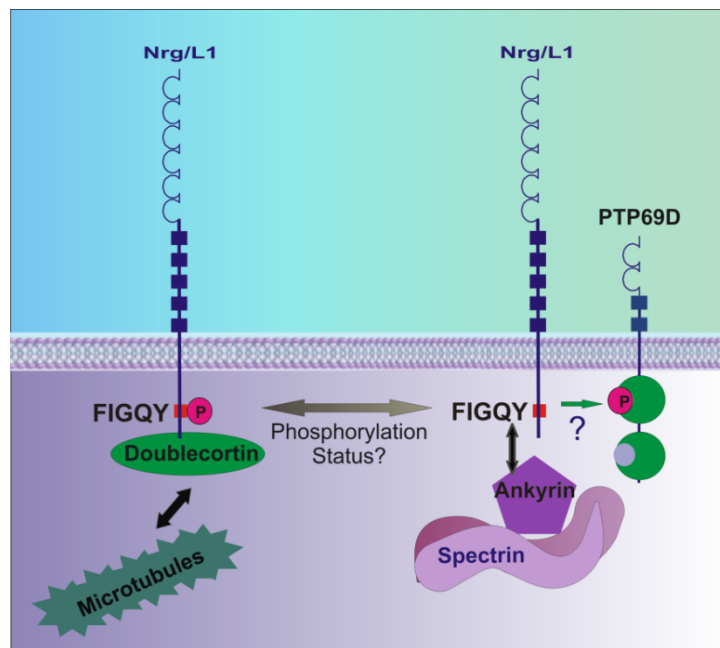
Figure A.1 Possible Theory of PTP69D interaction with Neuroglian

PTP69D could be the phosphatase involved in dephosphorylating the tyrosine residue in the FIGQY motif.

motif of Nrg suggesting that it is the cause for the synaptic phenotypes seen in this mutant (Godenschwege et al., 2006). This was supported by the finding that the expression of a mutant *nrg* construct (UAS-*nrg*^{167Y1234F}) where the tyrosine was converted to phenylalanine (Y to F) was shown to not be able to rescue the synaptic phenotypes of the *nrg*^{849} mutants. Moreover this mutant construct had a disruptive effect on giant synapse formation when expressed in a wild type background (Godenschwege et al., 2006). The experiments demonstrated that proper regulation of the phosphorylation status of Nrg is critical for giant synapse formation. However, currently the mechanism by which phosphorylation of Nrg is regulated in synapse formation and how the balance between the phosphorylated and unphosphorlyated isoforms contributes to this function is unknown. My studies have described a role of PTP69D in terminal growth and synapse formation. This raises the question whether PTP69D could potentially be the protein altering the phosphorylation status of Nrg directly or indirectly (Figure 6.1).

To test whether PTP69D and NRG genetically interact *in vivo* in the GF circuit. In order to test for a putative interaction between Nrg and PTP69D in the GFC various *Ptp69D* mutant alleles were crossed into in *nrg849* hemizygous and heterozygous backgrounds. The following genotypes were tested and compared to control flies (*nrg*^{849}/>, *nrg*^{849}/+, *Ptp69D**/+, and *nrg*^{849}; A307/UAS-*Ptp69D*-RNAi) for their ability to rescue the GF phenotype physiologically. We found that PTP69D did not rescue the nrg^{849} phenotype (Table 6.1).

Table A.1 Interaction of *Ptp69D* mutants with *nrg^{849}*

Genotype	n	wt in %
nrg^{849}/>; Tm3 or TM6/+ (control)	32	0
nrg^{849}/+; Tm3 or TM6/+ (control)	18	94
nrg^{849}/>; *Ptp^{10}*/+	20	5
nrg^{849}/+; *Ptp^{10}*/+	20	55
nrg^{849}/>; *Ptp^{18}*/+	22	5
nrg^{849}/+; *Ptp^{18}*/+	20	50
nrg^{849}/>; *Ptp^{20}*/+	20	0
nrg^{849}/+; *Ptp^{20}*/+	20	55
nrg^{849}/>; *Ptp^{21}*/+	20	0
nrg^{849}/+; *Ptp^{21}*/+	20	40
nrg^{849}/>; A307/ UAS-*Ptp69D*-RNAi^{40631}	8	0
nrg^{849}/+; A307/ UAS-*Ptp69D*-RNAi^{40631}	8	0
nrg^{849}/>; A307/+; UAS-*Ptp69D*-RNAi^{104761}/+	4	0
nrg^{849}/+; A307/+; UAS-*Ptp69D*-RNAi^{104761}/+	12	0

The results are listed as number of GFS (n) and percentage physiologically wild type (wt%), which is defined as a GF-TTM response latency under 1ms and a minimum of 80% following frequency at 100Hz.

Additionally, to test whether PTP69D dephosphorylates the FIGQY motif of Neuroglian, we examined the phosphorylation status of *Ptp69D* mutants (*Ptp69D^{10}, Ptp69D ^{18}, Ptp69D ^{20} and Ptp69D^{21}*) via Western blot using anti-phospho FIGQY Nrg antibodies. We anticipated that if PTP69D was the phosphatase involved in dephosphorylating the FIGQY motif that the phosphorylation would be increased in *Ptp69D ^{20} and Ptp69D^{21}* mutants (Figure 6.2a). This is because these alleles have

mutations in the catalytic domain which would affect their ability to function in removal

of the phosphate. We also predicted two scenarios for *Ptp69D[10]* and *Ptp69D [18]* mutants

(Figure 6.2b). In the first scenario they could have a decreased phosphorylation status

because they have functional catalytic domains because their mutations are in the

extracellular domain. Alternatively, they could have increased phosphorylation status

because they are unable to be recruited to their substrate because of mutations in the

immunoglobulin and fibronectin domains thus preventing removal of the phosphate from

the FIGQY motif. We found that PTP69D doesn't regulate FIGQY phosphorylation of

Nrg through the phosphatase domain.   Interestingly we did observe increased

phosphorylation of *Ptp69D[10]* and *Ptp69D [18]* mutants (Figure 6.3), suggesting that

PTP69D is involved in dephosphorylation of Nrg indirectly possibly through the

recruitment of another phosphatase.
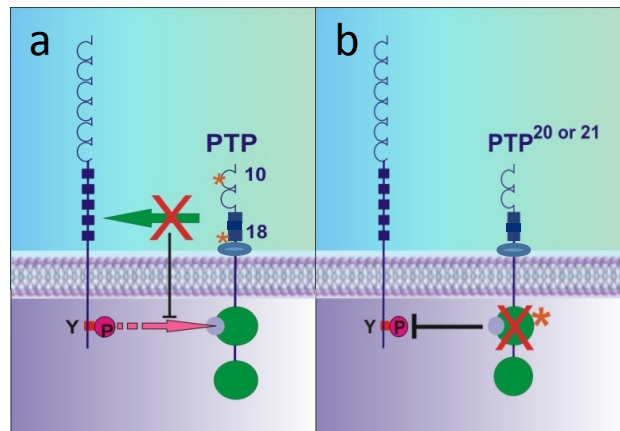
Figure A.2 Working hypothesis of PTP69D action on dephosphorylation of Nrg.

α –phospho Nrg

Loading control (α -tubulin)
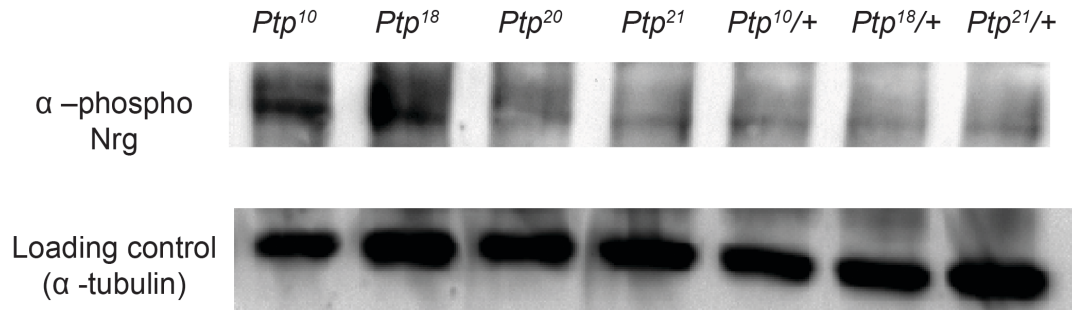
Figure A.2 Western Blot of phosphorylation status of *Ptp69D* mutants

A.2 Generation of Distracted UAS-construct

The distracted cDNA was obtained from *Drosophila* Genomics Resource Center (DGRC, Indiana) in a pot2 vector. The DGRC vector clones are delivered on Whatman FTA paper. To process the clones the following procedure was conducted:

1. The clone disc was placed in a 1.5mL microfuge tube, 50µL of 1X sterile TE was added and pipetted up and down twice.

2. The tube was placed on ice.

3. Then 50µL of DH5α competent cells were added and allowed to incubate on ice for 30 minutes. At the incubation midpoint the tube was vortexed briefly, 1 second.

4. The tube was then heat shocked for 2 minutes at 37^0C.

5. The cells were transferred to 1mL of LB media and incubated with shaking at 37^0C for one hour.

6. The cells were then plated on Chloramphenicol LB plates and incubated at 37^0C.

7. The resulting clones were used in the following cloning experiment.

To determine the restriction sites and analyze construct sequence the Invitrogen Vector NTI program was used. The molecular cloning scheme is illustrated in Figure A.1. Restriction enzymes were obtained from New England Biolabs. Mini and Maxi preps were carried out by protocols established by Qiagen. Electroporation into XL1-Blue competent cells (Strategene) was conducted in an Eppendorf Electroporater 2510. Gel visualization was conducted using the BioRad Molecular Imager® Gel Doc System. To

generate transgenic *Drosophila* lines the pUAST-*dsd* constructs was sent out for injections into embryos and generation of individual stable balanced transformants to BestGene (Chino Hills, CA).
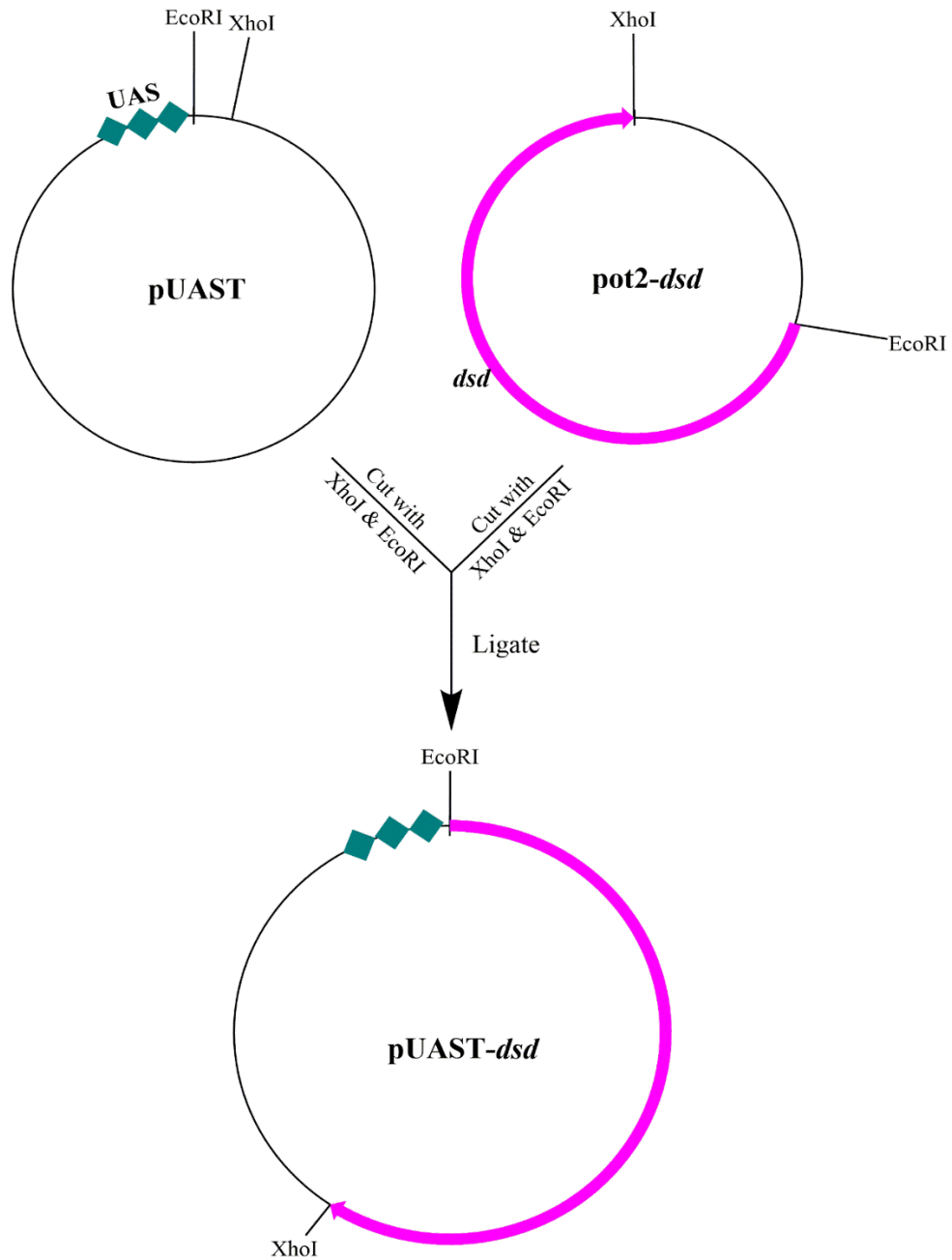
Figure A.3 Cloning scheme for *pUAST-dsd*

A.3   Real Time PCR Protocol

The following protocols were created with the help of Dr. David Brunell.

A.3.1 RNA Isolation

Materials:

- Trizol Reagent

- Microcentrifuge at 4°C

- Microcentrifuge tubes

- 75% ethanol

- CHCl$_3$

- Micropipetters with tips

- RNAse-free water

- Isopropanol

Procedure:

1.   Homogenize flies (5 to 10 flies are sufficient) in 0.5mL Trizol Reagent using a sterilized blue homogenizer pestle. Then add another 500µl Trizol Reagent for a total of 1ml.

2.   Centrifuge at maximum speed for 10 min at 4°C

3.   Transfer the supernatant to a clean microcentrifuge tube.

4.   Allow the sample to incubate at room temperature for 5 min.

5.   Add 200 μl of CHCl₃, vortex for 15 sec, and then incubate the sample at room temperature for 2-3 min.

6.   Centrifuge at full speed for 15 min at 4°C.

7.   Transfer the aqueous phase to a clean microcentrifuge tube. Note: <u>Do not</u> disturb the interphase! The DNA is in the interphase and the proteins are in the pink-colored organic phase.

8.   Precipitate the RNA by adding 500μl isopropanol and 1μl 10mg/ml glycogen. Mix by inverting once.

9.   Incubate the samples at room temperature for 10 min.

10.   Centrifuge at maximum speed for 10 min at 4°C.

11.   Pour off the supernatant without disturbing the pellet.

12.   Wash the RNA pellet with 1 ml 75% ethanol.

13.   Vortex sample for 15 sec and centrifuge at 12,000 rpm for 10 min at 4°C.

14.   Decant the ethanol. Centrifuge again for a few seconds to collect the residual ethanol. Remove all visible ethanol with a micropipette.

15.   Allow the pellet to air dry for a few minutes before resuspending the pellet in 30 - 50μl of RNAse free water. (Note: Resuspend in 30μl if you cannot see the pellet or 50μl if a pellet is clearly visible.)

16.   Determine the amount and quality of RNA using the Eppendorf Biophotometer (Spectrophotometer) with Hellma TrayCell by placing a 1μl drop of the sample into the depression on the TrayCell and recording the RNA concentration obtained.

17.   Prepare RNA samples for electrophoresis by combining 2μg RNA and water in a total volume of 15μl for each sample.

18.   Add 5μl Sample Buffer

19.   Heat at 65°-70°C for 10 minutes.

20.   Briefly chill the sample on ice.

21.   Load RNA samples onto a 2.5% agarose gel with ethidium bromide.

22.   Run the gel at ~150V until the tracking dye has traveled about 2/3 the length of the gel.

23.   Observe RNA samples with UV with a BioRad Molecular Imager® Gel Doc System. (Note two bands should be observed 28S and 18S)

A.3.2   Reverse Transcriptase PCR

The following genotypes were used for the following experiment: A307, 215b/TM6β,
A5.8.1, and EP3400. A5.8.1 and 215b/TM6β are "jumpout lines" generated by Randall
W. Phillis (University of Massachusetts – Amherst). EP3400 is a P-element line that was
obtained from the Bloomington Stock Center.

Procedure:

1.   Obtain a microcentrifuge tube containing 5μl water with 0.5μg random
       hexamers.

2.   Add 5μl of total *Drosophila* RNA for a final volume of 10μl.

3.   Heat the sample at 70°C for 10 min.

4.   Chill the sample on ice for 3 min.

5.   Centrifuge for a few seconds in the microcentrifuge at maximum speed.

6.   Add 10μl of the following mixture:

           4μl 5X Reverse Transcription Buffer

           2μl 100mM DTT

           1μl 10mM dNTP's

           1μl RNAse inhibitor

           1μl reverse transcriptase (200U/μl – Superscript II)

7.   Centrifuge for a few seconds in the microcentrifuge at maximum speed.

8.   Incubate at 42°C for 60 min.

9. Add 1µl 100mM EDTA and heat at 90°C for 2 min to inactivate the reverse transcriptase.

10. Add 79µl water to bring the final sample volume to 100µl.

11. Add the following to each 200µl PCR-tube, keeping it on ice as much as possible:

    30µl 2X PCR Reaction Mix

    10µl diluted cDNA reaction products

13. Mix thoroughly by pipetting up and down several times.

14. Transfer 20µl to a clean 200µl PCR-tube.

15. Add 5µl oligonucleotide primer (20pmol concentration) for DSD to tube

16. Use the following PCR profile:

    One cycle at 94°C for 1 minute

    40 cycles of 94°C for 20 sec, 52°C for 30 sec and 68°C for one min.

    Chill to 4°C and hold.

17. Load the DNA marker and the samples (with Sample Buffer) onto a 2.5% agarose gel with ethidium bromide.

18. Run the gel at 100-150V until the bromophenol blue dye is midway down the gel.

19. Observe the PCR products with UV with a BioRad Molecular Imager® Gel Doc System.

A.3.3   Real Time PCR

Primer Design:

The genomic DNA sequence of *dsd* was obtained from Flybase (http://flybase.bio.indiana.edu/) and the accession number (NT_033777.2) obtained from the National Center for Biotechnology Information (NCBI, www.ncbi.nlm.nih.gov). The primers were made using Invitrogen's D-LUX primer designer software (https://www.invitrogen.com/). The open reading frame for target design was selected and the program generated a number of primer sets. The best two primer sets were selected to be produced.   For each set the FAM dye was selected and 50nmoles of labeled and unlabeled primers were ordered. For internal control 18S ribosomal RNA was used and primers with VIC dye was ordered. The same sequences were ordered as non-LUX primers from Integrated DNA Technologies (http://www.idtdna.com/site).

Materials:

- *Drosophila dsd* LUX primers (FAM dye)

- *Drosophila* 18s ribosomal subunit LUX primers (VIC dye)

- SuperScript™ III Platinum® One-Step Quantitative RT-PCR kit (Invitrogen)

- RNase-free (DEPC-treated) water

- 96-well plates and optically-clear caps

- Microcentrifuge tubes

- Pipettors and barrier tips

Procedure:

Reaction mix (per well):

RT Platinum Taq Mix 1µL

2X SuperScript III Reaction Mix 25 µL

DEPC-treated water 22.8 µL

5' Primer (Stock 100µM) 0.1 µL

3' Primer (Stock 100µM) 0.1 µL

    Total 49 µL

1. The extracted RNA needs to be diluted to a concentration of 50 ng/µl. Based on the concentration measured with the spectrophotometer will determine how much sample needs to be diluted in RNase-free water. If sample is between 25 and 50 ng/µl, the amount can be directly pipetted into the reaction without dilution.

2. Create a set of standards. The following concentrations are needed: 200, 100, 50, 25 and 12.5 ng/µl. First, prepare 20 µl of a 200 ng/µl dilution (with RNase-free water). Then then make serial dilutions by taking 10 µl of the 200 ng/µl sample and transfer it to a separate tube and add 10 µl of water to create a 100 ng/µl solution. Continue for the remainder of the dilutions.

3. Make a master mix of the reaction mix above by making enough mix for 2.5 reactions. This allows for two reactions plus a little extra to allow for pipetting errors. After primers have been added add 2.5 µl of your diluted (50 ng/µl) RNA. After mixing by tapping the tube or gentle vortexing, pipet 50 µl into each well as shown in the plate map below. The standards and NTCs (no template controls) are loaded similarly. NTC wells have reaction mix but no RNA.

4. Load the plate as shown in the plate map (Table 6.2.) After all wells are loaded, the plate is capped, briefly centrifuge to remove air bubbles, then load into the Bio-Rad CFX96 Real-Time System. The protocol is as follows:

Step 1: 50°C for 15 minutes

Step 2: 95°C for 2 minutes

Step 3: 95°C for 15 seconds

Step 4: 55°C for 30 seconds

Step 5: 72°C for 30 seconds

Step 6: Read plate

Step 7: Goto step 3 for 39 more times

Step 8: Melting curve from 55°C to 90°C, read every 1.0°C, hold 10 seconds

5. The software was used to compute the relative gene expression levels in each of the genotypes. Alternatively, the Comparative CT method ($\Delta\Delta$CT) to quantitate the relative gene expression levels manually is found below.

Table A.2 Plate Map

|	**1**	**2**	**3**	**4**	**5**	**6**	**7**	**8**	**9**	**10**	**11**	**12**
A	NTC 18s	NTC 18s	NTC dsd	NTC dsd					18s A307	18s A307	dsd A307	dsd A307
B									18s 215b/TM6β	18s 215b/TM6β	dsd 215b/TM6β	dsd 215b/TM6β
C									18s A5.8.1	18s A5.8.1	dsd A5.8.1	dsd A5.8.1
D	STD 200ng 18s	STD 200ng 18s	STD 200ng dsd	STD 200ng dsd					18s EP3400	18s EP3400	dsd EP3400	dsd EP3400
E	STD 100ng 18s	STD 100ng 18s	STD 100ng dsd	STD 100ng dsd								
F	STD 50ng 18s	STD 50ng 18s	STD 50ng dsd	STD 50ng dsd								
G	STD 25ng 18s	STD 25ng 18s	STD 25ng dsd	STD 25ng dsd								
H	STD 12.5ng 18s	STD 12.5ng 18s	STD 12.5ng dsd	STD 12.5ng dsd								

NTC: No template control (minus RNA)
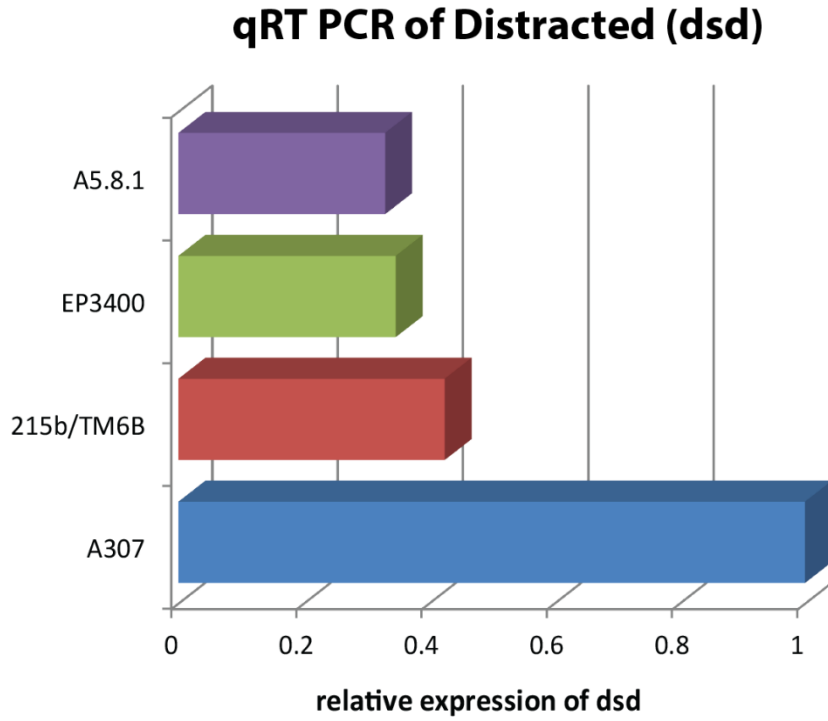
Figure A.4 Relative Quantitation of *dsd* in *Drosophila* mutants.

Distracted is reduced by 60% or more in mutants.

A.3.4 Comparative CT method (ΔΔCT)

1. Download the real-time data file ina .CSV (commaseparated value) format which can be read with most spreadsheet software, like Excel. There are six fields in the spreadsheet:

   Well The physical location on the plate of the sample

   Dye The type of fluorophore used (FAM or VIC)

   Type Indicates whether the well is a blank, standard or sample

   Label A user-friendly label for the gene associated with the given dye

   C(T) The interpolated cycle number where the fluorescence level crosses the threshold

   ng The amount of starting material determined by the real-time instrument by interpolating from the standard curve

2. The instrument was configured to recognize certain wells as containing standards. After obtaining CT data, the instrument did a least-squares fit of straight lines to the standards (there are two sets of standards, one for Dsd and one for 18s). Next, the CT values for each sample were converted to ng of starting material by interpolating from the appropriate standard curve. Using the mass values from the data file, construct a relative quantitation table shown below. It will be helpful to refer to the plate map. Average the two mass values for each sample and enter into columns   and   in the table below. Normalize DSD to 18s for each sample by dividing column   by column   and placing the result in column . Then, when all samples are normalized to 18s, determine which one shows the lowest level of DSD expression

138

(but should not be zero). Using this sample as the calibrator, compute the values for

column ____ by dividing each sample's value in column ____ by the calibrator's value.

Sample	DSD	18s	DSD normalized to 18s	Sample normalized to sample #_
			②/③	④/④$_c$
			②/③	④/④$_c$
			②/③	④/④$_c$
			②/③	④/④$_c$

3. Using the average of the standard C_T values from the data file, complete the table below. The ΔC_T value is simply the C_T value for Dsd minus the C_T value for 18s.

Standard (ng)	C_T, DSD	C_T, 18s	ΔC_T, DSD - 18s
12.5			
25			
50			
100			
200			

4. Graph the ΔC_T values from the table above and determine the slope of the least squares trend line. If the slope is less than 01 then you can safely use the $\Delta\Delta C_T$ method to find relative gene expression levels.

139

5. Complete the $\Delta\Delta C_T$ table (shown below), the calibrator should be the sample with the greatest ΔC_T.

Sample	C_T DSD	C_T 18s	ΔC_T DSD – 18s	$\Delta\Delta C_T$ $\Delta C_T - \Delta C_{T(calibrator)}$	$2^{-\Delta\Delta C_T}$
1					
2					
3					
4					

A.4   Electrophysiological analysis of other mutants in the GFC

All the results are listed as number of GFS (n) and percentage physiologically wild type (wt%), which is defined as a GF-TTM response latency under 1ms and a minimum of 80% following frequency at 100Hz..

Distracted (*dsd*) -

Genotype	n	wt in %
dsd^{36221}/*cyo* (control)	8	100%
dsd^{36221}	16	75%
dsd^{36221}/EP3400	14	100%
EP3400	20	100%
EP3030	16	100%

Epidermal Growth Factor (EGF) Receptor -

Genotype	n	wt in %
5144 EGF/CyO	30	90%
A307; UAS *EGFR* DN^{5364}	22	77%
A307; UAS *EGFR* B ^{5368}	14	71%
15366 EGF/CyO	20	70%

Breathless (*btl*) – Protein Tyrosine Kinase (PTK); Fibroblast growth factor (FGF) receptor subfamily.

Genotype	n	wt in %
A307 Dicer2; UAS *btl* RNAi[548]	20	100%
A307 Dicer2; UAS *btl* RNAi[950]	18	100%
A307 Dicer2; UAS *btl* RNAi[27106]	20	100%

Heartless (*htl*) – Protein Tyrosine Kinase (PTK); Fibroblast growth factor (FGF) receptor subfamily.

Genotype	n	wt in %
A307; UAS *htl* DN[5366]	30	77%
A307; UAS *htl* RNAi[40627]	16	100%
A307 Dicer2; UAS *htl* RNAi[6692]	32	78%

PTP10D – *Drosophila* RPTP

Genotype	n	wt in %
A307; UAS *Ptp10D* RNAi[8010]	14	100%

PTP52F – *Drosophila* RPTP

Genotype	n	wt in %
Ptp52F/ TM6β (control)	8	100%
Ptp69D/cyo (control)	10	100%
Ptp69D[10]/Ptp52F	10	100%
Ptp69D[18]/Ptp52F	10	100%
Ptp69D[20]/Ptp52F	10	100%

PTP99A – *Drosophila* RPTP

Genotype	n	wt in %
Ptp99A/TM6β (control)	10	100%
Ptp69D[10]/Ptp99A	10	60%
Ptp69D[18]/Ptp99A	10	80%
Ptp69D[20]/Ptp99A	10	40%
Ptp69D[21]/Ptp99A	10	80%
*A307/*UAS *Ptp99A* RNAi[8009GD]	6	83%

DLAR

Genotype	n	wt in %
A307; UAS *Dlar* RNAi[107996]	20	100%

Ableson Kinase

Genotype	n	wt in %
A307; UAS *Abl* RNAi[110186]	38	84%

Semaphorin

Genotype	n	wt in %
A307/Sema1aPi; *Ptp69D[10]*	10	70%
A307/Sema1aPi; *Ptp69D[20]*	10	50%

Fasciclin 2

Genotype	n	wt in %
A307; UAS *Fas2* RNAi[8392]	16	38%

Ephrin

Genotype	n	wt in %
Eph RS5; *Ptp69D*^{10}	10	100%
Eph KDm2; *Ptp69D*^{10}	20	80%
Eph RS5; *Ptp69D*^{20}	10	100%
Eph KDm2; *Ptp69D*^{20}	16	75%

REFERENCES

Allen, M. J., Drummond, J. A., & Moffat, K. G. (1998). Development of the giant fiber neuron of Drosophila melanogaster. *J Comp Neurol, 397*(4), 519-531.

Allen, M. J., & Godenschwege, T. A. (2010). Electrophysiological recordings from the Drosophila giant fiber system (GFS). *Cold Spring Harb Protoc, 2010*(7), pdb.prot5453. doi: 10.1101/pdb.prot5453

Allen, M. J., Godenschwege, T. A., Tanouye, M. A., & Phelan, P. (2006). Making an escape: development and function of the Drosophila giant fibre system. *Semin Cell Dev Biol, 17*(1), 31-41. doi: 10.1016/j.semcdb.2005.11.011

Allen, M. J., & Murphey, R. K. (2007). The chemical component of the mixed GF-TTMn synapse in Drosophila melanogaster uses acetylcholine as its neurotransmitter. *Eur J Neurosci, 26*(2), 439-445. doi: 10.1111/j.1460-9568.2007.05686.x

Allen, M. J., Shan, X., Caruccio, P., Froggett, S. J., Moffat, K. G., & Murphey, R. K. (1999). Targeted expression of truncated glued disrupts giant fiber synapse formation in Drosophila. *J Neurosci, 19*(21), 9374-9384.

Andersen, J. N., Mortensen, O. H., Peters, G. H., Drake, P. G., Iversen, L. F., Olsen, O. H., . . . Moller, N. P. (2001). Structural and evolutionary relationships among protein tyrosine phosphatase domains. *Mol Cell Biol, 21*(21), 7117-7136. doi: 10.1128/mcb.21.21.7117-7136.2001

Ariño, J., & Alexander, D. (2004). *Protein phosphatases*. New York: Springer-Verlag.

145

Arregui, C. O., Balsamo, J., & Lilien, J. (2000). Regulation of signaling by protein-tyrosine phosphatases: potential roles in the nervous system. *Neurochem Res, 25*(1), 95-105.

Barford, D., Das, A. K., & Egloff, M. P. (1998). The structure and mechanism of protein phosphatases: insights into catalysis and regulation. *Annu Rev Biophys Biomol Struct, 27*, 133-164. doi: 10.1146/annurev.biophys.27.1.133

Barr, A. J., Ugochukwu, E., Lee, W. H., King, O. N., Filippakopoulos, P., Alfano, I., . . . Knapp, S. (2009). Large-scale structural analysis of the classical human protein tyrosine phosphatome. *Cell, 136*(2), 352-363. doi: 10.1016/j.cell.2008.11.038

Beltran, P. J., & Bixby, J. L. (2003). Receptor protein tyrosine phosphatases as mediators of cellular adhesion. *Front Biosci, 8*, d87-99.

Benson, D. L., Colman, D. R., & Huntley, G. W. (2001). Molecules, maps and synapse specificity. *Nat Rev Neurosci, 2*(12), 899-909. doi: 10.1038/35104078

Besco, J., Popesco, M. C., Davuluri, R. V., Frostholm, A., & Rotter, A. (2004). Genomic structure and alternative splicing of murine R2B receptor protein tyrosine phosphatases (PTPkappa, mu, rho and PCP-2). *BMC Genomics, 5*(1), 14. doi: 10.1186/1471-2164-5-14

Bixby, J. L. (2001). Ligands and signaling through receptor-type tyrosine phosphatases. *IUBMB Life, 51*(3), 157-163. doi: 10.1080/152165401753544223

Blagburn, J. M., Alexopoulos, H., Davies, J. A., & Bacon, J. P. (1999). Null mutation in shaking-B eliminates electrical, but not chemical, synapses in the Drosophila giant fiber system: a structural study. *J Comp Neurol, 404*(4), 449-458.

Blanchetot, C., Chagnon, M., Dube, N., Halle, M., & Tremblay, M. L. (2005). Substrate-trapping techniques in the identification of cellular PTP targets. *Methods, 35*(1), 44-53. doi: 10.1016/j.ymeth.2004.07.007

Boerner, J., & Godenschwege, T. A. (2010). Application for the Drosophila ventral nerve cord standard in neuronal circuit reconstruction and in-depth analysis of mutant morphology. *J Neurogenet, 24*(3), 158-167. doi: 10.3109/01677063.2010.489624

Boerner, J., & Godenschwege, T. A. (2011). Whole mount preparation of the adult Drosophila ventral nerve cord for giant fiber dye injection. *J Vis Exp*(52). doi: 10.3791/3080

Brand, A. H., & Perrimon, N. (1993). Targeted gene expression as a means of altering cell fates and generating dominant phenotypes. *Development, 118*(2), 401-415.

Campos, A. R., Rosen, D. R., Robinow, S. N., & White, K. (1987). Molecular analysis of the locus elav in Drosophila melanogaster: a gene whose embryonic expression is neural specific. *Embo j, 6*(2), 425-431.

Chagnon, M. J., Uetani, N., & Tremblay, M. L. (2004). Functional significance of the LAR receptor protein tyrosine phosphatase family in development and diseases. *Biochem Cell Biol, 82*(6), 664-675. doi: 10.1139/o04-120

Davies, R. W., & Morris, B. J. (2004). *Molecular biology of the neuron Molecular and cellular neurobiology* (pp. 1 online resource (xvii, 480 p.)). Retrieved from http://ezproxy.lib.usf.edu/login?url=http://dx.doi.org/10.1093/acprof:oso/9780198 509981.001.0001

den Hertog, J., Blanchetot, C., Buist, A., Overvoorde, J., van der Sar, A., & Tertoolen, L. G. (1999). Receptor protein-tyrosine phosphatase signalling in development. *Int J Dev Biol, 43*(7), 723-733.

Desai, C., & Purdy, J. (2003). The neural receptor protein tyrosine phosphatase DPTP69D is required during periods of axon outgrowth in Drosophila. *Genetics, 164*(2), 575-588.

Desai, C. J., Gindhart, J. G., Goldstein, L. S., & Zinn, K. (1996). Receptor tyrosine phosphatases are required for motor axon guidance in the Drosophila embryo. *Cell, 84*(4), 599-609.

Desai, C. J., Krueger, N. X., Saito, H., & Zinn, K. (1997). Competition and cooperation among receptor tyrosine phosphatases control motoneuron growth cone guidance in Drosophila. *Development, 124*(10), 1941-1952.

Desai, C. J., Popova, E., & Zinn, K. (1994). A Drosophila receptor tyrosine phosphatase expressed in the embryonic CNS and larval optic lobes is a member of the set of proteins bearing the "HRP" carbohydrate epitope. *J Neurosci, 14*(12), 7272-7283.

Desai, C. J., Sun, Q., & Zinn, K. (1997). Tyrosine phosphorylation and axon guidance: of mice and flies. *Curr Opin Neurobiol, 7*(1), 70-74.

Dietzl, G., Chen, D., Schnorrer, F., Su, K. C., Barinova, Y., Fellner, M., . . . Dickson, B. J. (2007). A genome-wide transgenic RNAi library for conditional gene inactivation in Drosophila. *Nature, 448*(7150), 151-156. doi: 10.1038/nature05954

Edwards, A. C., & Mackay, T. F. (2009). Quantitative trait loci for aggressive behavior in Drosophila melanogaster. *Genetics, 182*(3), 889-897. doi: 10.1534/genetics.109.101691

Enneking, E. M., Kudumala, S. R., Moreno, E., Stephan, R., Boerner, J., Godenschwege, T. A., & Pielage, J. (2013). Transsynaptic coordination of synaptic growth, function, and stability by the L1-type CAM Neuroglian. *PLoS Biol, 11*(4), e1001537. doi: 10.1371/journal.pbio.1001537

Ensslen-Craig, S. E., & Brady-Kalnay, S. M. (2005). PTP mu expression and catalytic activity are required for PTP mu-mediated neurite outgrowth and repulsion. *Mol Cell Neurosci, 28*(1), 177-188. doi: 10.1016/j.mcn.2004.08.011

Fauman, E. B., & Saper, M. A. (1996). Structure and function of the protein tyrosine phosphatases. *Trends Biochem Sci, 21*(11), 413-417.

Fischer, E. H., Charbonneau, H., & Tonks, N. K. (1991). Protein tyrosine phosphatases: a diverse family of intracellular and transmembrane enzymes. *Science, 253*(5018), 401-406.

Flint, A. J., Tiganis, T., Barford, D., & Tonks, N. K. (1997). Development of "substrate-trapping" mutants to identify physiological substrates of protein tyrosine phosphatases. *Proc Natl Acad Sci U S A, 94*(5), 1680-1685.

Frangioni, J. V., Beahm, P. H., Shifrin, V., Jost, C. A., & Neel, B. G. (1992). The nontransmembrane tyrosine phosphatase PTP-1B localizes to the endoplasmic reticulum via its 35 amino acid C-terminal sequence. *Cell, 68*(3), 545-560.

Garrity, P. A., Lee, C. H., Salecker, I., Robertson, H. C., Desai, C. J., Zinn, K., & Zipursky, S. L. (1999). Retinal axon target selection in Drosophila is regulated by a receptor protein tyrosine phosphatase. *Neuron, 22*(4), 707-717.

Garver, T. D., Ren, Q., Tuvia, S., & Bennett, V. (1997). Tyrosine phosphorylation at a site highly conserved in the L1 family of cell adhesion molecules abolishes ankyrin binding and increases lateral mobility of neurofascin. *J Cell Biol, 137*(3), 703-714.

Godenschwege, T. A., Kristiansen, L. V., Uthaman, S. B., Hortsch, M., & Murphey, R. K. (2006). A conserved role for Drosophila Neuroglian and human L1-CAM in central-synapse formation. *Curr Biol, 16*(1), 12-23. doi: 10.1016/j.cub.2005.11.062

Godenschwege, T. A., Simpson, J. H., Shan, X., Bashaw, G. J., Goodman, C. S., & Murphey, R. K. (2002a). Ectopic expression in the giant fiber system of Drosophila reveals distinct roles for roundabout (Robo), Robo2, and Robo3 in dendritic guidance and synaptic connectivity. *Journal of Neuroscience, 22*(8), 3117-3129. doi: 20026291

Godenschwege, T. A., Simpson, J. H., Shan, X., Bashaw, G. J., Goodman, C. S., & Murphey, R. K. (2002b). Ectopic expression in the giant fiber system of Drosophila reveals distinct roles for roundabout (Robo), Robo2, and Robo3 in dendritic guidance and synaptic connectivity. *J Neurosci, 22*(8), 3117-3129. doi: 20026291

Greenspan, R. J. (2004). *Fly pushing : the theory and practice of Drosophila genetics* (2nd ed.). Cold Spring Harbor, N.Y.: Cold Spring Harbor Laboratory Press.

Gurd, J. W. (1997). Protein tyrosine phosphorylation: implications for synaptic function. *Neurochem Int, 31*(5), 635-649.

Hofmeyer, K., & Treisman, J. E. (2009). The receptor protein tyrosine phosphatase LAR promotes R7 photoreceptor axon targeting by a phosphatase-independent signaling mechanism. *Proc Natl Acad Sci U S A, 106*(46), 19399-19404. doi: 10.1073/pnas.0903961106

Jacobs, K., Todman, M. G., Allen, M. J., Davies, J. A., & Bacon, J. P. (2000). Synaptogenesis in the giant-fibre system of Drosophila: interaction of the giant fibre and its major motorneuronal target. *Development, 127*(23), 5203-5212.

Jenett, A., Rubin, G. M., Ngo, T. T., Shepherd, D., Murphy, C., Dionne, H., . . . Zugates, C. T. (2012). A GAL4-driver line resource for Drosophila neurobiology. *Cell Rep, 2*(4), 991-1001. doi: 10.1016/j.celrep.2012.09.011

Jiang, G., den Hertog, J., Su, J., Noel, J., Sap, J., & Hunter, T. (1999). Dimerization inhibits the activity of receptor-like protein-tyrosine phosphatase-alpha. *Nature, 401*(6753), 606-610. doi: 10.1038/44170

Johnson, K. G., & Van Vactor, D. (2003). Receptor protein tyrosine phosphatases in nervous system development. *Physiol Rev, 83*(1), 1-24. doi: 10.1152/physrev.00016.2002

Kashio, N., Matsumoto, W., Parker, S., & Rothstein, D. M. (1998). The second domain of the CD45 protein tyrosine phosphatase is critical for interleukin-2 secretion and substrate recruitment of TCR-zeta in vivo. *J Biol Chem, 273*(50), 33856-33863.

151

Kaufmann, N., DeProto, J., Ranjan, R., Wan, H., & Van Vactor, D. (2002). Drosophila liprin-alpha and the receptor phosphatase Dlar control synapse morphogenesis. *Neuron, 34*(1), 27-38.

Kennerdell, J. R., & Carthew, R. W. (2000). Heritable gene silencing in Drosophila using double-stranded RNA. *Nat Biotechnol, 18*(8), 896-898. doi: 10.1038/78531

King, D. G., & Wyman, R. J. (1980). Anatomy of the giant fibre pathway in Drosophila. I. Three thoracic components of the pathway. *J Neurocytol, 9*(6), 753-770.

Kizhatil, K., Wu, Y. X., Sen, A., & Bennett, V. (2002). A new activity of doublecortin in recognition of the phospho-FIGQY tyrosine in the cytoplasmic domain of neurofascin. *J Neurosci, 22*(18), 7948-7958.

Krueger, N. X., Reddy, R. S., Johnson, K., Bateman, J., Kaufmann, N., Scalice, D., . . . Saito, H. (2003). Functions of the ectodomain and cytoplasmic tyrosine phosphatase domains of receptor protein tyrosine phosphatase Dlar in vivo. *Mol Cell Biol, 23*(19), 6909-6921.

Krueger, N. X., Van Vactor, D., Wan, H. I., Gelbart, W. M., Goodman, C. S., & Saito, H. (1996). The transmembrane tyrosine phosphatase DLAR controls motor axon guidance in Drosophila. *Cell, 84*(4), 611-622.

Kurusu, M., & Zinn, K. (2008). Receptor tyrosine phosphatases regulate birth order-dependent axonal fasciculation and midline repulsion during development of the Drosophila mushroom body. *Mol Cell Neurosci, 38*(1), 53-65. doi: 10.1016/j.mcn.2008.01.015

Kwon, S. K., Woo, J., Kim, S. Y., Kim, H., & Kim, E. (2010). Trans-synaptic adhesions between netrin-G ligand-3 (NGL-3) and receptor tyrosine phosphatases LAR,

protein-tyrosine phosphatase delta (PTPdelta), and PTPsigma via specific domains regulate excitatory synapse formation. *J Biol Chem, 285*(18), 13966-13978. doi: 10.1074/jbc.M109.061127

Li, L., & Dixon, J. E. (2000). Form, function, and regulation of protein tyrosine phosphatases and their involvement in human diseases. *Semin Immunol, 12*(1), 75-84. doi: 10.1006/smim.2000.0209

Liang, L., Lim, K. L., Seow, K. T., Ng, C. H., & Pallen, C. J. (2000). Calmodulin binds to and inhibits the activity of the membrane distal catalytic domain of receptor protein-tyrosine phosphatase alpha. *J Biol Chem, 275*(39), 30075-30081. doi: 10.1074/jbc.M004843200

Lim, S. H., Kwon, S. K., Lee, M. K., Moon, J., Jeong, D. G., Park, E., . . . Lee, J. R. (2009). Synapse formation regulated by protein tyrosine phosphatase receptor T through interaction with cell adhesion molecules and Fyn. *EMBO J, 28*(22), 3564-3578. doi: 10.1038/emboj.2009.289

Majeti, R., Bilwes, A. M., Noel, J. P., Hunter, T., & Weiss, A. (1998). Dimerization-induced inhibition of receptor protein tyrosine phosphatase function through an inhibitory wedge. *Science, 279*(5347), 88-91.

Maness, P. F., & Schachner, M. (2007). Neural recognition molecules of the immunoglobulin superfamily: signaling transducers of axon guidance and neuronal migration. *Nat Neurosci, 10*(1), 19-26. doi: 10.1038/nn1827

Marlo, J. E., & Desai, C. J. (2006). Loss of phosphatase activity in Ptp69D alleles supporting axon guidance defects. *J Cell Biochem, 98*(5), 1296-1307. doi: 10.1002/jcb.20862

Maurel-Zaffran, C., Suzuki, T., Gahmon, G., Treisman, J. E., & Dickson, B. J. (2001). Cell-autonomous and -nonautonomous functions of LAR in R7 photoreceptor axon targeting. *Neuron, 32*(2), 225-235.

Muqit, M. M., & Feany, M. B. (2002). Modelling neurodegenerative diseases in Drosophila: a fruitful approach? *Nat Rev Neurosci, 3*(3), 237-243. doi: 10.1038/nrn751

Murphey, R. K., Froggett, S. J., Caruccio, P., Shan-Crofts, X., Kitamoto, T., & Godenschwege, T. A. (2003). Targeted expression of shibire ts and semaphorin 1a reveals critical periods for synapse formation in the giant fiber of Drosophila. *Development, 130*(16), 3671-3682.

Newsome, T. P., Asling, B., & Dickson, B. J. (2000). Analysis of Drosophila photoreceptor axon guidance in eye-specific mosaics. *Development, 127*(4), 851-860.

Perrimon, N. (1998). New advances in Drosophila provide opportunities to study gene functions. *Proc Natl Acad Sci U S A, 95*(17), 9716-9717.

Pfeiffer, B. D., Jenett, A., Hammonds, A. S., Ngo, T. T., Misra, S., Murphy, C., . . . Rubin, G. M. (2008). Tools for neuroanatomy and neurogenetics in Drosophila. *Proc Natl Acad Sci U S A, 105*(28), 9715-9720. doi: 10.1073/pnas.0803697105

Phelan, P., Nakagawa, M., Wilkin, M. B., Moffat, K. G., O'Kane, C. J., Davies, J. A., & Bacon, J. P. (1996). Mutations in shaking-B prevent electrical synapse formation in the Drosophila giant fiber system. *J Neurosci, 16*(3), 1101-1113.

Pilz, D. T., Matsumoto, N., Minnerath, S., Mills, P., Gleeson, J. G., Allen, K. M., . . . Ross, M. E. (1998). LIS1 and XLIS (DCX) mutations cause most classical

lissencephaly, but different patterns of malformation. *Hum Mol Genet, 7*(13), 2029-2037.

Schindelholz, B., Knirr, M., Warrior, R., & Zinn, K. (2001). Regulation of CNS and motor axon guidance in Drosophila by the receptor tyrosine phosphatase DPTP52F. *Development, 128*(21), 4371-4382.

Serra-Pagès, C., Streuli, M., & Medley, Q. G. (2005). Liprin phosphorylation regulates binding to LAR: evidence for liprin autophosphorylation. *Biochemistry, 44*(48), 15715-15724. doi: 10.1021/bi051434f

Sharp, P. A. (1999). RNAi and double-strand RNA. *Genes Dev, 13*(2), 139-141.

Song, J. K., Giniger, E., & Desai, C. J. (2008). The receptor protein tyrosine phosphatase PTP69D antagonizes Abl tyrosine kinase to guide axons in Drosophila. *Mech Dev, 125*(3-4), 247-256. doi: 10.1016/j.mod.2007.11.005

Soulsby, M., & Bennett, A. M. (2009). Physiological signaling specificity by protein tyrosine phosphatases. *Physiology (Bethesda), 24*, 281-289. doi: 10.1152/physiol.00017.2009

Stewart, A. E., Dowd, S., Keyse, S. M., & McDonald, N. Q. (1999). Crystal structure of the MAPK phosphatase Pyst1 catalytic domain and implications for regulated activation. *Nat Struct Biol, 6*(2), 174-181. doi: 10.1038/5861

Stoker, A. (2005). Methods for identifying extracellular ligands of RPTPs. *Methods, 35*(1), 80-89. doi: 10.1016/j.ymeth.2004.07.011

Stoker, A., & Dutta, R. (1998). Protein tyrosine phosphatases and neural development. *Bioessays, 20*(6), 463-472. doi: 10.1002/(SICI)1521-1878(199806)20:6<463::AID-BIES4>3.0.CO;2-N

Stoker, A. W. (2001). Receptor tyrosine phosphatases in axon growth and guidance. *Curr Opin Neurobiol, 11*(1), 95-102.

Stoker, A. W. (2005). Protein tyrosine phosphatases and signalling. *J Endocrinol, 185*(1), 19-33. doi: 10.1677/joe.1.06069

Streuli, M., Krueger, N. X., Hall, L. R., Schlossman, S. F., & Saito, H. (1988). A new member of the immunoglobulin superfamily that has a cytoplasmic region homologous to the leukocyte common antigen. *J Exp Med, 168*(5), 1523-1530.

Streuli, M., Krueger, N. X., Tsai, A. Y., & Saito, H. (1989). A family of receptor-linked protein tyrosine phosphatases in humans and Drosophila. *Proc Natl Acad Sci U S A, 86*(22), 8698-8702.

Sun, Q., Bahri, S., Schmid, A., Chia, W., & Zinn, K. (2000). Receptor tyrosine phosphatases regulate axon guidance across the midline of the Drosophila embryo. *Development, 127*(4), 801-812.

Sun, Q., Schindelholz, B., Knirr, M., Schmid, A., & Zinn, K. (2001). Complex genetic interactions among four receptor tyrosine phosphatases regulate axon guidance in Drosophila. *Mol Cell Neurosci, 17*(2), 274-291. doi: 10.1006/mcne.2000.0939

Tanouye, M. A., & Wyman, R. J. (1980). Motor outputs of giant nerve fiber in Drosophila. *J Neurophysiol, 44*(2), 405-421.

Thaker, H. M., & Kankel, D. R. (1992). Mosaic analysis gives an estimate of the extent of genomic involvement in the development of the visual system in Drosophila melanogaster. *Genetics, 131*(4), 883-894.

Thomas, J. B., & Wyman, R. J. (1982). A mutation in Drosophila alters normal connectivity between two identified neurones. *Nature, 298*(5875), 650-651.

Tian, S. S., Tsoulfas, P., & Zinn, K. (1991). Three receptor-linked protein-tyrosine phosphatases are selectively expressed on central nervous system axons in the Drosophila embryo. *Cell, 67*(4), 675-685.

Tonks, N. K., Charbonneau, H., Diltz, C. D., Fischer, E. H., & Walsh, K. A. (1988). Demonstration that the leukocyte common antigen CD45 is a protein tyrosine phosphatase. *Biochemistry, 27*(24), 8695-8701.

Tonks, N. K., & Neel, B. G. (1996). From form to function: signaling by protein tyrosine phosphatases. *Cell, 87*(3), 365-368.

Trimarchi, J. R., & Murphey, R. K. (1997). The shaking-B2 mutation disrupts electrical synapses in a flight circuit in adult Drosophila. *J Neurosci, 17*(12), 4700-4710.

Vactor, D. V., Sink, H., Fambrough, D., Tsoo, R., & Goodman, C. S. (1993). Genes that control neuromuscular specificity in Drosophila. *Cell, 73*(6), 1137-1153.

Van Vactor, D. (1998). Protein tyrosine phosphatases in the developing nervous system. *Curr Opin Cell Biol, 10*(2), 174-181.

Wallace, M. J., Fladd, C., Batt, J., & Rotin, D. (1998). The second catalytic domain of protein tyrosine phosphatase delta (PTP delta) binds to and inhibits the first catalytic domain of PTP sigma. *Mol Cell Biol, 18*(5), 2608-2616.

Walsh, F. S., & Doherty, P. (1997). Neural cell adhesion molecules of the immunoglobulin superfamily: role in axon growth and guidance. *Annu Rev Cell Dev Biol, 13*, 425-456. doi: 10.1146/annurev.cellbio.13.1.425

Williams, M. J. (2009). The Drosophila cell adhesion molecule Neuroglian regulates Lissencephaly-1 localisation in circulating immunosurveillance cells. *BMC Immunol, 10*, 17. doi: 10.1186/1471-2172-10-17

Wills, Z., Bateman, J., Korey, C. A., Comer, A., & Van Vactor, D. (1999). The tyrosine kinase Abl and its substrate enabled collaborate with the receptor phosphatase Dlar to control motor axon guidance. *Neuron, 22*(2), 301-312.

Wills, Z., Marr, L., Zinn, K., Goodman, C. S., & Van Vactor, D. (1999). Profilin and the Abl tyrosine kinase are required for motor axon outgrowth in the Drosophila embryo. *Neuron, 22*(2), 291-299.

Zhang, Z. Y. (1998). Protein-tyrosine phosphatases: biological function, structural characteristics, and mechanism of catalysis. *Crit Rev Biochem Mol Biol, 33*(1), 1-52. doi: 10.1080/10409239891204161

Zinn, K. (1993). Drosophila protein tyrosine phosphatases. *Semin Cell Biol, 4*(6), 397-401.